Distribution Agreement

In presenting this thesis or dissertation as a partial fulfillment of the requirements for an advanced degree from Emory University, I hereby grant to Emory University and its agents the non-exclusive license to archive, make accessible and display my thesis or dissertation in whole or in part in all forms of media, now or hereafter known, including display on the world wide web. I understand that I may select some access restrictions as part of the online submission of this thesis or dissertation. I retain all ownership rights to the copyright of the thesis or dissertation. I also retain the right to use in future works (such as articles or book) all or part of this thesis or dissertation.

Signature:

_____ _____

Michael Joseph Jutras Date

Recognition memory signals in the macaque hippocampus

By

Michael Joseph Jutras
Doctor of Philosophy

Graduate Division of Biological and Biomedical Sciences
Neuroscience

_____

Elizabeth Buffalo, Ph.D.
Advisor

_____

Jocelyne Bachevalier, Ph.D.
Committee Member

_____

Stephan Hamann, Ph.D.
Committee Member

_____

Joseph Manns, Ph.D.
Committee Member

_____

Donald Rainnie, Ph.D.
Committee Member

_____

Stuart Zola, Ph.D.
Committee Member

Accepted:

_____

Lisa A. Tedesco, Ph.D.
Dean of the James T. Laney School of Graduate Studies

_____

Date

Recognition memory signals in the macaque hippocampus

By

Michael Joseph Jutras
Sc.B., Brown University, 2003

Advisor: Elizabeth A. Buffalo, Ph.D.

An abstract of
a dissertation submitted to the Faculty of the Graduate School of Emory University in partial fulfillment of the requirements for the degree of Doctor of Philosophy in the Graduate Division of Biological and Biomedical Science
Neuroscience
2011

Abstract

Recognition memory signals in the macaque hippocampus

By Michael Joseph Jutras

Recognition memory, the ability to perceive recently encountered items as familiar, relies on structures in the medial temporal lobe, including the hippocampus. However, neurophysiological studies have thus far provided little evidence for the existence of recognition memory signals in the monkey hippocampus, despite the existence of such signals in surrounding cortical areas. Studies of the effects of hippocampal damage in monkey and humans have shown the visual paired comparison, or visual preferential looking task (VPLT), to be a test of recognition memory that is sensitive to hippocampal damage. Accordingly, to examine possible recognition memory signals in the hippocampus, I recorded hippocampal activity in rhesus monkeys as they performed the VPLT. Hippocampal neurons responded significantly to stimulus presentation relative to the baseline pre-stimulus period, and a substantial proportion of these visually-responsive neurons showed significant firing rate modulations that reflected whether stimuli were novel or familiar. Additionally, these firing rate modulations were correlated with recognition memory performance on the VPLT such that larger modulations by stimulus novelty were associated with better performance. I also observed an increase in temporally correlated activity across the hippocampus, i.e., neuronal synchronization, in the gamma frequency band during encoding that predicted the strength of subsequent recognition. Finally, I observed theta-band oscillations in hippocampal LFPs that were strongly coupled to the monkeys' eye movements, undergoing a phase resetting with each new fixation. The phase of the network theta oscillation at fixation onset and the degree of spike-field phase synchronization in the theta band across the trial were correlated with the strength of stimulus encoding. In addition, the amplitude of hippocampal gamma, which has been linked to successful memory formation, was modulated at theta frequency. Taken together, these findings suggest that neuronal activity in the hippocampus is organized at multiple levels, is related to the strength of memory formation, and is intimately connected to behavior. Findings from this research could be used to develop new criteria for identifying aberrant neural activity in humans exhibiting symptoms of memory loss. The possibility that a disruption in neuronal synchronization may underlie the memory impairment in these patients also suggests that therapies aimed at alleviating this disruption could be used to treat memory loss.

Recognition memory signals in the macaque hippocampus

By

Michael Joseph Jutras
Sc.B., Brown University, 2003

Advisor: Elizabeth A. Buffalo, Ph.D.

A dissertation submitted to the Faculty of the Graduate School of Emory University in partial fulfillment of the requirements for the degree of Doctor of Philosophy in the Graduate Division of Biological and Biomedical Science
Neuroscience
2011

Contents

List of Figures

List of Tables

Acknowledgements

First and foremost, I would like to thank my mentor, Dr. Elizabeth Buffalo. It has been an immense privilege to be a student under her guidance and a researcher in her lab, and I am truly grateful for the years of collaboration that produced this dissertation. I am also proud to have been the first graduate student under her mentorship and to have played a role in building the lab up to the great environment it is today, but it would not have been possible without her incredible guidance, patience, support, and enthusiasm. While working with her, I've learned that being a successful scientist requires more than just skill at the bench, but also a willingness to ask tough questions about your results as well as imagination and openness to new scientific ideas.

I would also like to thank my fellow students in the Emory Neuroscience program, and especially those in the class of 2004. While graduate school has in many ways been a long, arduous journey, I feel very fortunate to have had the opportunity to spend my years at Emory with such a group of bright, supportive, inspiring peers. I have truly appreciated going through my graduate training with classmates who are not only passionate about science, but have also been such great friends through our years together. I am also grateful for the excellent academic and social environment provided by the Emory Neuroscience faculty.

Of course I owe a great deal of gratitude to my thesis committee: Dr. Jocelyne Bachevalier, Dr. Stephan Hamann, Dr. Joseph Manns, Dr. Donald Rainnie, and Dr. Stuart Zola. Each of the members of my committee has helped the development of this project as well as contributed to my own growth as a scientist, not only through committee meetings but also through journal clubs, practice talks and the occasional informal

meeting, and I'm happy to acknowledge their contribution to this dissertation as well as their excellent mentorship. I would also like to thank Dr. Pascal Fries for his valuable input regarding the various analytical techniques which were vital to this project.

I am also indebted to my labmates, not only for the many ways in which they have contributed to this research project, but also for providing such an incredible work environment, for which I am eternally grateful. Part of my reason for choosing a career in neuroscience research was due to my admiration for the passion that neuroscientists have for their research, and I have to say that every single person I have had the pleasure of working with in the Buffalo lab has exhibited that enthusiasm, especially the many talented undergraduates that have made their way through the lab. I would especially like to acknowledge those whose technical assistance has, in varying ways, contributed to this project: Emily Stanley, Kiril Staikov, and Melissa Wilcox. Also, I'd like to thank fellow graduate student Nathan Killian, whose input has greatly contributed to this project as well as to my own scientific growth.

Thank you also to Megan Tompkins, who has been there with me through so much of this journey. Finally, I'd like to thank my parents, and my sister Tricia. I would not be where I am today without all your encouragement and support through the years, and I cannot thank you enough for everything you've done for me.

Funding for my dissertation research was provided by training grants from the National Institute of General Medical Sciences, grant 5T32GM008605-10, and the National Institute of Mental Health, grant MH082559.

Chapter 1

Introduction and Background

Overview

The ability to form memories of the surrounding environment exerts a profound influence over all of life. Memory allows organisms to navigate and grow within their environment, find food, avoid predators, recognize social cues, and a myriad of other tasks that aid in survival. While the brains of animals and humans have evolved complex systems for forming and storing memories, evidence of information storage can be observed even at the level of molecular cascades within cells. Our experience gives us a subjective sense for the significant role that memory plays in our everyday lives, but nothing quite conveys this significance as much as when this ability fails us. Impaired memory is a component of diseases such as Alzheimer's disease, schizophrenia, temporal lobe epilepsy, and depression. The desire to understand memory formation, the systems responsible for memory and the causes of memory deficits has propelled decades of research in the hopes of developing new therapies for patients afflicted with memory loss. While memory has long been known to be a function of brain activity, the knowledge that localized damage to specific areas in the brain will dramatically alter the manner in which

memories can be stored and accessed has only come about within the last half century. From the early clues that memory formation begins with the activity of neurons in certain memory centers in the brain, neuroscience research and technological advances have subsequently progressed to a point where this activity can be measured as it occurs. These methods offer great promise for understanding the progression of changes during the course of neurodegenerative diseases that negatively impact memory.

This introduction reviews the available literature in order to provide background relevant to the research described in this thesis. Our current understanding of the nature of memory and the specific roles of various brain areas in memory comes primarily from studies in human amnesic patients as well as in animal models of memory deficits. In addition, increasing understanding of memory formation has come from a growing body of research measuring this process using a number of methods, both invasive and noninvasive. These studies provide a basis for the experiments reported in the current thesis, which utilize electrophysiological methods for understanding the natural process of recognition memory formation in the nonhuman primate brain.

Background: Hebbian learning and memory formation

The work contained in this thesis falls under a tradition of basic research that ultimately seeks to answer a simple question: how does the brain learn? Some of the most enduring ideas addressing this question came from Donald Hebb, whose theories on the workings of neurons and the storage of information in the brain continue to resonate in the field of neuroscience to this day. While he was not the first to suggest that learning is a process related to the connections among neurons in the brain, in *The Organization of*

Behavior he advanced the hypothesis that learning specifically involves the strengthening of a synaptic connection between neurons following repeated, correlated activation of one neuron by another through this connection[1]. In addition, he proposed the existence of groups of neurons which he referred to as "cell assemblies" that form a functional unit in information processing, i.e., neurons that tend to fire together. Subsequent research has supported the idea that neurons "learn" through changes in the strength of their connections with each other[2], and that these changes can come about as a result of variations in patterns of activity occurring in cell assemblies, in terms of both rate and the specific timing of activity. The experiments contained in this thesis were designed to study such patterns of activity at the systems level in the hippocampus, a brain region that is critical for memory formation.

Memory systems in the brain

Evidence for the importance of the medial temporal lobe (MTL), including the hippocampus and neighboring cortical regions (Figure 1.1), in memory can be traced to over a century ago, when von Bechterew presented a clinical case report describing a patient with profound memory impairment. An autopsy on this patient showed softening of the hippocampus and neighboring cortical areas on both sides of the brain[3]. Later, there were several other clinical case studies that suggested a connection between MTL damage and impaired memory[4-6].

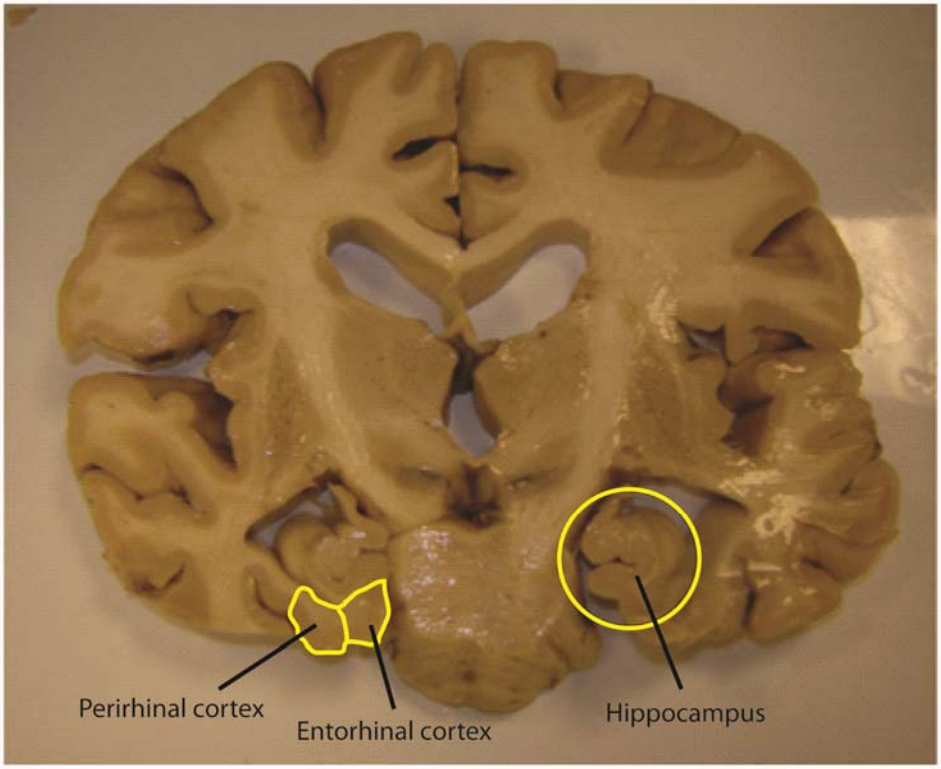

Figure 1.1: The medial temporal lobe of the human brain. This image shows a coronal section through the human brain at the level of the anterior hippocampus, with the regions of the medial temporal lobe labeled. Image provided by Dr. Yoland Smith, Yerkes National Primate Research Center.

However, it was not until the 1950s that the link between memory and MTL structures was rigorously tested. Much of our understanding of memory systems in the brain began with studies of patients with bilateral damage to the MTL, such as patient HM. These patients' surgeries were performed in order to alleviate the symptoms of severe intractable epilepsy, and in the case of HM and others, involved the removal of most of the MTL on both sides of the brain. Following the surgery, HM's language, perception, and reasoning were unaffected, and knowledge acquired before the surgery was generally well preserved (although there was a period of retrograde amnesia which affected a period of time preceding the surgery). However, he exhibited profound amnesia for the experiences of daily life, and although he could retain and utilize

information for a brief period of time in immediate memory, his long term memory was severely disrupted[7,8].

Through the use of appropriate behavioral tasks with patients like HM, Brenda Milner and other researchers revealed compelling evidence for multiple memory systems in the brain. For instance, HM retained the ability to learn new motor skills after the surgery, although he was unable to remember the training sessions involved in learning the skill and could not recall having performed the task before. This example illustrates a key distinction between two memory systems: explicit (or declarative) memory, which involves the ability to consciously recall information about facts and events; and implicit (or nondeclarative) memory, which includes motor (skill) learning as well as perceptual learning and other types of learning that are not necessarily accessible to conscious knowledge. Damage to specific regions of the brain can potentially produce deficits in one or the other of these memory systems. However, these two memory systems are critically reliant on separate regions of the brain for normal function[9]. While motor and perceptual learning generally involve the striatum, cerebellum, and motor or sensory cortices, explicit memory in humans and other primates is critically dependent on regions in the MTL.

Many different forms of explicit memory are thought to rely on the MTL memory system for normal function. These include episodic memory, the memory for the day to day occurrences in one's life; semantic memory, the ability to recall information about facts and events not necessarily based in one's own life; and recognition memory, which is simply the ability to perceive a recently encountered item as familiar. This thesis will focus on recognition memory for visual stimuli in the primate.

Recognition memory and the medial temporal lobe

Along with the development of appropriate animal models for memory disruption, the development of appropriate behavioral testing paradigms has been essential for understanding the neural correlates of memory. With the knowledge that explicit memory was disrupted in humans following damage to MTL structures while other functions including implicit memory and immediate (or working) memory remained intact, researchers attempted to replicate these effects in animals in order to elucidate the specific regions of the temporal lobe that are critical for normal explicit memory.

One problem that was encountered early on was that animals with MTL lesions will often show normal performance on the same memory tasks for which amnesic human patients show a deficiency. For example, monkeys[10] and rats[11] with lesions of the same regions that were surgically ablated in HM showed no impairment in performance compared to controls when tested on the same tasks on which HM was impaired[12]. Specifically, delayed visual discrimination tasks that were often used in early studies to show impaired performance among amnesic patients compared to healthy controls can be learned gradually over many trials by monkeys with medial temporal lesions. This difference is now known to be due to the fact that animals will utilize any methods at their disposal to successfully complete such reward-based tasks, and many of these tasks could, in fact, be successfully completely using means other than explicit memory, such as through habit learning[13]. This form of memory depends on the basal ganglia and is independent of the MTL[14,15]. Because animals can utilize alternative brain pathways to complete such reward-based tasks, any purported test of explicit memory function must

necessarily be solvable without relying on alternative skills, especially those (such as habit learning) that can come into use during the prolonged training periods that are often involved in animal behavioral studies.

An important development came with the use of single trial memory tasks, in which memory for stimuli is assessed on a trial-by-trial basis. For example, in the delayed matching (DMS) or nonmatching to sample (DNMS) task, monkeys are first presented with a sample object, which the monkey displaces to receive a food reward. Recognition memory for the sample object is tested by presenting the monkey with the sample object alongside a new object after a delay period. The monkey is trained over many trials to displace the sample object (for DMS) or the novel object (for DNMS) in order to receive a reward[16,17]. In the trial-unique version of this task, unique objects are used for each trial so that successful performance could be obtained by comparing the relative familiarity of each pair of objects. Monkeys with large MTL lesions are consistently impaired on this task, especially when a large delay between trial phases is imposed[18-25].

These findings supported the MTL as an area of focus for studies of explicit memory function. Additional studies have considered the role of specific regions within the MTL memory system in memory performance. This system includes the hippocampal formation (dentate gyrus, subiculum, and the cornu ammonis, usually delineated into areas CA1 and CA3), entorhinal cortex, perirhinal cortex, and parahippocampal cortex (whose homologue in rodents is believed to be the postrhinal cortex). While earlier lesion studies involved surgical removal of the entire MTL,

including the hippocampus, amygdala, and surrounding cortex, later studies investigated the effects of specific lesions. These will be discussed in further detail below.

The visual paired comparison (VPC) task

While DMS was developed earlier as a test of recognition memory, DNMS came into more widespread use because the test subject was rewarded for consistently choosing the novel object in each test phase. Both humans and other primates are inherently attracted to novelty, and so this version of the task proved far easier to train monkeys to complete successfully because it took advantage of this bias. However, along with the DNMS task paradigm, yet another test of visual recognition memory was developed which took advantage of the innate preference that primates normally display for novel stimuli. This test was originally developed to study early visual development, with the reasoning that an animal that consistently exhibits preference for one stimulus over another has the ability to detect differences in form and pattern between the two stimuli[26]. Joseph Fagan first used this test to assess recognition memory in human infants[27]. Based on the insight that differential time spent looking at a novel stimulus versus a previously seen target stimulus must indicate successful memory for the target stimulus, Fagan developed a task wherein infants were presented with two identical stimuli side by side for a period of time, then following this presentation (immediately or after a delay) the recently viewed stimulus was presented alongside a novel stimulus. Infants showed preferred viewing for the novel stimulus over the familiar, and thus less interesting, stimulus, even when a delay of 2 hours separated the successive presentations[27]. Because this task takes advantage of an innate preference for novelty that is conserved across

mammalian species, it does not require verbal instruction or training, making it a simple, straightforward tool for studying recognition memory in many species.

The visual paired comparison (VPC) task and novel object recognition (NOR) task were subsequently developed from this paradigm to test recognition memory in primates[28] and rodents[29], respectively. In VPC, the subject is presented with two images side by side, and the eye position is measured (typically non-invasively by measuring the corneal reflection) to determine which image the subject is looking at. In NOR, rodents are allowed to explore physical objects in their environment, and the time spent sniffing or whisking these objects is measured. In both tasks, the amount of exploration time is compared between novel and repeated stimuli to assess memory for the repeated stimulus. These tasks have been shown to be sensitive to MTL damage in humans[30], monkeys[31-33], and rats[34]. Additional findings specific to the hippocampus will be discussed below.

Hippocampal contribution to recognition memory

The hippocampus is anatomically positioned to receive highly processed information largely via projections from the entorhinal cortex, which in turn receives information from widespread neocortical regions via the perirhinal and parahippocampal cortices[35-38] (Figure 1.2). Importantly, sensory information arriving at the hippocampus through these relays is multimodal in nature. Thus, deficits in explicit memory resulting from damage to the MTL is never specific to one sensory domain, but affects visual, auditory, and somatosensory modalities alike. Each relay point of information flow through the MTL involves one or more synaptic connections, along with opportunities for

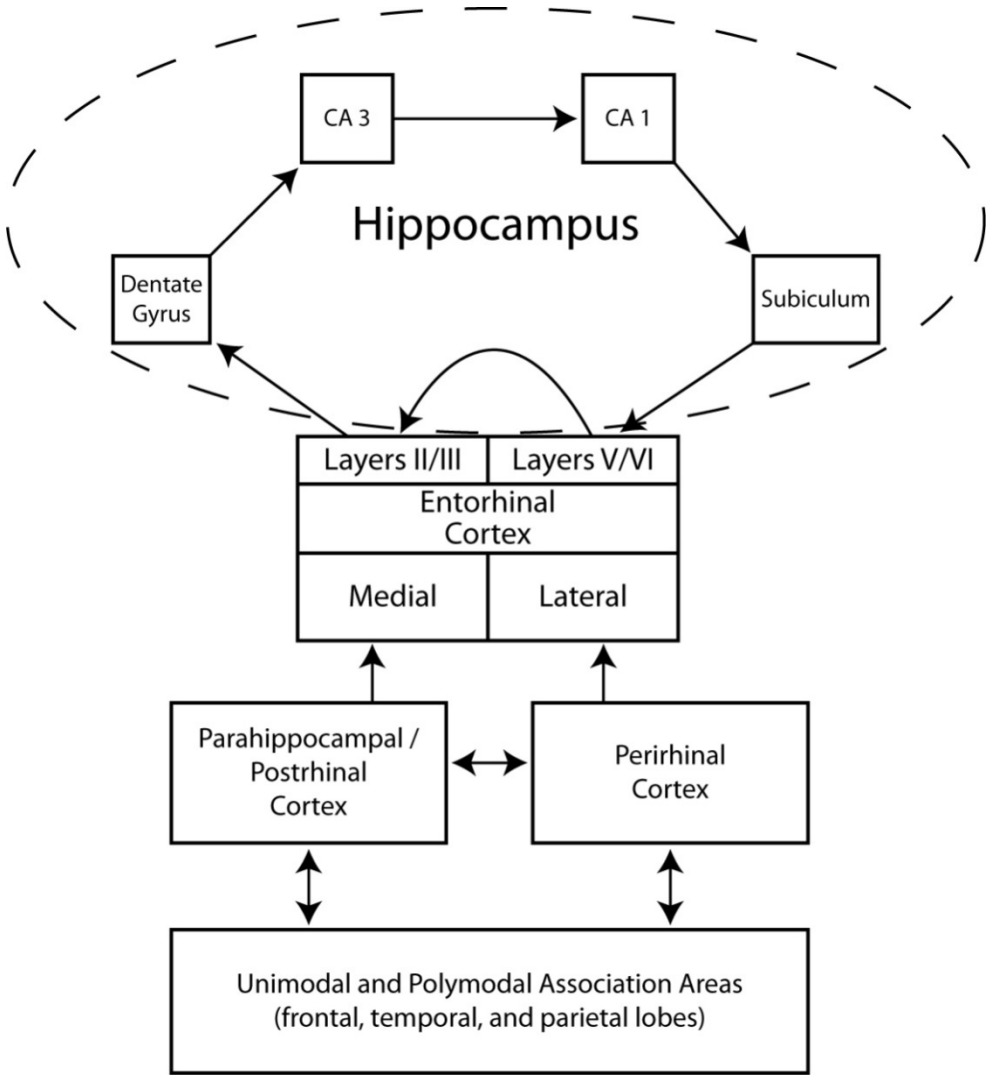

Figure 1.2: Schematic of the medial temporal lobe memory system. The diagram shows the anatomical connectivity of the hippocampal formation (dentate gyrus, CA3, CA1, and subiculum), and the entorhinal, perirhinal, and parahippocampal (postrhinal in the rat) cortices. This is a simplified representation of the way information is projected from the parahippocampal and perirhinal cortices to layers II/III of the entorhinal cortex, then in turn through a mainly unidirectional, feed-forward pathway from the superficial layers of the entorhinal cortex through the subregions of the hippocampal formation, and finally returning to the deep layers of the entorhinal cortex.

further processing through local inhibition and input from other regions of the brain. This pattern of anatomical connectivity of the MTL memory system suggests differing levels of function in each region's contribution to the neural operations underlying memory. While the anatomical connectivity between regions of the MTL has guided the

investigation of these areas' contributions to recognition memory, the complexity of this system has largely frustrated many attempts at simplistic matching of structure to function.

Studies of monkeys with lesions of specific MTL regions have provided some insight into the contribution of each region to recognition memory. There is widespread agreement that the perirhinal cortex is critical for recognition memory, as monkeys with perirhinal lesions consistently display a deficit in performance on DNMS compared to controls[18,19,22,39-43]. In contrast, inconsistent findings have been reported regarding the impact of hippocampal lesions on DNMS performance[33,42,44-46], eliciting debate among researchers as to the extent of hippocampal involvement in recognition memory performance[47,48]. While studies using DNMS to assess recognition memory have yielded inconsistent results, damage limited to the hippocampus produces consistent deficits in performance on VPC in humans[49] and monkeys[33,42] and on NOR in rats[34]. Monkeys with hippocampal lesions will show significantly less novelty preference on VPC than controls with delays as short as 10 seconds[33], making VPC a compelling behavioral assay of hippocampal function.

The discrepancy in these data regarding hippocampal-lesioned monkeys and recognition memory performance continues to provoke discussion among memory researchers regarding the contribution of the hippocampus to recognition memory, as well as the precise psychological basis of these two tasks. Although at first glance both VPC and DNMS would seem to test the same cognitive processes, they are in fact drastically different in terms of the amount of training involved to learn the rule-based task parameters of DNMS, along with the degree of motivation involved, since DNMS is

explicitly rewarded while VPC is not. Because monkeys are highly motivated to complete DNMS trials successfully, they are likely to resort to any strategy available in order to complete the task. Thus, it is conceivable that hippocampectomized monkeys may rely on strategies that are unavailable to monkeys with perirhinal lesions, such as holding information about the sample "on-line" during the delay in order to successfully make the correct choice during the test phase. Such strategies may also come about with excessive pretraining, which is avoided in VPC. Another consideration is the possibility that the two tasks simply involve separate memory systems altogether. Because subjects are not explicit rewarded for performing VPC, as they are for DNMS, the behavior measured during VPC performance could be linked to implicit mechanisms of sensory memory that rely on brain regions that are distinct from those critically involved in recognition memory. However, it is unlikely that VPC relies on implicit memory processes because in humans, VPC performance is predictive of subsequent recognition memory performance in a two-alternative forced-choice test, while performance in perceptual priming (an implicit memory process) is unrelated to recognition memory performance[50]. One last consideration comes from Nemanic et al., 2004, suggesting that VPC's greater sensitivity to hippocampal damage may be indicative of the associative nature of hippocampal processing, especially for completely novel stimuli:

> In VPC, animals are passively exploring two-dimensional black/white novel stimuli, not actively memorizing the sample to select a future response (i.e., incidental learning). It is presumably more ecological for monkeys (and humans) passively witnessing a new event to keep a trace (however weak it is) of the whole event, because anything can later prove to be behaviorally relevant (i.e., the

> stimulus, its elements, and its spatial and temporal contexts). This incidental encoding could favor the formation of conjunctive representation not only of the different elements of the sample but also of its location and contexts.[42]

Because the hippocampus is widely considered to play an important role in associative memory, the memory for relationships between multiple items[51-53], it is difficult to rule out the possibility that the relational content of images may contribute to greater hippocampal processing during the formation of an image's representation in memory, even during passive viewing. Indeed, previous work suggests that processes related to single-item and associative memory may be closely related in the hippocampus[54], which may make attempts to disambiguate these processes during recognition memory tasks difficult. However, neural signals related to such associations in the hippocampus may take many presentations to develop[55], while recognition for the images used in VPC is evident after a single presentation.

Despite these considerations, studies have consistently shown that normal performance on VPC is drastically affected by hippocampal damage, making this task paradigm an effective assay of hippocampal activity related to the mnemonic processing of visual stimuli. One goal of the current thesis is to investigate neuronal activity in the hippocampus during recognition memory performance in order to further our knowledge of this region's contribution to memory. The experiments designed for this thesis draw from previous work by Wilson and Goldman-Rakic, which adapted the preferential looking paradigm in order to enable investigations of the neurophysiological correlates of viewing preferences of monkeys for complex images[56]. In that study, completely novel images were presented one at a time rather than side by side, and the amount of time

spent looking at each picture was measured as an index of the monkey's interest in the picture. Consistent with studies using VPC, monkeys spent substantially less time, on average, viewing images when they were shown for repeated presentations compared to when the images were completely novel. Because the monkey has a choice to either continue looking at each image or to look away from the image, and will do the latter when interest in the image diminishes (such as when recognition of the image becomes apparent), this preferential looking paradigm is comparable to VPC which compares gaze durations for the repeated (and less interesting) image to a completely novel image. The fact that images appear one at a time makes this task paradigm especially amenable to neurophysiological study, since the visual receptive field of neurons in the temporal lobe could encompass most of the field of view[57], which would complicate any analysis of neuronal activity when two images are presented side by side. Thus, this task paradigm was adapted for use in the current thesis as the Visual Preferential Looking Task (VPLT).

Hippocampal physiology - background

While studies of amnesic patients and MTL-lesioned animals elucidated the subtle distinctions between different types of memory and the structures that are critically involved in the neuronal operations of memory formation, the realm of physiology research has allowed us to observe these operations as memories are formed. Although the intimate connection between the MTL and memory wasn't fully appreciated until the 1950s, studies of neuronal physiology in the hippocampus go back possibly as far as 1933, when Saul and Davis, recording with large electrodes in the region of the cat hippocampus, described "huge discharges, about five times a second, which are very

regular and have waves of very constant and definite shape"[58]. Jung and Kornmüller followed this report in 1938 with an observation of a large amplitude, sinusoidal wave pattern in the rabbit hippocampus at between 4 and 7 Hz, which they named "theta" activity[59]. While subsequent studies in a number of species initially seemed to link this activity to attention, arousal, locomotion and a number of other behaviors, the growing body of evidence linking the hippocampus to memory provided a well-defined behavioral context within which later studies would explore neuronal signals in the hippocampus, in attempts to relate these signals to memory formation. The unique cytoarchitecture and placement of the hippocampus within the brain (along with other considerations) also facilitated the development of a number of novel techniques for recording neural activity, such as the first use of microelectrodes for recording extracellular neuronal signals[60] and the development of field potential analysis[61,62]. While many other methods have been used to investigate the physiology of hippocampal neurons, such as recordings from slices and isolated cultures of neurons, this introduction will focus on data obtained from the brains of awake, behaving subjects, except where it is relevant to discuss data obtained using other methods.

Hippocampal circuitry

Hippocampal neurons fall into two major classes: principal cells and interneurons. Principal cells form the major output pathway from hippocampal subregions. They are morphologically defined as granule and mossy cells in the dentate gyrus, and pyramidal cells in all other hippocampal subregions. Their projections make excitatory connections onto other neurons, utilizing the neurotransmitter glutamate to mediate this excitation.

While these principal cells are the classic "projection" neurons that provide the means for signal transmission between hippocampal subregions, there is also a fair amount of interconnectivity among the principal neurons within CA3 (and to some extent, in CA1) through recurrent excitatory axon collaterals, allowing for a high degree of complexity in local information processing in these subregions. For instance, this organization is thought to facilitate the arbitrary associations between multiple items in memory that occurs during the process of episodic memory formation[63,64].

Hippocampal interneurons are distinguished from principal cells by their γ-aminobutyric acid (GABA)-ergic projections[65]. As a group, the interneurons are much more morphologically, physiologically, and neurochemically diverse than principal cells. While GABA is generally an inhibitory neurotransmitter, and GABAergic interneurons are thought to set the overall "tone" of excitation/inhibition in many areas of the brain, this is in fact an oversimplification of the complex role interneurons can play in local hippocampal circuitry. For instance, many interneurons make inhibitory synapses on other nearby interneurons, with the net result being an increase in excitation. Due to their innate firing properties and connectivity, interneurons also provide an important pacemaker function in the generation of oscillatory activity in hippocampal networks[66]. Although the interneurons only make up approximately 5.8%[67] to 11%[68] of the total population of hippocampal neurons, each may contact in excess of 1000 postsynaptic target neurons[69-71], allowing for a high level of control over the dynamics of local neuronal networks. The functionality of these networks is greatly enhanced by recurrent circuits formed through coupling between interneurons, both through GABAergic

synaptic connections[72] as well as through electrical synapses[73,74], which serve to promote a high degree of synchronization of the interneuron network.

The hippocampal tri-synaptic circuit consists of glutamatergic projections from the entorhinal cortex to the dentate gyrus, then in turn from the principal cells of the dentate gyrus to CA3, and finally from CA3 to CA1. This relatively simple circuit is made more complex by the fact that afferents to each subregion activate local principal neurons as well as local interneurons. This complexity is compounded by the high degree of interconnectivity within the neurons of each subregion, with local glutamatergic connections from principal cells to interneurons as well as projections from interneurons to principal cells. The net result of this organization is to provide a background against which the precise timing of neuronal activity is important in the transmission of information between and within subregions[75].

Memory-related single neuron activity in the MTL

The recording of single neurons in the hippocampus of awake, behaving animals goes back to the early 1970s, when Ranck[76] and O'Keefe[77] independently categorized hippocampal neurons into two main classes based on anatomical and physiological properties (e.g. firing rates, action potential width, and relative locations in the hippocampus). One of these neuron classes, the complex spiking neuron, is otherwise known as the "place cell" due to the fact that these cells are highly attuned to the position of the rat in its environment, exhibiting peak firing rates when the rat is in a particular location. The discovery of these cells led to the development of the cognitive map theory of hippocampal function, which posits that the hippocampus mediates the psychological

representation of space as well as context-dependent memory[53]. The other neuron class, the theta cell, displays activity that is highly correlated with the aforementioned theta activity (which will be described later in further detail). These two cell classes most likely correspond to principal cells and interneurons, respectively[78]. While these two cell types have been primarily investigated in the rat, there are indications that both monkey[79] and human[80] hippocampal neurons can be classified based on similar criteria.

The discovery of place cells in the rodent hippocampus spawned an entire field of research that has provided insight into the nature of memory formation. However, the basis for much of the experimental work contained in this thesis can be traced more directly back to electrophysiological studies of recognition and working memory in the monkey MTL. The early experiments in this realm were driven in part by disagreement, stemming from lesion studies, concerning the individual contributions of the hippocampus and neighboring cortical areas in the MTL to performance on recognition memory tasks[81-84]. These studies typically involved task paradigms similar to those used in lesion studies: monkeys were trained to signal recognition of a visual stimulus (using a computer screen or projector rather than physical objects) that had been previously presented, with a delay period interceding successive presentations, in order to receive a reward. Variations on this basic task structure include DMS[85-87] (Figure 1.3A), the Konorski conditional delayed matching task[88-91], and a serial recognition task[91-93]. The general approach used in these studies was to record the activity of single neurons using microelectrodes as monkeys performed these tasks, and compare neuronal response properties (in terms of the rate of action potential firing) to stimuli when they were presented during the encoding phase of the task (the "sample") to the same stimuli when

they were repeated during the test phase of the task. Results from these studies have shown clear evidence for memory-related signals in the perirhinal and entorhinal cortex[85-88,94,95]. Such signaling took the form of a reduction in firing rate for stimuli when they were repeated compared to when they were first presented, an effect that has been called "match suppression"[86] (Figure 1.3B). These results seem to be consistent with the well-recognized role of the MTL cortical areas in recognition memory.

In contrast to these results, several of these same studies found no evidence of

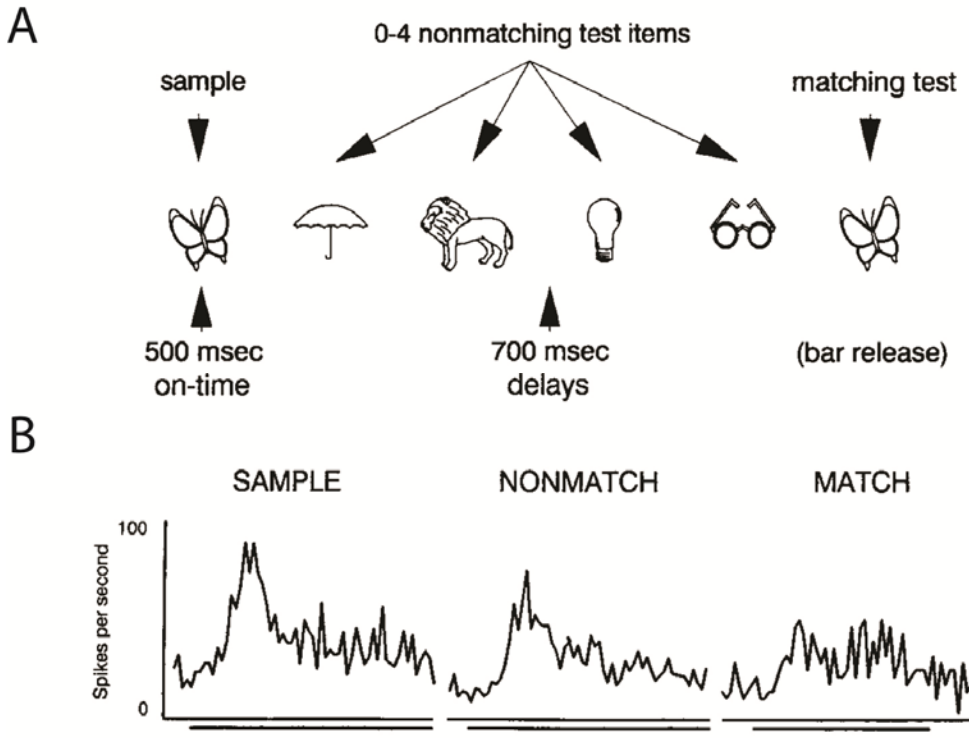

Figure 1.3: Match suppression in a temporal lobe neuron during DMS. (A) Schematic outline of the DMS task. Monkeys are trained to hold a touch-sensitive bar and release it when the sample stimulus reappears following a variable number of nonmatching stimuli on each trial. (B) Average firing responses to stimuli appearing as samples, nonmatches, and matches for an example neuron in inferior temporal cortex, illustrating the match suppression effect that occurs in response to stimuli that match the sample stimulus on each trial. Reprinted from Miller et al. (1993), with permission.

such signals in monkey hippocampus[88,89,96], while others found only very few such signals[92,93,97]. One concern with the tasks used in these studies is that they typically involved the repetitive use of highly familiar stimuli, rather than the use of completely novel stimuli as in VPC and VPLT. Because the sample stimuli used in these tasks had actually been previously viewed by the monkey, it is questionable whether the monkeys were actually using recognition memory rather than working memory to complete these tasks. One study by Hampson and colleagues[98], in which monkeys performed a DMS task using completely trial-unique stimuli, has provided some insight into the mechanisms by which hippocampal neurons encode stimulus features. In that study, many hippocampal neurons increased their firing rate during specific phases of the task (e.g. Sample, Delay, or Match), and some neurons were also selectively responsive to distinct categories of stimuli. A later study, showing increases in hippocampal glucose metabolism during performance of trial-unique DMS, is consistent with these findings[99]. A recent study utilizing single neuron recordings in human epileptic patients, using completely novel stimuli, also reported a substantial number of hippocampal neurons that signal the novelty or familiarity of stimuli with firing rate changes[100]. These results suggest that stimulus novelty may be a critical factor for hippocampal involvement.

Local field potentials

While each single neuron in the hippocampus provides a basic unit of computing power, this information is integrated on a much larger scale through the organization of these neurons into neural networks. Network activity can be measured using relatively large electrodes, which can record the aggregate electrical signals generated by the

processes of the neuronal ensemble surrounding the electrode tip. These extracellular voltage fluctuations are generally referred to as local field potentials (LFPs) and are commonly thought to reflect the input of a neuronal ensemble and the dendritic processing within the associated network: synchronized synaptic signals[101,102], subthreshold membrane oscillations[103], and spike afterpotentials[104,105] are all thought to contribute to this signal. Because fluctuations in the LFP signal represent the aggregate synchronous activity of many neurons in a particular region, the study of these signals is essentially an analysis of synchronized activity in the brain.

Neuronal synchronization and memory formation[1]

The concept that the precise synchronization of neuronal activity is one of the underlying mechanisms by which information is stored in neural tissue has been well-characterized at the level of single neurons. For instance, changes in synaptic connectivity can be induced by the precise timing of spiking activity of multiple neurons in relation to one another, an effect known as spike timing-dependent plasticity (STDP)[106]. The ability of synchronized activity between two neurons to induce long-term potentiation (LTP) or long-term depression (LTD) of the synapse(s) connecting those neurons depends on whether the activity falls within a particular critical window (10-20 ms), as well as whether the presynaptic spike precedes or follows the postsynaptic spike within this window[107-111]. The size of the window varies depending on the cell type as well as the dendritic location of intercellular connections[112-115]. Because LTP and LTD can lead to long-lasting changes in neuronal properties, including receptor

[1] Edited from Jutras, M. J. & Buffalo, E. B. Synchronous neural activity and memory formation. *Curr Opin Neurobiol* **20**, 150-155, (2010).

trafficking and spine motility, these studies provide a direct link between synchronous neuronal firing and the modifications that may underlie memory formation in the brain.

Growing evidence from electrophysiogical and imaging studies suggests that precisely timed neuronal activity at the network level can be linked to improved memory performance. In particular, many studies in recent years have furthered the idea that gamma- (30-100 Hz) and theta- frequency (3-8 Hz) synchronization, and the interaction between these two rhythms, may engender the critical conditions by which synchrony among neural networks can support the specific processes underlying learning at the cellular level in the brain.

Gamma-band oscillations and memory formation

Neuronal ensembles often synchronize their activity at particular frequencies, producing oscillations that can be measured either noninvasively or with subdural arrays or electrodes planted deep within the brain. Modulations in oscillatory activity are often seen as humans and animals engage in cognitive tasks. Gamma-band oscillations, in particular, have been associated with neuronal processing when the brain is in an "active" state, such as during attentional or mnemonic processing[116-118]. In the hippocampus, gamma-band oscillations rely on interactions between inhibitory networks and local collaterals of principal cells providing excitatory signals to the network[119,120]. Gamma-band synchronization may affect signal transmission by two distinct mechanisms. First, gamma-band synchronization may provide input gain modulation through the influence of rhythmic network inhibition on local principal cells. Because these oscillations arise from strong, perisomatic inhibition from networks of local interneurons[120,121], the efficacy

of excitatory input to neurons within the oscillating network is highest when this input arrives out of phase with this rhythmic inhibition. In this way, gamma-band oscillations can align rhythmic inhibition among neuronal groups, ensuring that the interactions between groups are the strongest when their phases are well-aligned with each other[122] (Figure 1.4). Second, neurons under the common influence of gamma-band oscillation will tend to fire within 10 ms of each other (roughly the equivalent of a gamma-band half-cycle). This synchronization may enhance the impact of multiple excitatory neurons to downstream areas, where they converge on a common target. This feedforward coincidence detection may involve increased temporal summation of excitatory postsynaptic potentials, resulting in an increased likelihood that downstream neurons will fire. In this way, gamma-band oscillations may serve to enhance the impact of projection neurons[123-125]. As mentioned above, correlated activity within this time window (10-20 ms) is a necessary condition for STDP. Accordingly, gamma-band oscillations may promote interactions among neurons that bring about the synaptic changes thought to be necessary for memory formation.

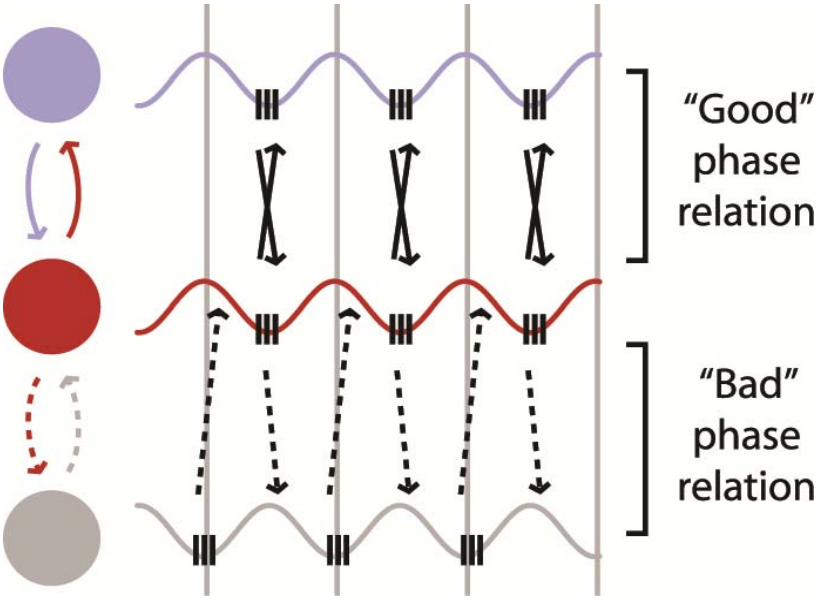

Figure 1.4: Phase synchronization promotes effective neuronal communication. Schematic illustration of oscillatory activity (LFP oscillations with spikes in troughs) for three groups of neurons. Phase alignment among rhythmically-active neuronal ensembles promotes effective communication between these ensembles (top) while misalignment results in less effective communication (bottom). Reprinted from Womelsdorf et al. (2007), with permission.

Although much research has focused on the role of gamma-band synchronization in selective attention[126-129], many recent studies have observed synchronous activity in the medial temporal lobe (MTL) during performance of memory tasks in rodents[130-132] and humans[117,133-142]. Changes in neuronal activity have been observed, with respect to memory formation, in oscillatory power, which reflects the energy per unit time within a particular frequency range, and coherence, which is a measure of linear predictability that captures phase and amplitude correlations. In particular, studies of intracranial electroencephalography (iEEG) signals in human epileptic patients have shown that when subjects study lists of words and are subsequently asked to freely recall as many words as possible, gamma-band power in the MTL is higher during the encoding of subsequently

recalled words than unrecalled words[142]. Using a similar task, Fell and colleagues have shown that gamma-band coherence between iEEG signals in the hippocampus and the rhinal cortex also predicts successful memory encoding[117,135].

Coupling between gamma-band and theta-band oscillations

Modulations in gamma-band oscillations are often observed with respect to the phase of slower oscillations. This has primarily been observed in the theta-frequency band[143-145], but instances of cross-frequency coupling with the alpha-frequency (8-13 Hz) band have also been noted[146]. For example, Canolty and colleagues found that power in the fast gamma-frequency (80-150 Hz) band was highest at the trough of the theta-band oscillation in the human electrocorticogram[144]. Cross-frequency coupling may represent a mechanism for inter-areal communication. In support of this idea, it was recently observed that gamma-band oscillations in hippocampal area CA1 of the rat hippocampus can be divided into fast and slow components, each occurring at a particular phase of the theta-band oscillation, and each associated with a different source of afferent input to CA1[147]. Slow (~25-50) gamma-band oscillations in CA1 were most prominent during the descending phase of the theta-band oscillation and were synchronous with slow gamma-band oscillations in CA3, while fast (~65-150) gamma-band oscillations in CA1 peaked during the trough of the theta-band oscillation and synchronized with fast gamma-band oscillations in medial entorhinal cortex. These results suggest that hippocampal theta-band oscillations may play a role in regulating information flow from entorhinal cortex and CA3 to CA1 in a way that optimizes memory encoding and retrieval. Also, spike-field coherence in the theta-band is enhanced during the encoding of visual stimuli

in human hippocampus[148]. The hippocampal theta-band oscillation has been shown to exert an influence over activity in other areas of the cortex, as well. In one recent study, neurons in primary sensory cortices and the medial prefrontal cortex were transiently coherent with locally-generated gamma-band oscillations during exploration or REM sleep, and "bursts" of gamma-band oscillations as well as with theta-band oscillations generated in the hippocampus[149]. Taken together, these findings support the idea that rhythmic modulation in the gamma- and theta-frequency bands interact in support of memory formation and that theta-band phase can convey important information about the flow of information in the MTL during encoding processes[150].

Phase resetting as a mechanism of processing

Because the phase of the theta-band oscillation can have important implications for gamma-band oscillations, gamma-band coherence, and thus memory formation, it is important to consider behavioral factors that may influence theta-band phase at any given moment. During working memory tasks, stimulus presentation induces shifts in the phase of the hippocampal theta-band oscillation[151,152]. Such phase-resetting has recently been studied in monkey visual and auditory cortices[153,154], where it appears to play a role in modulating neuronal responses to incoming sensory stimuli. Particularly noteworthy in this regard is the finding that oscillations in monkey primary auditory cortex undergo phase-reset upon somatosensory stimulation[154]. This modulation affected the neuronal response to auditory stimuli such that auditory inputs arriving at a specific phase of the

Process associated with theta phase:	**Outcome:**	**Role in memory formation:**
LTP/LTD induction[155-157] Gamma-band oscillations[143,144,147,149]	Stimulation at peak of theta in rodent hippocampus produces LTP; stimulation at trough produces LTD. Slow gamma-band amplitude in monkey auditory cortex is highest at falling phase of theta[143]; fast gamma-band power in human cortex is highest at trough of theta[144]; slow gamma-band synchronization between rodent CA3 and CA1 occurs at falling phase of CA1 theta while fast gamma synchronizes entorhinal cortex and CA1 at trough of CA1 theta[147]; gamma-band bursts in rodent neocortex and hippocampus occur preferentially at peak and falling phase of hippocampal theta, respectively[149].	Hippocampal theta-band oscillations provide a background for regulating the processing of input from sensory areas. Gamma-band oscillations are modulated by the phase of theta, providing a foundation for patterns of signaling between brain regions that may be important for memory encoding and retrieval
Process eliciting phase reset:	**Outcome:**	**Role in memory formation:**
Stimulus onset[151-154] Fixation onset[153]	Phase reset in hippocampal theta occurs in rodents[151] and humans[152] during performance of a working memory task; theta-band phase resets in monkey auditory cortex upon somatosensory stimulation, allowing incoming auditory stimuli to elicit amplified neuronal responses depending on resulting theta-band phase[154]. Theta-band phase reset occurs in monkey primary visual cortex upon fixation onset in the dark, and theta-band phase upon stimulus onset determines amplitude of evoked neural response[153].	Phase resetting of theta-band oscillations with stimulus and fixation onset may ensure that sensory input occurs at an "ideal phase" of the oscillation; this may have important implications for mechanisms of plasticity thought to underlie memory formation.

Table 1.1: Memory-related mechanisms associated with theta-band oscillatory activity.

low-frequency oscillation produced an amplified neuronal response. Interestingly, similar effects have been seen in monkey primary visual cortex with respect to eye movements. Theta-band phase reset occurs upon fixation onset when monkeys make saccades in complete darkness, and the oscillatory phase at stimulus onset determines the strength of the subsequent neural response[153]. Such phenomena are thought to represent a mechanism by which salient events (e.g. saccades or microsaccades[153,158]) trigger a reset in ongoing oscillatory activity to an "ideal phase" in order to optimize the processing of incoming information. If theta-band phase influences the patterns of signaling in the MTL through modulations in the power of gamma-band oscillatory activity, as seen in other systems[143,144], then resetting to an ideal phase upon salient environmental or behavioral events may set different regions of the MTL to the optimum state of synchronization for memory formation and retrieval. Because LTP is optimally induced at particular phases of the theta-band oscillation in the hippocampus [155-157], hippocampal theta-band phase-resetting may also have important implications for memory formation through enhanced plasticity. These various mechanisms associated with theta-band oscillations, and their proposed role in memory formation, are summarized in Table 1.1. Interestingly, other recent evidence indicates that the amplitude of theta-band oscillations in the human MTL even before stimulus encoding can predict subsequent recognition[141], suggesting that oscillatory activity may play an important functional role in generating a cognitive state associated with successful memory formation.

Hypothesis and Aims:

The Visual Preferential Looking Task (VPLT) was developed based on the VPC task paradigm, which is known to be highly sensitive to lesions of the hippocampus. The use of this task may help identify neural signals in the hippocampus related to recognition memory. The following experiments were performed in order to test this hypothesis:

Aim 1: *Determine the extent to which firing rates of hippocampal neurons correlate with memory performance on the Visual Preferential Looking Task.* Damage restricted to the hippocampus produces a severe deficit in performance of the VPLT in both humans and monkeys; thus, modulations in hippocampal single-unit activity were predicted to correlate with performance on this task. To test this hypothesis, I recorded spiking activity from hippocampal neurons as monkeys performed the VPLT. I measured the proportion of hippocampal neurons that displayed modulations in firing rate that differentiated novel from familiar stimuli, and tested whether the magnitude of this modulation was correlated with recognition memory performance.

Aim 2: *Characterize hippocampal local field potentials during performance on the Visual Preferential Looking Task.* I recorded LFPs simultaneously with spiking activity in the hippocampus as monkeys performed the VPLT. I used spectral analysis techniques to examine the power, phase, and amplitude of LFP activity and correlated these measures with task parameters. I hypothesized, based on preliminary data and results from previous studies, that modulations in the LFP, such as in the power, amplitude, and phase of oscillatory activity, would reflect memory formation.

Aim 3: *Determine the extent to which synchrony among hippocampal neurons correlates with memory performance on the Visual Preferential Looking Task.* Research

in humans and monkeys has shown that the precise timing of neuronal activity, in particular the synchronization of neuronal firing in the gamma-band (30-100 Hz), may play an important role in cognition. Using data collected for Aims 1 and 2, I calculated gamma-band synchrony within the hippocampus to determine the degree to which neural synchrony is associated with successful memory encoding. Based on preliminary data, I hypothesized that neuronal populations in the hippocampus would exhibit gamma-band coherence and that the amount of coherence among hippocampal neurons during stimulus encoding would predict subsequent recognition memory performance.

Conclusion

Researchers have long appreciated the important role of the hippocampus in explicit memory, although despite many years of study, the role of this structure in recognition memory is still poorly understood. However, there have been a number of findings in recent years that provide hope in increasing our understanding of the neuronal substrates of recognition memory. The development of the preferential viewing paradigm to assess hippocampal-dependent memory provides a powerful tool for investigating hippocampal signals related to memory formation. In addition, there have been many recent advances in our understanding of the role of synchronized neuronal activity in memory formation. For instance, recent research supports gamma-band neuronal synchronization as a potential mechanism of encoding of sensory information. Performance of the VPLT relies only on the monkey's innate preference for novelty, thus avoiding the necessity for a lengthy training period, during which monkeys could potentially develop alternative strategies for task completion that do not rely on the

hippocampus. The potential benefit of this study is increased due to the use of the VPC in an ongoing clinical trial as an early diagnostic tool for Alzheimer's disease (Stuart Zola, personal communication). While any electrophysiology experiment is by definition correlative, and positive results would at best only associate particular neuronal mechanisms with memory formation without necessarily proving a causal relationship, these studies would pave the way for additional work using pharmaceutical, genetic, or other methods in order to investigate a deterministic relationship between synchronous neural activity and recognition memory.

Chapter 2

The activity of single neurons in the macaque hippocampus related to recognition memory[2]

Introduction

Recognition memory refers to the ability to perceive a previously encountered item as familiar. The neural processing necessary for this ability has long been attributed to structures in the medial temporal lobe (MTL) including the hippocampus and the adjacent entorhinal, perirhinal, and parahippocampal cortices[20,23,24]. However, there remains significant controversy regarding the role of the hippocampus in recognition memory. While several studies have reported impaired recognition memory performance following damage limited to the hippocampus in both humans[159-162] and monkeys[33,46,163], other studies have reported a lack of impairment[42,44,164-166]. For example, there are inconsistent findings regarding the role of the hippocampus in performance of the delayed nonmatching-to-sample task (DNMS)[33,42,44,46]. This task requires subjects to remember a previously encountered visual stimulus or object and to choose a different

[2] Reproduced with edits from original publication: Jutras, M. J. & Buffalo, E. B. Recognition memory signals in the macaque hippocampus. *Proc Natl Acad Sci U S A*, (2009).

visual stimulus or object after a delay in order to receive a reward. While it is widely accepted that the perirhinal cortex is critical for performance of DNMS[40,42], these inconsistent findings have called into question the extent to which the hippocampus contributes to performance[44].

Studies in humans have led to the proposal that the hippocampus is essential for recollection, but is not critical for simple recognition memory, or judgments of familiarity [167]. Studies of developmental as well as adult-onset amnesia have reported cases in which hippocampal damage produced intact recognition memory but impaired episodic memory, or the ability to recollect information pertaining to the specific event during which the stimulus was first encountered[164-166,168] (but see [161]). The 'Remember-Know' procedure has often been used to try to distinguish impairments in simple recognition from deficits in recall[165,166,169-171]. However, this depends on the assumption that 'Remember' judgments reflect recollection while 'Know' judgments reflect familiarity. It has recently been proposed that these findings can just as easily be explained in terms of memory strength[172], with 'Remember' and 'Know' judgments often reflecting strong and weak memories, respectively[173-177]. In support of this idea, activity in the hippocampus as measured by fMRI has been related to memory strength, even for familiarity-based, or recognition, memories[174].

If the hippocampus is critical for recognition memory performance, hippocampal neurons would be expected to modulate their evoked activity depending on whether a given stimulus is novel or familiar. While this kind of modulation has been described among neurons in the entorhinal and perirhinal cortices[85-88,94], physiological studies in non-human primates have generally reported only very low percentages of hippocampal

neurons[92,93], or in many cases no neurons at all[88,89,97], displaying such modulation. This apparent inconsistency between the findings from lesion and physiology studies has added to the controversy surrounding the role of the hippocampus in recognition memory.

Previous neurophysiological studies of recognition memory signals in the monkey MTL have typically involved training monkeys to maintain the representation of a visual stimulus in memory during a delay period in order to later signal recognition of that stimulus for a reward. Specific variations on this basic task structure used for physiological studies include the delayed match-to-sample task[85-87], the Konorski conditional delayed matching task[88-91], and the serial recognition task[91-93]. Another task that has been used to examine recognition memory in monkeys and humans is the visual preferential looking task (VPLT). Unlike the delayed matching tasks, this task does not require any specific training, but relies on the subject's innate preference for novelty. In the VPLT, recognition is assessed by comparing subjects' preferences for visual stimuli. When given a choice between a novel and a repeated stimulus, control subjects spend about 70% of the time viewing the novel stimulus, which indicates that they have formed a memory of the repeated stimulus. Lesions restricted to the hippocampus in both monkeys and humans produce significant impairment on this task[30,31,33,42]. Accordingly, this task may be useful for identifying recognition memory signals in the hippocampus.

In the current study, we used the VPLT to examine recognition memory signals in the monkey hippocampus. This task capitalizes on primates' innate preference for novel over familiar stimuli, requires minimal training, and allows for the measurement of varying degrees of performance. We analyzed the relationship between the activity of

isolated hippocampal neurons and performance on the VPLT in monkeys. Here we report that a substantial proportion of hippocampal neurons modulate their firing rates depending on whether pictures are novel or repeated. Furthermore, these modulations in firing rate are associated with trial-to-trial variability in recognition memory performance.

Methods

Electrophysiological recording, data collection and preprocessing

Procedures were carried out in accordance with NIH guidelines and were approved by the Emory University Institutional Animal Care and Use Committee. Neuronal recordings were carried out in two adult male rhesus monkeys (*Macaca mulatta*), which were obtained from the breeding colony at the Yerkes National Primate Research Center. Their mean weight at the start of the experiment was 6.8 ± 1.1 kg, and their mean age was 4 years and 5 months. Prior to implantation of recording hardware, monkeys were scanned with magnetic resonance imaging (MRI) to localize the hippocampus and to guide placement of the recording chamber. Using this information, a cilux plastic chamber (Crist Instrument Co., Hagerstown, MD) for recording neural activity, and a titanium post for holding the head were surgically implanted.

A post-surgical MRI was performed to determine recording locations. Before the scan, a cilux plastic grid was inserted in the recording chamber, and a 23-gauge guide tube was lowered through the center hole in the grid and through the dura mater. A sterile, 24-gauge glass tube was then lowered through the guide tube and 20 mm into the

brain. This tube was clearly visible in the MRI scan and allowed us to calibrate our recording depths.

During testing, each monkey sat in a dimly illuminated room, 60 cm from a 19" CRT monitor, running at 120 Hz, non-interlaced refresh rate. Eye movements were recorded using a non-invasive infrared eye-tracking system (ISCAN, Burlington, Massachusetts). Stimuli were presented using experimental control software (CORTEX, www.cortex.salk.edu). At the beginning of each recording session, the monkey performed a calibration task, which involved holding a touch-sensitive bar while fixating a small (0.3°) gray fixation point, presented on a dark background at various locations on the monitor. The monkey had to maintain fixation within a 3° window until the fixation point changed to an equiluminant yellow at a randomly chosen time between 500 ms and 1100 ms after fixation onset. The monkey was required to release the touch sensitive bar within 500 ms of the color change for delivery of a drop of applesauce. During this task, the gain and offset of the oculomotor signals were adjusted so that the computed eye position matched targets that were a known distance from the central fixation point.

Following the calibration task, the monkey was tested on the Visual Preferential Looking Task (VPLT). The monkey initiated each trial by fixating a white cross (the fixation target, 1°) at the center of the computer screen. After maintaining fixation on this target for 1 s, the target disappeared and a square picture stimulus subtending 11° was presented. Stimuli were obtained from Flickr (http://www.flickr.com/). A total of 9000 stimuli were used in this study. The stimulus disappeared when the monkey's direction of gaze moved off the stimulus, or after a maximum looking time of 5 seconds. The VPLT was given in 51 daily blocks of 6, 8, or 10 trials each, chosen

pseudorandomly, for a total of 400 trials each day. The median delay between successive presentations was 8.1 seconds. Reward was not delivered during blocks of the VPLT; however, 5 trials of the calibration task were presented between each block to give the monkey a chance to earn some reward and to verify calibration. The number of trials in each VPLT block was varied to prevent the monkey from knowing when to expect the rewarded calibration trials.

The recording apparatus consisted of a multi-channel microdrive (FHC Inc., Bowdoinham, Maine) holding a manifold consisting of a 23-gauge guide tube containing 4 independently moveable tungsten microelectrodes (FHC Inc., Bowdoinham, Maine), with each electrode inside an individual polyamide tube. Electrode impedance was in the range of 1-2 MΩ, and electrode tips were separated horizontally by 190 μm. For each recording, the guide tube was slowly lowered through the intact dura mater and advanced to ~3.5 mm dorsal to the hippocampus with the use of coordinates derived from the MRI scans. The electrodes were then slowly advanced out of the guide tube to the hippocampus. No attempt was made to select neurons based on firing pattern. Instead, we collected data from the first neurons we encountered in the hippocampus. At the end of each recording session, the microelectrodes and guide tube were retracted. All recordings took place in the anterior part of the left hippocampus. Recording sites were located in the CA3 field, dentate gyrus, and subiculum. Recording sites were located in the CA3 field, dentate gyrus, and subiculum (see Figure 2.1).

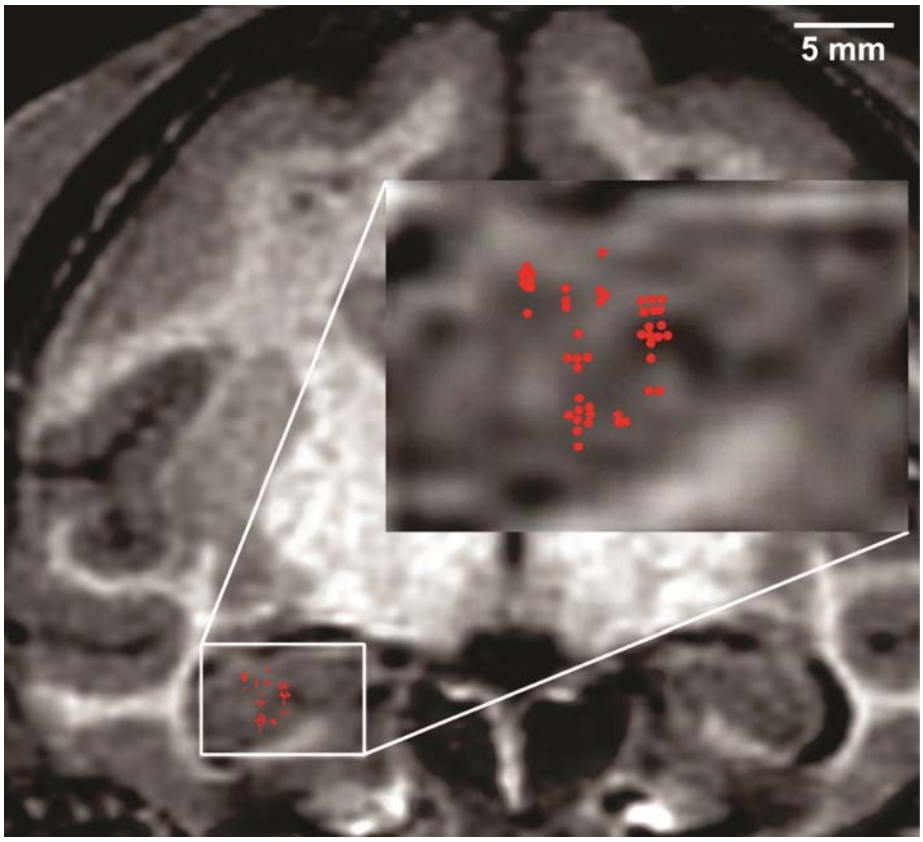

Figure 2.1: Recording locations of visually-responsive hippocampal neurons. Approximate recording sites for visually-responsive units in both monkeys, superimposed on a coronal MRI image from one of the monkeys. This image was taken at the level of the anterior hippocampus (13 mm anterior to interaural plane). Because recordings took place in multiple anterior-posterior planes, recording locations depicted may not align perfectly with regions of high cell density on the representative MRI image.

Data amplification, filtering, and acquisition were performed with a Multichannel Acquisition Processor (MAP) system from Plexon Inc. (Dallas, TX). The neural signal was split to separately extract the spike and the LFP components. For spike recordings, the signals were filtered from 250 Hz – 8 kHz, further amplified and digitized at 40 kHz. A threshold was set interactively, in order to separate spikes from noise, and spike waveforms were stored in a time window from 150 μs before to 700 μs after threshold

crossing. Each recording typically yielded 2 to 6 units; single units were sorted offline using Offline Sorter (Plexon, Inc.).

Data analysis

All analyses were performed using custom programming in Matlab (The Mathworks, Inc., Natick, MA) and using FieldTrip (http://www.ru.nl/fcdonders/fieldtrip/), an open source toolbox for the analysis of neurophysiological data.

We recorded from 131 hippocampal units in two monkeys (67 in Monkey A and 64 in Monkey B, respectively). For each neuron, the average firing rate was calculated for the period including pre-stimulus fixation as well as stimulus presentation, for each trial. A baseline period of 800 ms preceding stimulus onset was used to calculate the average background firing rate for each neuron. The response latency for each neuron was determined by first calculating the spike density function of the neuron's firing activity for each trial using a Gaussian kernel with a standard deviation of 100 ms, dividing this smoothed activity into 10 ms bins starting with stimulus onset, then finally using a Student's t-test to compare the activity in each bin, across trials, to the baseline firing rate. Upon identifying the first instance in which three consecutive bins showed a significant difference ($p < 0.05$) from the baseline firing rate, the onset time of the first bin was designated as the response latency for the neuron.

Significant responsiveness to visual stimuli was determined by first calculating the average firing rate for the period from 100-600 ms after stimulus onset for each trial, then using a Student's t-test to compare this activity for all trials in either the Novel or

Repeat conditions to the average firing rate during a baseline period of 800 ms preceding stimulus onset. For trials where the monkey's looking time was less than 600 ms, the firing rate after the monkey's scan path left the picture boundary was not included when calculating the average firing rate. Neurons passing the criteria of significance to $p < 0.05$ for the trials in each condition were designated as visually-responsive for that condition. To designate neurons as differentially-responsive, the same 500 ms time period was used to calculate average firing rate for each trial; a Student's t-test was used to determine whether the firing rates across trials of the Novel condition were significantly different from firing rates across trials of the Repeat condition for each neuron. A Gaussian kernel with a standard deviation of 100 ms was used to smooth neuronal firing rates for visualization purposes in Figures 2.4 and 2.5.

To quantify recognition memory performance and firing rate modulations on a trial-by-trial basis, for each session, all stimuli for which the looking times were at least 600 ms for the Novel presentation were sorted in terms of increasing percent change in looking time between the Novel and Repeat presentations (recognition memory performance). Bins of 30 stimuli each were defined, starting with the first 30 stimuli in the progression. Each subsequent bin overlapped with the previous bin by 20 stimuli, and included the next 10 stimuli (Figure 2.2A). For each neuron, within each bin of 30 stimuli, average firing rates were calculated for the Novel and Repeat presentations (using the time period 100-600 ms after stimulus onset), and were normalized by dividing by the baseline firing rate of the neuron (the 800 ms preceding stimulus onset). The average firing rate for Repeat trials was subtracted from the average firing rate for Novel trials to obtain a difference; the absolute value of this difference was then taken, giving a

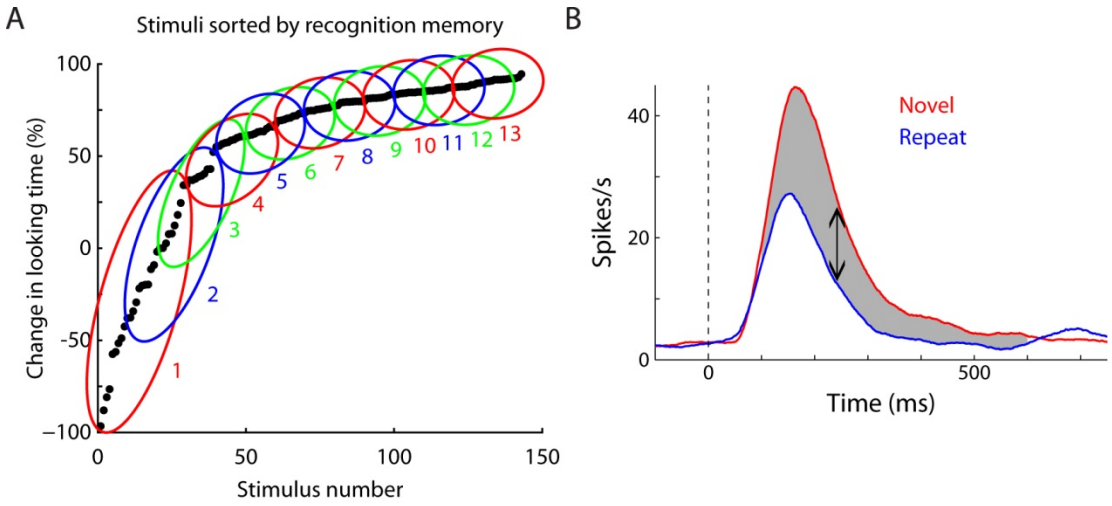

Figure 2.2: Analysis of trial-by-trial correlations between firing rate modulation and recognition memory. (A) Points represent stimuli from a sample recording session, sorted from lowest to highest recognition memory (i.e., most negative to most positive percent change in looking time). The designation of bins is represented by colored circles drawn to encompass 30 stimuli each. (B) Firing rates for Novel (red) and Repeat (blue) trials for a sample neuron, illustrating the calculation of the "firing rate difference": the difference between the firing rates for the two conditions during the time period covered by the gray shaded area (100-600 ms after stimulus onset). This difference was calculated separately for each bin of stimuli as represented in (A).

"firing rate difference" value for each neuron, and each bin (Figure 2.2B). This was done to include cells whose firing rates increased and those whose firing rates decreased between subsequent stimulus presentations. For each bin of stimuli, the average memory performance (percent change in looking time) was also calculated across the stimuli in that bin. Finally, the correlation between memory performance and firing rate difference was calculated across all neurons and all bins. To visually represent this correlation, the "firing rate difference" data were further distributed into 10 bins, based on the memory performance value of each data point. For each bin of data points, the average firing rate difference and memory performance value were calculated. In addition, we constructed a

histogram of correlation coefficients for all neurons and determined whether this population deviated significantly from a zero median population using a sign test.

Stimuli were repeated with varying numbers of intervening trials; thus, it was also possible to measure the degree to which firing rate modulations varied with increasing lag intervals between presentations. To determine whether firing rate modulations were influenced by the delay between successive stimulus presentations, stimuli were divided into three categories: those with no intervening stimuli between presentations (Lag 0), those with one to three intervening stimuli (Lag 1-3), and those with four to eight intervening stimuli (Lag 4-8). Firing rates for Novel and Repeat trials were then calculated for each differentially-responsive neuron, for the 15% of stimuli in each category for which the monkey showed the best subsequent recognition memory (High Recognition) and the 15% of stimuli for which the monkey showed the worst subsequent recognition memory (Low Recognition). The firing rate difference for each condition, in each category, was then calculated as described above, using the 100-600 ms period after stimulus onset and normalized to the baseline firing rate.

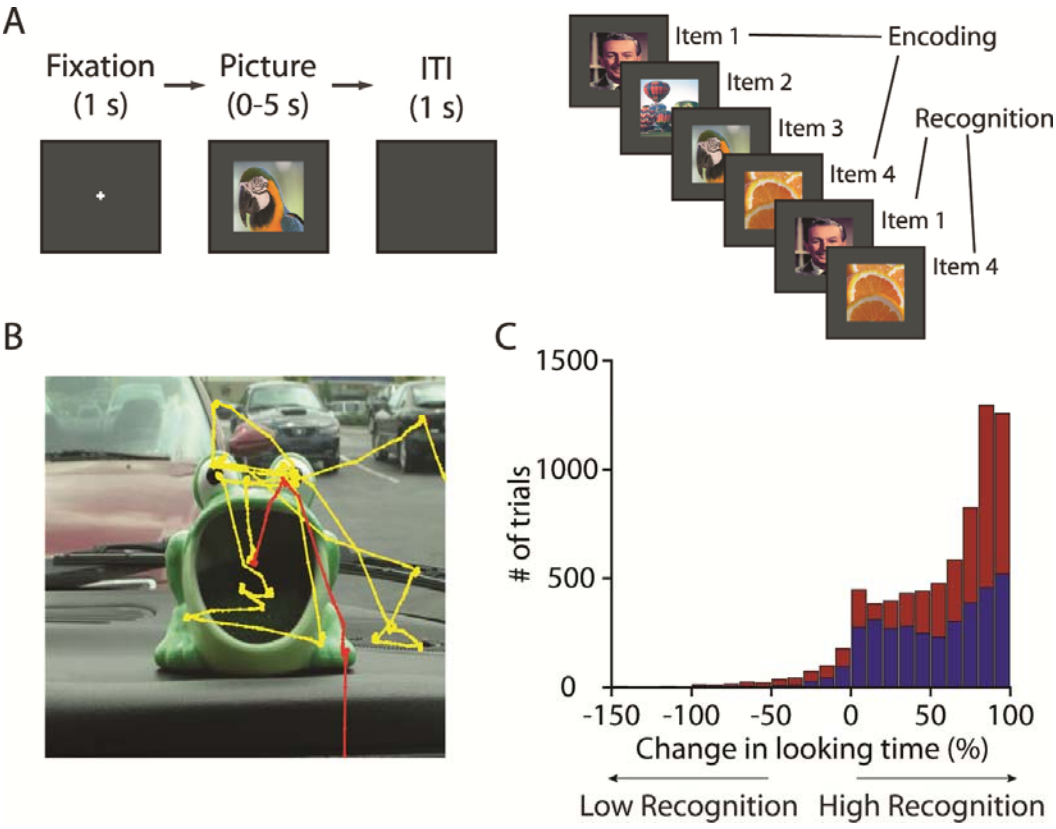

Figure 2.3: Visual Preferential Looking Task and performance. (A) VPLT design. Two-hundred novel stimuli were presented in each test session, with up to 8 trials intervening between the first and second presentations. Each trial began with a required 1 second fixation period and trials were separated by a 1 second intertrial interval. (B) An example of the monkey's scan path over the first (yellow) and second (red) presentations of a stimulus. The monkey spent much less time viewing the stimulus in the second presentation. (C) Combined behavioral data from 45 test sessions in two monkeys. Histogram depicts the change in looking time for all stimuli as a percentage of the amount of time the monkey spent looking at the first presentation of each stimulus (blue: Monkey A; red: Monkey B). A positive change represents stimuli for which looking times were longer during the first presentation. For clarity, trials with a percent change in looking time of less than -150% are not shown (these represented a total of 5 trials, or 0.2 trials per session, for Monkey A and 22 trials, or 1.1 trials per session, for Monkey B).

Results

Behavioral Results

We recorded extracellular spikes from hippocampal neurons in two rhesus monkeys performing the VPLT (Figure 2.3A). Each recording session, monkeys were presented with large (11°) complex visual stimuli, one at a time, on a computer screen. Two hundred novel stimuli were each presented twice during a given session, with up to 8 intervening stimuli between successive presentations. Each stimulus remained on the screen until the monkey's gaze moved off the stimulus or for a maximum of 5 seconds. In this way, the monkey controlled the duration of stimulus presentation, and this duration provided a measure of the monkey's stimulus preference. We compared the amount of time the monkey spent looking at each stimulus during its first (Novel) and second (Repeat) presentation. Adult monkeys show a strong preference for novelty; therefore, a significant reduction in looking time from the first to the second presentation of a stimulus indicated that the monkey had formed a memory of the stimulus[56]. Figure 2.3B depicts an example of the monkey's eye movements during the first (yellow trace) and second (red trace) presentations of a stimulus. In this example, and across the majority of stimuli, the monkeys spent significantly more time looking at the stimulus when it was novel compared to when it was repeated ($p < 0.001$**;** average looking times for Novel and Repeat trials were 2.7 s and 0.8 s, respectively). To control for varying interest in individual stimuli, recognition memory performance was calculated as the absolute change in looking time between presentations as a percentage of the amount of time the monkey spent looking at the first presentation of each stimulus. Across 45 sessions, the monkeys demonstrated robust recognition memory performance. There was

a significant ($p < 0.001$) decrease in looking time for the repeated presentation (average looking times for Novel and Repeat trials were 2.3 s and 0.8 s, respectively). The median reduction in looking time was 70.7% (67.3% in Monkey A and 72.8% in Monkey B). Figure 2.3C shows the distribution of the change in looking time across presentations of each stimulus for both monkeys.

Pictures were repeated with a variable number of intervening stimuli (see Methods for details), which allowed us to analyze the degree to which performance varied with increasing delays. There was a significant relationship between the change in looking time and number of intervening stimuli (Kruskal-Wallis test, $F[8,5848] = 36.48$, $p < 0.01$). As the number of intervening stimuli increased, the median change in looking time became more negative. This effect was driven by trials in which stimuli were repeated without an intervening stimulus, which made up 33% of all trials presented to both monkeys. After removing these trials, there was no significant relationship between

Total hippocampal single units recorded: 131				
	Novel only	Repeat only	Both	Total
Visually responsive single units	21 (**25%**)	15 (**18%**)	48 (**57%**)	84
Increase in firing rate	5 (24%)	4 (27%)	21 (44%)	30 (**36%**)
Decrease in firing rate	16 (76%)	11 (73**%**)	27 (56%)	54 (**64%**)

Table 2.1: Single unit response properties. Stimulus response properties of all single units showing significant differences in firing rate between baseline and the 100-600 ms period after stimulus onset ($p \leq 0.05$). Percentages in bold are based on the total number of responsive single units; all other percentages calculated from the total number of single units in response category: Novel, Repeat, or Both.

behavior and number of intervening stimuli (F[7,3884] = 9.16, $p > 0.1$). This is consistent with previous findings that control monkeys show very little forgetting in this task across increasing delays[31,33]. When we excluded stimuli that repeated without an intervening stimulus, the population effects for neuronal activity (reported below) remained the same.

Hippocampal neurons modulate their firing rate with stimulus repetition

We recorded from 131 hippocampal neurons in two monkeys performing the VPLT. For each neuron, the average firing rate across all 200 stimuli was calculated for each of two conditions: Novel and Repeat. The primary response pattern of each neuron (i.e. the directionality and condition specificity) was assessed by analyzing the time period from

Total differentially-responsive single units: 30	Novelty Responses	Familiarity Responses
Enhanced	7 (**23%**)	4 (**13%**)
Baseline firing rate (spk/s)	6.0 ± 3.0	6.0 ± 3.6
Response latency (ms)	134.6 ± 58.8	283.5 ± 135.2
Depressed	10 (**33%**)	9 (**30%**)
Baseline firing rate (spk/s)	6.6 ± 1.2	8.7 ± 3.4
Response latency (ms)	96.0 ± 21.1	162.1 ± 28.8

Table 2.2: Differentially-responsive single unit properties. Numbers of Enhanced and Depressed neurons, further divided into those that gave Novelty responses (higher firing rate for Novel stimuli) and those that gave Familiarity responses (higher firing rate for Repeat stimuli). Percentages in bold are based on the total number of differentially-responsive single units. Measures for average baseline firing rate and response latency for each category are presented ± SEM.

100-600 ms after stimulus presentation. This duration was chosen to encompass the major part of each visually-responsive neuron's deviation from baseline firing rate. Eighty-eight neurons (67%) were visually responsive, in that they demonstrated a significant change in firing rate during stimulus presentation compared to baseline during either or both presentations (Table 2.1). The majority (63%) of these neurons exhibited a decrease in firing rate upon stimulus presentation. There were no significant differences between neurons with enhanced firing rates and those with depressed firing rates in either response latency (131 ± 27 ms and 152 ± 11 ms, respectively; Student's *t*-test, $p > 0.1$) or baseline firing rate (7.63 ± 1.30 spk/s and 7.45 ± 0.97 spk/s, respectively; $p > 0.1$). Each stimulus was presented exactly twice, once as Novel and once as a Repeat. Because a minimum of 20-30 trials are necessary to obtain a reliable measure of firing rate, the experimental design did not allow for an analysis of stimulus specificity. The neuronal effects we describe are averaged across different visual stimuli.

The degree to which the novelty of visual stimuli influenced the activity of hippocampal neurons was measured by analyzing the difference in firing rate across the two conditions (Novel vs. Repeat). The firing rates of thirty visually-responsive units (36%) were significantly modulated by stimulus novelty. These differentially-responsive cells fell into four categories, depending on whether their firing rates were enhanced or depressed upon stimulus onset, and whether firing rates were higher for Novel stimuli (Novelty responses) or for Repeat stimuli (Familiarity responses) (Table 2.2). Baseline firing rates were not significantly different between Novelty response cells (6.3 ± 1.4

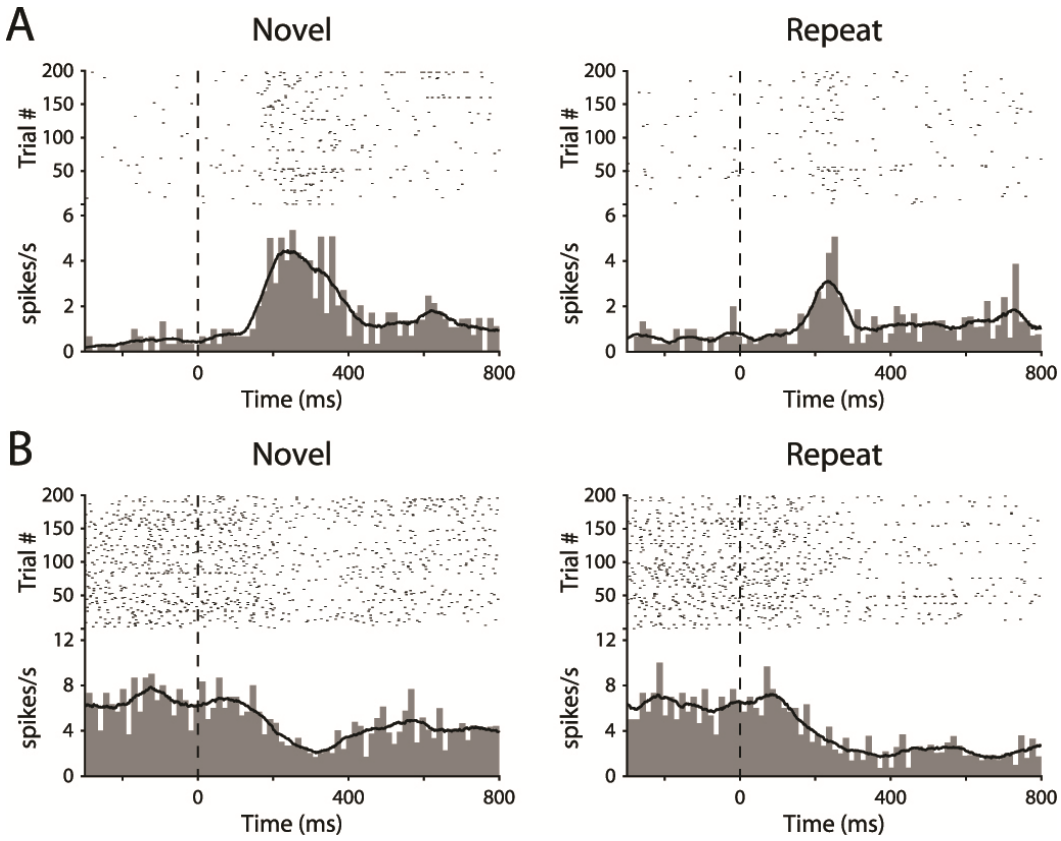

Figure 2.4: Example differentially-responsive single units. Raster plots, peristimulus time histograms, and smoothed firing rates for two example hippocampal neurons. The responses of each neuron are averaged for the 200 stimuli, and are plotted separately for Novel (first presentation) and Repeat (second presentation) stimuli.

spk/s) and Familiarity response cells (7.9 ± 2.5 spk/s; $p > 0.1$). However, there was a trend for Novelty response cells (112 ± 27 ms) to have a shorter response latency than Familiarity response cells (200 ± 45 ms; $p = 0.09$). The responses of two representative differentially-responsive neurons are shown in Figure 2.4. These data suggest that information about the novelty of visual stimuli is represented in the firing rate of hippocampal neurons in monkeys, consistent with recent findings from human epileptic patients[100,178].

One advantage of the VPLT is that it provides for the ability to analyze the strength of recognition memory by considering the magnitude of the change in looking time for each stimulus across presentations. This offers a distinct advantage over many other recognition memory tasks, where performance for each trial can only be rated as correct or incorrect, and after training, the number of incorrect trials is usually so low that it is difficult to relate modulations in neural activity to performance. We hypothesized that changes in the firing rates of differentially responsive neurons would be correlated with memory strength, assessed through performance on the VPLT. To test this, we defined recognition memory strength as the difference in looking times for the Novel and Repeat presentations, normalized to the looking time during the Novel presentation (as per Figure 2.3C). Assuming that this difference in looking time is correlated with the strength of memory encoding, the stimuli with the largest reductions in looking time are those for which the monkey formed the strongest memories. For two example neurons, we calculated the firing rate during both Novel and Repeat presentations for the 30 stimuli for which the monkey showed the best subsequent recognition memory (High Recognition) and the 30 stimuli for which the monkey showed the worst subsequent recognition memory (Low Recognition). Each condition represented approximately 19% of all analyzed trials. The firing rate was increased by stimulus onset for one neuron and was decreased for the other neuron (Figure 2.5). Both of these neurons showed a significant modulation of firing rate by stimulus novelty for the High Recognition trials ($p < 0.05$) but not for the Low Recognition trials ($p > 0.1$).

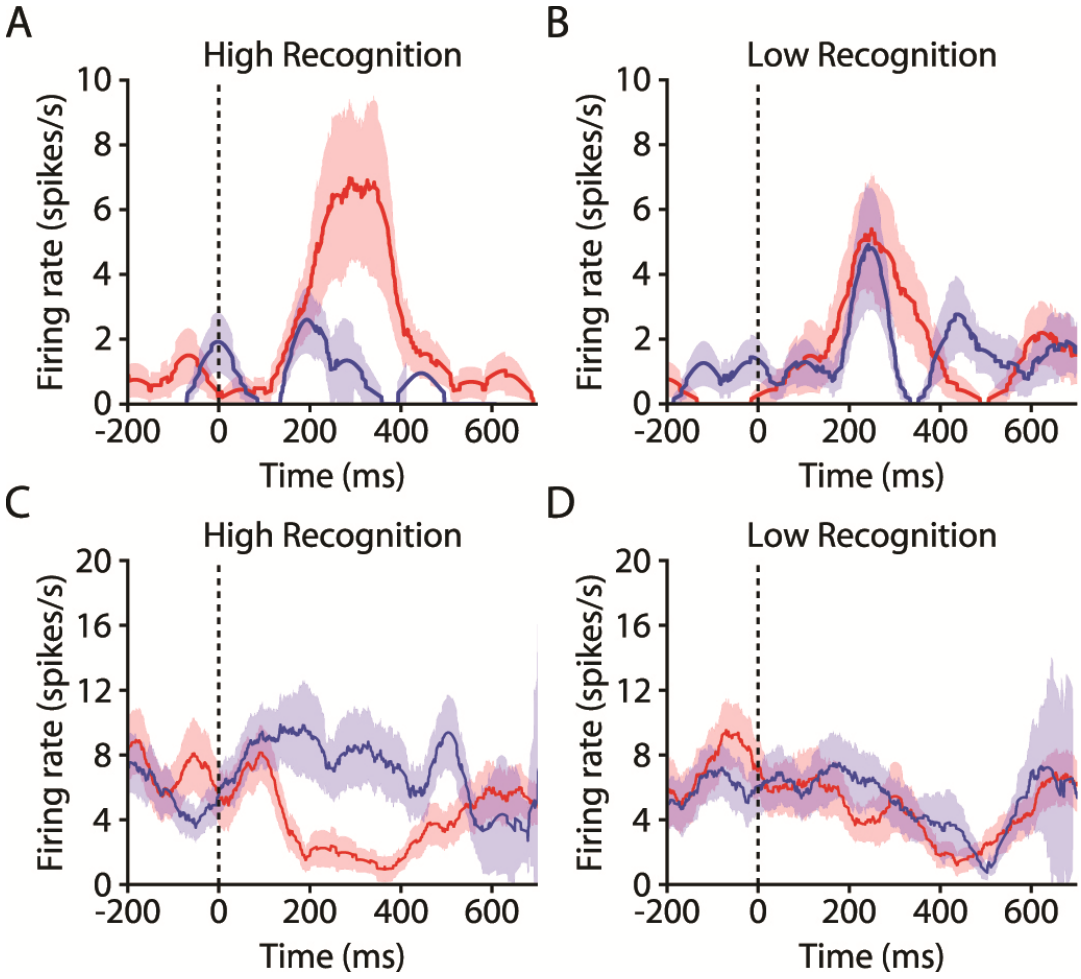

Figure 2.5: Example differentially-responsive single units on High and Low Recognition trials. (A) Firing rates for one enhanced differentially-responsive neuron averaged across Novel (red) and Repeat (blue) presentations, for High Recognition stimuli. (B) Same as (A), but for Low Recognition trials. Red and blue shaded areas represent SEM. Stimulus-evoked firing rates were significantly higher for novel trials versus repeat trials in the High Recognition condition ($p < 0.05$) but not in the Low Recognition condition ($p > 0.1$). (C & D) Same as (A) and (B), but for one depressed differentially-responsive neuron. Stimulus-evoked firing rates were significantly lower for novel trials versus repeat trials in the High Recognition condition ($p < 0.05$) but not in the Low Recognition condition ($p > 0.1$).

Across the population of differentially responsive neurons, we considered whether firing rate changes were correlated with memory performance throughout each recording session, rather than for just the highest and lowest extremes of memory performance (see Methods for details). Briefly, we organized the stimuli from each VPLT session by increasing recognition memory performance (least negative to most negative change in looking time). Stimuli were grouped into bins of 30, and within each bin, we determined average measures for the difference in firing rates between Novel and Repeat trials and memory performance. The Pearson correlation coefficient was calculated across all bins in the session, for each neuron. Figures 2.6A and 2.6B depict the relationship between the magnitude of the firing rate modulation and memory performance for two example neurons. In both cases, firing rate differences between Novel and Repeat trials were positively correlated with recognition memory performance ($p < 0.01$). To examine the effects across the population, these data were further sorted into 10 bins based on memory performance (see Methods for details). Across all differentially-responsive neurons, there was a significant correlation between the magnitude of the firing rate modulation and memory performance ($p < 0.01$; Figure 2.6C). Figure 2.6D shows the distribution of correlation coefficients for the population of differentially-responsive cells, which was significantly greater than zero (sign test, $p < 0.05$).

To determine the relative contribution of enhanced cells and depressed cells to this correlation, we performed the same analysis for each subset of the differentially-responsive cells; the results of this analysis are depicted in Figures 2.7A and 2.7B. The correlation was significant for the enhanced cells ($p < 0.01$; Figure 2.7A), and there was a trend towards significance for the depressed cells ($p = 0.06$; Figure 2.7B). We also

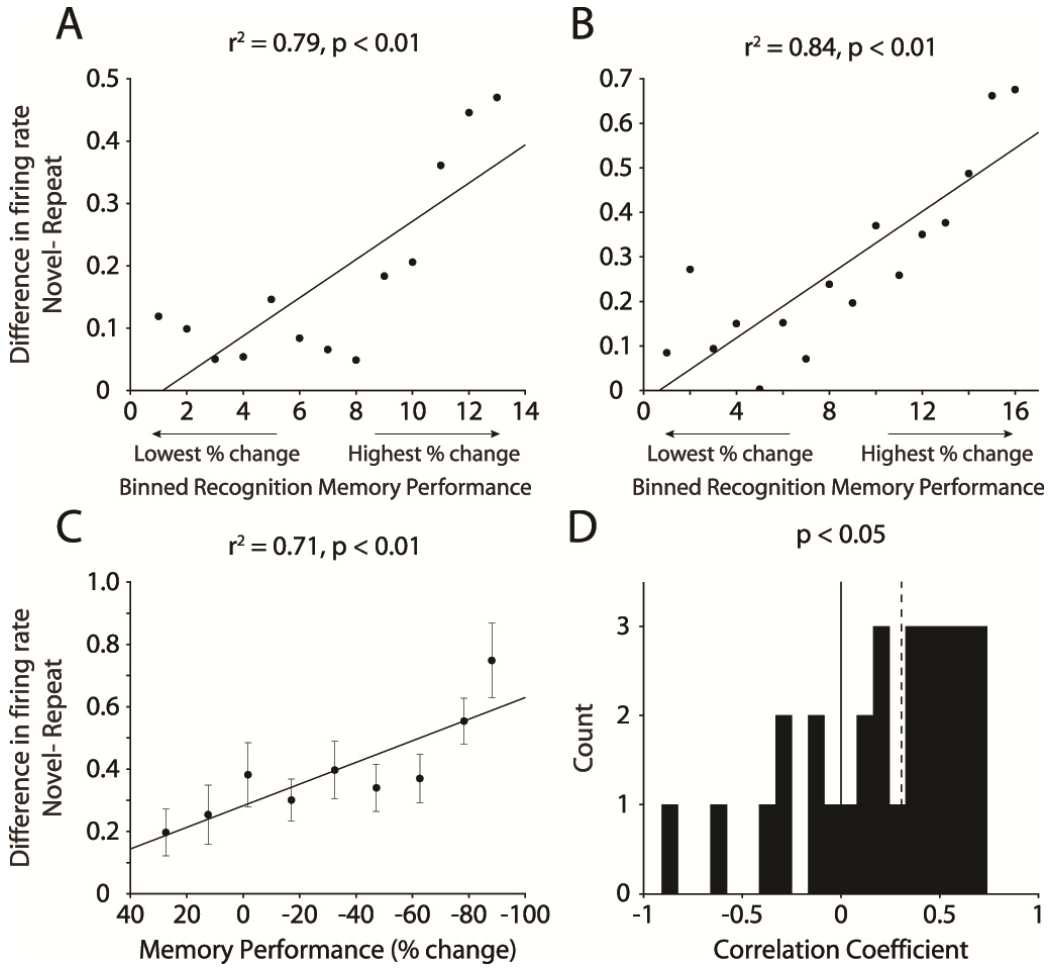

Figure 2.6: Correlation between firing rate modulation and memory performance. (A & B) Difference in firing rates for two sample neurons, across 30-trial bins organized from trials with lowest to highest percent change in looking time between encoding and recognition. Black lines represent linear regression of data points. (C) Difference in firing rates across all differentially-responsive neurons (n = 30), organized from lowest to highest percent change in looking time. Memory performance and firing rate difference were significantly correlated ($p < 0.01$). Error bars represent SEM. Black line represents linear regression of data points. (D) Histogram of correlation coefficients for all differentially responsive cells. The distribution was significantly positive (sign test, $p < 0.05$). Dashed line: median.

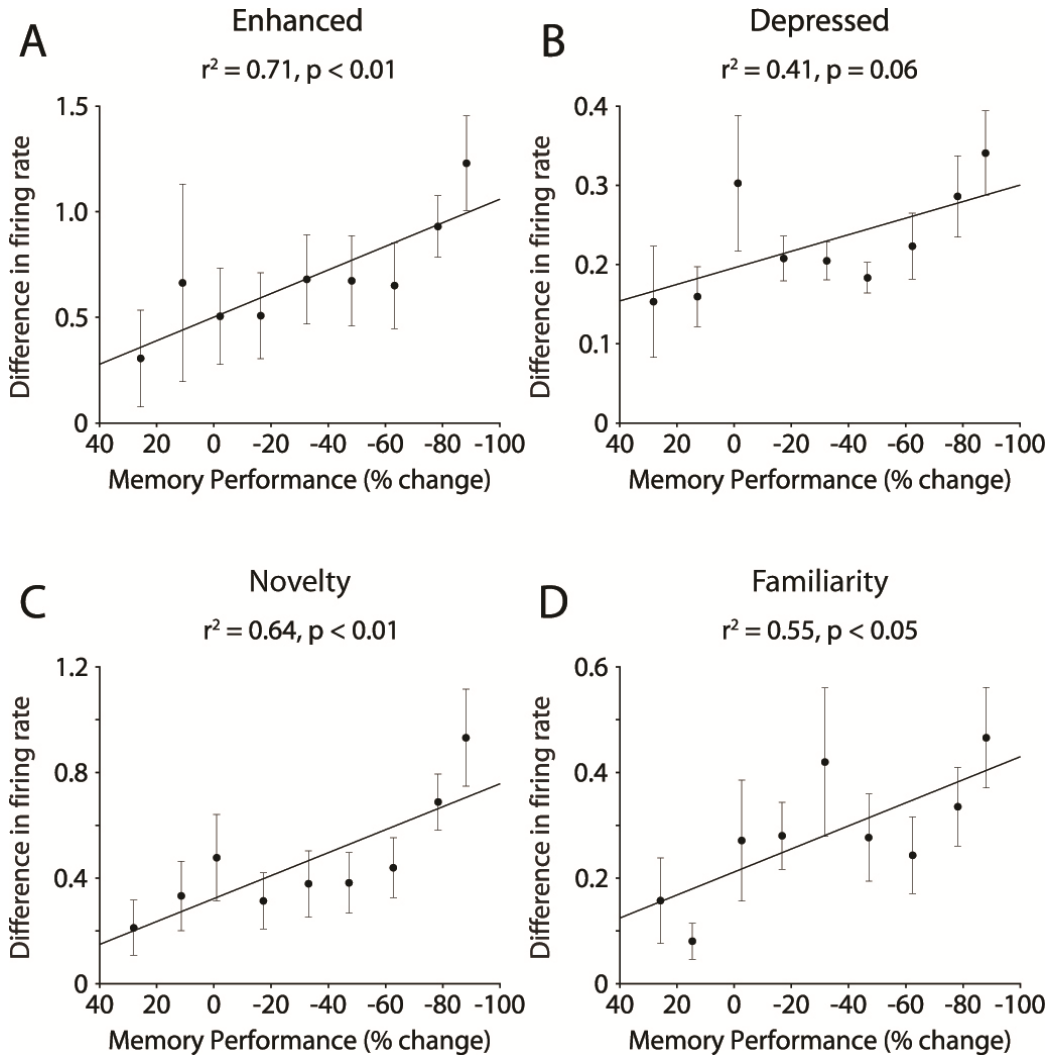

Figure 2.7: Correlation between firing rate modulation and memory performance for neuronal subgroups. (A) Difference in firing rates across all differentially-responsive neurons whose firing rates increased with visual stimulation (*n* = 11), organized from lowest to highest percent change in looking time. Error bars represent SEM. Black line represents linear regression of data points. (B) Same as (A), but for depressed differentially-responsive neurons (n = 19). (C) Same as (A), but for differentially-responsive neurons with Novelty responses (n = 17). (D) Same as (A), but for differentially-responsive neurons with Familiarity responses (n = 13).

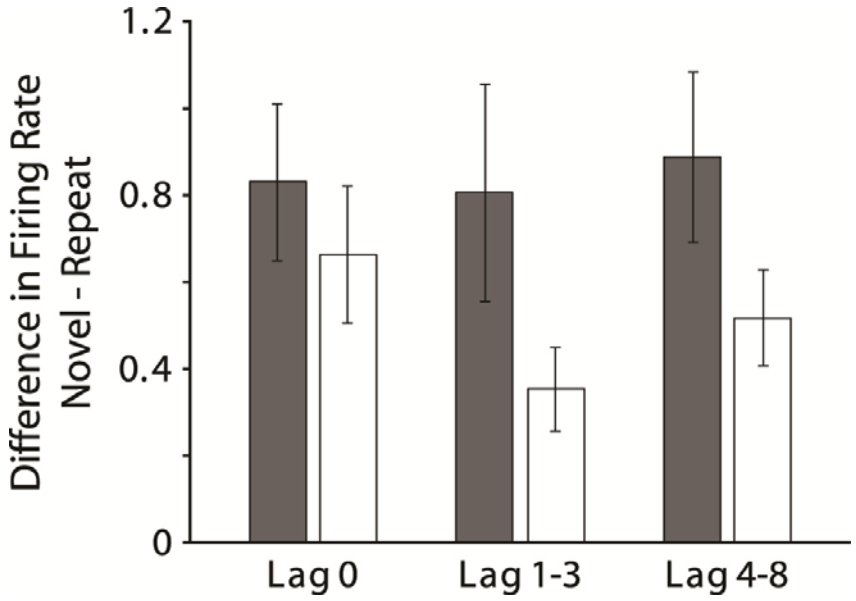

Figure 2.8: Firing rate modulation across lag categories. Average difference in firing rates across differentially-responsive neurons, normalized by baseline firing rate, for stimuli with no intervening trials (Lag 0), stimuli with 1-3 intervening trials (Lag 1-3), and stimuli with 4-8 intervening trials (Lag 4-8). Each bar represents the average firing rate difference for the 15% of trials with the highest recognition memory (gray bars) and the 15% of trials with the lowest recognition memory (white bars) in each lag category.

performed the analysis separately for cells with Novelty responses and cells with Familiarity responses. Both subgroups showed significant correlations between difference in firing rate and memory performance ($p < 0.05$; Figures 2.7C & 2.7D).

The average firing rate modulation across differentially responsive neurons for High and Low Recognition trials, for all three Lag categories is depicted in Figure 2.8. Paired *t*-tests revealed that the firing rate modulation was significantly different for the Lag 1-3 and Lag 4-8 categories ($p < 0.05$), but not for the Lag 0 category ($p > 0.1$). Behavioral performance did not vary across lag categories for High Recognition and Low Recognition trials (repeated-measures two-way ANOVA, no main effect of lag, $F[2,220] = 0.85$, $p > 0.1$).

Discussion

Using a behavioral task that is sensitive to restricted lesions of the hippocampus[30,31,33,42], we found that a substantial proportion of hippocampal neurons differentiate between novel and familiar stimuli through changes in firing rate. Furthermore, modulations in firing rate were correlated with variability in recognition memory performance throughout the session. For individual neurons and across the population of differentially-responsive neurons, there was a significant positive correlation between the magnitude of the modulation by stimulus novelty and performance, such that changes in firing rate for successive presentations of visual stimuli were greater when these stimuli were better remembered. These findings provide evidence that recognition memory performance may be supported by hippocampal activity at the cellular level.

These data stand in contrast to previous studies of recognition memory signals in the monkey hippocampus. These previous studies used either the Konorski conditional delayed matching task[88-90] or the serial recognition task[92,93]. In the Konorski conditional delayed matching task, two stimuli (varying in familiarity to the animal) are presented sequentially with a 0.5 second delay, and monkeys are trained to signal whether the two stimuli are the same or different. Despite the relatively large incidence of neurons in cortical areas surrounding the hippocampus whose firing rates decreased with stimulus repetition, no hippocampal neurons showed alterations in firing rates that reflected whether stimuli were novel or had recently been seen[88,89]. One exception was a study by Wilson et al., which reported that 34% of visually-responsive hippocampal units responded differently during the second stimulus presentation depending on whether or

not it matched the first stimulus presentation[90]. Because these stimuli were already familiar to the monkeys, these signals could reflect neural coding of relative familiarity. However, because the subjects were trained to respond to the right panel for a match and the left panel for a non-match, it is also possible that these responses instead reflected spatial coding[172,179,180]. Other studies used the serial recognition task, in which novel stimuli are presented sequentially, with familiar stimuli intervening at various frequencies. Monkeys are typically trained in a go/no go paradigm, licking a tube when stimuli are familiar in order to obtain fruit juice and refraining from licking when stimuli are novel to avoid the taste of saline. Studies using this task have identified very small numbers (<3%) of hippocampal neurons that alter their firing rates for the novel and repeat stimulus presentations[92,93].

One primary difference between the VPLT and these tasks is the degree of stimulus novelty. In the delayed matching task, images depicting a variety of different geometric shapes were used, and these were of varying familiarity to the animal[88-91]. One study in particular described stimuli as often differing only in terms of size while keeping other attributes the same[90]. In the serial recognition task, many of the stimuli were considered "novel" as long as they were not presented earlier that session. However, the stimuli may have been seen previously, a couple of months[92] or even days[93] prior. In the VPLT, 200 completely novel stimuli were used for each recording session, with a total of 9000 unique stimuli across all sessions. Because we observed changes in firing rate after only a single stimulus presentation in the VPLT, it is possible that recognition of previously seen stimuli affected the results in previous studies.

Recent studies have suggested that the hippocampus plays a role in working memory, i.e., in tasks requiring active maintenance of stimuli[181-183]. The design of the present study allowed us to examine whether the observed modulations in firing rate were related to the number of intervening stimuli between the novel and repeated stimulus presentation. The data revealed that there was no significant relationship overall between the modulation of the neural response for high and low recognition conditions and the number of stimuli intervening between presentation. However, the difference in the firing rate modulation related to memory strength was not significant when stimuli were presented back to back, while this difference was significant when there was at least one intervening stimulus. These data support the idea that the neural signal for recognition memory in the hippocampus is not specifically related to working memory.

The VPLT has also been used extensively in rats, where it is called the Visual Paired Comparison task or the Spontaneous Object Recognition task[34,184] (see Mumby, 2001[185] for review). It has been suggested that the open-field version of this task may not provide a 'pure' assessment of object recognition memory, but may instead assess memory for objects in a specific context[184]. Because the stimuli used in the present study were complex, natural images, it is possible that memory for spatial relational components of the stimuli contributed to the observed modulations in hippocampal neuronal activity. However, it has been shown that hippocampal activity signaling object-context associations often takes many trials to develop[55], while the firing rate changes we see using the VPLT occur after only one presentation. In addition, our results are consistent with previous findings in the human hippocampus[100] where learning-related changes in hippocampal signals were seen after one trial. Importantly,

although the task used in that study included a spatial-relational component, the firing rate modulation in the hippocampus did not depend on performance on that aspect of the task. Taken together, we suggest that these data provide evidence for a recognition memory signal in the hippocampus that is independent of spatial relationships.

Our results are consistent with findings from hippocampal recordings in human epileptic patients for both visual[100,178,186] and verbal memory[187]. Significantly, human hippocampal neurons demonstrate modulations in firing rates after a single presentation for visual stimuli[100,178,186], similar to the present findings in the monkey hippocampus. One study[186], using a task in which subjects were instructed to make an old/new judgement on sequentially-presented pictures, found that 82% of neurons in the human hippocampus were visually responsive. Of these responsive neurons, 18% differentiated between novel and repeated stimuli, with roughly the same number of enhanced and depressed responses. Interestingly, when compared to the responses of MTL cortical neurons in the same study, there was a much higher incidence of depressed responses in the hippocampus (at least 80% of all depressed differentially-responsive neurons were recorded in the hippocampus). Along with our findings, this suggests that this response type plays a relatively more important role in memory processing in the hippocampus than in the MTL cortex. Our results are also consistent with Rutishauser et al.[100], who reported 20% of neurons differentiated between novel and familiar stimuli, with about equal numbers of novelty and familiarity neurons.

Previous studies showed that the firing rates of human hippocampal neurons during the encoding of word pairs predicted recall success[187], and hippocampal activation during encoding (measured using fMRI) has been correlated with subsequent item

memory strength[174]. The robustness of this effect when averaged across many stimuli, in our analysis as well as others[100], suggests that hippocampal neurons may act in some circumstances as "novelty detectors". That is, the firing of hippocampal neurons may not necessarily reflect specific information about the stimulus being viewed, but rather a more general novelty or familiarity signal that is common to all stimuli. By contrast, most previous investigations of neural signals in the perirhinal and entorhinal cortices related to recognition memory have demonstrated significant stimulus-specific firing rate changes related to the repetition of very few stimuli[85-87,94,95]. However, there are exceptions; one study[92], for example, reported that many neurons in the perirhinal and entorhinal cortices in the monkey signaled the relative familiarity of stimuli, without controlling for stimulus specificity. In the present study, because each stimulus was only presented twice, and we did not explicitly control for stimulus content, we were unable to examine stimulus or category specificity. However, the presence of a significant effect of stimulus repetition on the firing rates of hippocampal neurons when responses were averaged across all stimuli is consistent with the idea that the hippocampus provides an "abstract" recognition memory signal[188]. Accordingly, this pattern of activity may support recognition memory by combining stimulus-selective information from the perirhinal and entorhinal cortices with a more general, abstract signal of novelty or familiarity.

In summary, consistent with findings from studies of the effects of lesions of the hippocampus on recognition memory, we found that a substantial number of hippocampal neurons show modulations in firing rate that are significantly correlated with performance on a recognition memory task. These findings support the idea that the

hippocampus plays a significant role in recognition memory and provide evidence for a neural signal that may underlie recognition memory performance.

Chapter 3

Gamma-band synchronization in the macaque hippocampus and memory formation[3]

Introduction

Accumulating evidence suggests that along with changes in the firing rates of individual neurons, the precise timing of neuronal activity may play an important role in cognition. Synchronization of neuronal activity in the gamma-frequency band (30 to 100 Hz) has been related to selective attention[126-129,189,190] and working memory[191]. Additionally, studies of intracranial electroencephalography in epilepsy patients suggest that gamma-band synchronization may be an important component in successful memory encoding[117,142]. By aligning periods of inhibition, gamma-band synchronization establishes precise coordination in the spike times of neurons responding to behaviorally relevant stimuli [122,192]. Gamma-band synchronization among a group of neurons ensures that presynaptic spikes arrive at mutual downstream targets within ~10 ms of each other. Since mutual synaptic input is followed reliably by postsynaptic spikes, this precise

[3] Reproduced with minor edits from original publication: Jutras, M. J., Fries, P. & Buffalo, E. A. Gamma-band synchronization in the macaque hippocampus and memory formation. *J Neurosci* **29**, 12521-12531, (2009).

temporal relationship provides the necessary conditions for long term changes in synaptic strength, which is considered to be one of the primary information storage principles in the brain [109,111]. However, to date, there has been little direct evidence for a relationship between gamma-band synchronization among hippocampal neurons and memory formation.

Recognition memory, the ability to perceive a recently encountered item as familiar, is degraded following damage to the hippocampus in humans and monkeys[33,161], although findings regarding the role of the hippocampus in recognition memory have not always been consistent across laboratories[42,44,45,47]. To add to this controversy, only a very small number of neurons have been reported to display recognition memory signals in the hippocampus proper[88,89,92,93,97] (but see [100]). The apparent inconsistency between the findings from lesion and physiology studies raises doubt about the contribution of the hippocampus to recognition memory.

All of these previous neurophysiological studies examined changes in firing rate that might act as a signal for recognition memory. However, it is possible that recognition signals in the hippocampus may take the form of enhanced neuronal synchronization among groups of neurons. Here, we examined the relationship between neuronal synchronization among hippocampal neurons and recognition memory performance on the Visual Preferential Looking Task in monkeys. This task has been shown to depend upon the integrity of the hippocampus in both monkeys[31,33,42] and humans[30]. We report that hippocampal neurons show gamma-band synchronization during encoding that is positively correlated with subsequent recognition memory performance. These changes in synchronization reflect enhanced interaction among

hippocampal neurons and may provide a mechanism for the synaptic changes necessary for successful memory formation.

Methods

Procedures were carried out in accordance with NIH guidelines and were approved by the Emory University Institutional Animal Care and Use Committee. Neuronal recordings were made in two adult male rhesus monkeys (*Macaca mulatta*), obtained from the breeding colony at the Yerkes National Primate Research Center. Their mean weight at the start of the experiment was 6.8 ± 1.1 kg, and their mean age was 4 years and 5 months. Prior to implantation of recording hardware, monkeys were scanned with magnetic resonance imaging (MRI) to localize the hippocampus and to guide placement of the recording chamber. Using this information, a cilux plastic chamber (Crist Instrument Co., Hagerstown, MD) for recording neural activity, and a titanium post for holding the head were surgically implanted. Post-surgical MRI was performed to localize recording sites.

Behavioral testing procedures

During testing, each monkey sat in a dimly illuminated room, 60 cm from a 19 inch CRT monitor that had a resolution of 800 x 600 pixels and a screen refresh rate of 120 Hz noninterlaced. Eye movements were recorded using a non-invasive infrared eye-tracking system (ISCAN, Burlington, Massachusetts).

Stimuli were presented using experimental control software (CORTEX, http://www.cortex.salk.edu). At the beginning of each recording session, the monkey

performed an eye-position calibration task, which involved holding a touch-sensitive bar while fixating a small (0.3°) gray fixation point, presented on a dark background at various locations on the monitor. The monkey was required to maintain fixation within a 3° window until the fixation point changed to an equiluminant yellow at a randomly chosen time between 500 ms and 1100 ms after fixation onset. The monkey was required to release the touch sensitive bar within 500 ms of the color change for delivery of a drop of applesauce. During this task, the gain and offset of the oculomotor signals were adjusted so that the computed eye position matched targets that were a known distance from the central fixation point.

Visual preferential looking task

Following the calibration task, the monkey was tested on the Visual Preferential Looking Task (VPLT; refer to Figure 2.3A for task design). The monkey initiated each trial by fixating a white cross (1°) at the center of the computer screen. After maintaining fixation on the cross for 1 s, the cross disappeared and the picture stimulus (11°) was presented. The stimulus disappeared when the monkey's direction of gaze moved off the stimulus, or after a maximum looking time of 5 s. Each trial was followed by a 1 s intertrial interval. The VPLT was given in 51 daily blocks of 6, 8, or 10 trials each, chosen pseudorandomly, for a total of 400 trials each day. Each session, monkeys were presented with a total of 200 unique, complex stimuli. Each stimulus was presented twice during a given session, with up to 8 intervening stimuli between successive presentations. A total of 9000 stimuli were used in this study.

Because the monkey controlled the duration of stimulus presentation, the duration of gaze on each stimulus provides a measure of the monkey's preference for the stimulus. We compared the amount of time the monkey spent looking at each stimulus during its first and second presentation. We designated the novel presentation of each stimulus the "encoding" phase and the repeated presentation the "recognition" phase of the task. Adult monkeys show a strong preference for novelty; therefore, a significant reduction in looking time between the two presentations of a stimulus indicated that the monkey had formed a memory of the stimulus and spent less time looking at the now familiar stimulus during its second presentation[56]. To control for varying interest in individual stimuli, recognition memory performance was calculated as the absolute change in looking time between presentations as a percentage of the amount of time the monkey spent looking at the first presentation of each stimulus.

Reward was not delivered during VPLT trials. However, 5 trials of the calibration task were presented between each VPLT block in order to give the monkey a chance to earn some reward and to verify calibration of the eye position. The number of trials in each VPLT block was varied to prevent the monkey from knowing when to expect the rewarded calibration trials.

Electrophysiological recording methods

The recording apparatus consisted of a multi-channel microdrive (FHC Inc., Bowdoin, Maine) holding a manifold consisting of a single 23-gauge guide tube containing 4 independently moveable tungsten microelectrodes (FHC Inc., Bowdoin, Maine), with each electrode inside an individual polyamide tube. Electrode impedance

was in the range of 1-2 MΩ, and electrode tips were separated horizontally by 190 µm. For each recording, the guide tube was slowly lowered through the intact dura mater and advanced to ~3.5 mm dorsal to the hippocampus with the use of coordinates derived from the MRI scans. The electrodes were then slowly advanced out of the guide tube to the hippocampus. No attempt was made to select neurons based on firing pattern. At the end of each recording session, the microelectrodes and guide tube were retracted. All recordings took place in the anterior part of the left hippocampus. Recording sites were located in the CA3 field, dentate gyrus, and subiculum (refer to Figure 2.1 for recording locations).

Data amplification, filtering, and acquisition were performed with a Multichannel Acquisition Processor (MAP) system from Plexon Inc. (Dallas, TX). The neural signal was split to separately extract the spike and the LFP components. For spike recordings, the signals were filtered from 250 Hz – 8 kHz, further amplified and digitized at 40 kHz. A threshold was set interactively, in order to separate spikes from noise, and spike waveforms were stored in a time window from 150 µs before to 700 µs after threshold crossing. Each recording typically yielded 2 to 6 units; single units were sorted offline using Offline Sorter (Plexon, Inc.). For LFP recordings, the signals were filtered with a passband of 0.7-170 Hz, further amplified and digitized at 1 kHz. Eye movement data were digitized and stored with a 240 Hz resolution.

The powerline artifacts were removed from the LFP in the following way: We estimated the amplitude of the powerline fluctuations with a Discrete Fourier Transformation (DFT) of long data segments which contained the data epochs of interest. We then computed the DFT at 60 and 120 Hz. Because the powerline artifact is of a

perfectly constant frequency and amplitude, and because the long data segments contained integer cycles of the artifact frequencies, essentially all the artifact energy is contained in those DFTs. We constructed sine waves with the amplitudes and phases as estimated by the respective DFTs, and subtracted those sine waves from the original long data segments. The epoch of interest was then cut out of the cleaned epoch. Power spectra of the cleaned epochs demonstrated that all artifact energy was eliminated, leaving a notch of a bin width of 0.1 Hz in the monkey recordings. The actual spectral data analysis was performed using the multi-taper method on 0.25 s data epochs, with a spectral smoothing of ±8 Hz. Thus, the original notch became invisible.

Data analysis

All analyses were performed using custom programming in Matlab (The Mathworks, Inc., Natick, MA) and using FieldTrip (http://www.ru.nl/fcdonders/fieldtrip/), an open source Matlab toolbox. To ensure that the monkeys had sufficient time to perceive the stimuli, analyses were limited to pairs of trials (corresponding to the two presentations of each stimulus) in which monkeys examined stimuli for at least 750 ms during the first presentation, which resulted in an average of 135 pairs of trials per session.

For each neuron, firing rate was calculated for the period including pre-stimulus fixation as well as stimulus presentation. Significant responses to stimuli were determined using a Student's t-test to compare activity for the period from 100-500 ms after stimulus onset to a baseline period of 300 ms preceding stimulus onset. Only neurons judged to be visually responsive, i.e., those which displayed a significant mean

firing rate modulation upon the first (encoding) presentation, were included in further analyses.

For the calculation of coherence and power spectra, the multi-taper method was used in order to achieve optimal spectral concentration[128,191,193,194]. Multitaper methods involve the use of multiple data tapers for spectral estimation. A 250 ms segment of data was multiplied by a data taper before Fourier transformation. A variety of tapers can be used, but an optimal family of orthogonal tapers is given by the prolate spheroidal functions or Slepian functions. For time length T and bandwidth frequency W, up to K=2TW-1 tapers are concentrated in frequency and suitable for use in spectral estimation. We used three Slepian tapers, providing an effective taper smoothing of ±8 Hz. For each taper, the data segment was multiplied with that taper and Fourier transformed, giving the windowed Fourier transform, $\tilde{x}_k(f)$:

$$\tilde{x}_k(f) = \sum_1^N w_k(t) x_t e^{-2\pi i f t}$$

where x_t, $(t = 1,2,..., N)$ is the time series of the signal under consideration and $w_k(t)$, $(k = 1,2,..., K)$ are K orthogonal taper functions. For spike signals, the firing rate was represented with a bin width of one millisecond and then subjected to spectral analysis like LFPs.

The multitaper estimates for the spectrum $S_x(f)$ and the cross-spectrum $S_{yx}(f)$ are given by the following:

$$S_x(f) = \frac{1}{K} \sum_1^K \left| \tilde{x}_k(f) \right|^2$$

$$S_{yx}(f) = \frac{1}{K} \sum_1^K \tilde{y}_k(f) \tilde{x}_k^*(f)$$

Spectra and cross-spectra are averaged over trials before calculating the coherency $C_{yx}(f)$ as follows:

$$C_{yx}(f) = \frac{S_{yx}(f)}{\sqrt{S_x(f)S_y(f)}}$$

Coherency is a complex quantity. Its absolute value is termed coherence and ranges from 0 to 1. A coherence value of 1 indicates that the two signals have a constant phase relationship (and amplitude covariation), a value of 0 indicates the absence of any phase relationship. Thus, coherence is a measure of linear predictability that captures phase and amplitude correlations.

Coherence spectra were calculated between the spiking activity obtained on one electrode and LFP activity derived from a different electrode. Both coherence and power analyses were limited to LFPs derived from electrodes that also had isolated single units in order to ensure that LFPs were obtained from cell layers. We did not calculate coherence between LFPs and spiking activity obtained on the same electrode. This gave us a maximum of 3 spike-LFP coherence spectra for each neuron. Spike-spike coherence spectra were also calculated between visually-responsive neurons recorded within the same recording session, using the same methods described above for the calculation of coherence spectra between spiking activity and LFP activity.

Spike-field coherence (SFC) typically increased relative to baseline within the first 500 ms of stimulus onset, and SFC for each neuron-LFP pair tended to cluster in either the low gamma (30-60 Hz) or high gamma (60-100 Hz) range. Neurons were thus designated either “low gamma” or “high gamma” based on the peak value of the mean coherence between the neuron and the LFPs measured on all other electrodes in the same

recording session across all encoding trials. Neurons whose peak coherence was below 60 Hz were designated "low gamma" (n = 43); neurons with coherence above 60 Hz were designated "high gamma" (n = 43).

Correlating neuronal activity with memory performance

Two methods were used to determine the relationship between neuronal activity and subsequent recognition memory performance. First, neuronal activity during encoding was compared for the stimuli that evoked the best and worst memory. The stimuli from each session were ranked in order of increasing recognition performance, quantified as the percent change in looking time between first and second presentations for each stimulus. The 30 encoding trials with the lowest percent change were designated "Low Recognition" and the 30 trials with the highest percent change were designated "High Recognition". After removing trials for which the looking time during the first stimulus presentation was 750 ms or less, 30 trials represented a median of 22.2% of all trials in the session. Comparisons between the two stimulus groups were made for neuronal firing rates, the evoked LFP response, spike and LFP power, spike-field coherence (SFC), and spike-spike coherence (SSC).

Neuronal firing rate. Each neuron's visual response magnitude was calculated across both groups of 30 trials from 100-500 ms after stimulus onset, expressed as a percentage of the baseline firing rate (such that a decrease in firing rate at stimulus onset assumed a negative value, and an increase in firing rate assumed a positive value). The absolute value of each neuron's percent change value was used to enable grouping of neurons with enhanced and depressed responses in the same analysis. Finally, a

Student's t-test was used to determine whether the magnitude of the visual response was significantly different for High and Low Recognition trials across the population.

Evoked LFP. To compare stimulus-evoked LFPs across the two conditions, we calculated an average LFP across all LFPs time-locked to stimulus onset, for High Recognition and Low Recognition trials. We then divided these signals into 10 ms bins and, using a Student's t-test, obtained a p-value for each bin. This allowed us to determine time points at which the two signals diverged significantly.

Spike and LFP spectra. Power spectra were calculated for each spike signal and all LFPs derived from electrodes that also had isolated single units, using the multi-taper method (see details above). For spike spectra, neurons with enhanced firing rate responses to stimulus onset were analyzed separately from neurons with depressed firing rate responses. Correlations between spectra and recognition memory were tested using a nonparametric permutation test (see details below).

Spike-field coherence. In order to compare the average SFC across all neuron-LFP pairs during encoding of High Recognition and Low Recognition conditions, the frequency range within the 30-100 Hz gamma-band for which each neuron-LFP pair showed the highest SFC at 100-400 ms after stimulus onset across all encoding trials was identified (average frequency window size was 21.4 ± 0.7 Hz). SFC was calculated within this frequency window across all High Recognition and Low Recognition trials, separately for each pair. Then, these values were averaged across all neuron-LFP pairs.

To test for statistical significance of differences between spectra during the High Recognition and Low Recognition conditions, we performed a nonparametric permutation test, with the median difference between conditions as our test statistic. The

test involves a comparison of the observed difference against a reference distribution of differences under the null hypothesis of no significant modulation of the spike or LFP power or SFC at individual frequencies between conditions. The reference distribution was obtained by performing the following procedure 10,000 times. For each recording site (or pairs of sites), a random decision was made to which condition the data from either condition was assigned. We then calculated the test statistic at each frequency for these randomly assigned conditions and stored only the minimal and maximal difference across frequencies. From the resulting distribution of 10,000 minimal and maximal differences, we determined the 2.5th and the 97.5th percentile. The empirically observed, nonrandomized difference at a particular frequency was considered statistically significant ($p < 0.05$), when it was larger than the 97.5th or smaller than the 2.5th percentile of the reference distribution. This procedure corresponds to a two-sided test with a global false positive rate of 5% and correction for the multiple comparisons across frequencies[195,196]. We used this non-parametric permutation approach, because 1) it is free of assumptions about the underlying distributions 2) it is not affected by partial dependence among the time-frequency tiles 3) it allows for correction for multiple comparisons without additional assumptions.

Along with single-unit activity, we also applied the non-parametric permutation test to the SFC calculated from multi-unit activity (MUA). During extracellular recording, we obtained spike waveforms simultaneously from 1-3 neurons per electrode, which gave us a total of 75 MUAs. After calculating SFC during encoding for all MUA-LFP pairs, each MUA was designated either “low gamma” or “high gamma” based on the peak value of the mean coherence between the MUA and the LFPs measured on all other

electrodes in the same recording session across all encoding trials. MUAs whose peak coherence was below 60 Hz were designated "low gamma" (n = 34); MUAs with coherence above 60 Hz were designated "high gamma" (n = 41).

Additionally, we identified neuron-LFP pairs showing significant gamma-band coherence using the following method. To test the significance of coherence values, we calculated the time-averaged coherence across the time period of 100-400 ms after stimulus onset for each pair, then transformed these values to Z-scores using the following formula:

$$Z = \operatorname{arctanh}\left(\sqrt{C}\right) \times \sqrt{2L}$$

where C is the coherence value and L is the number of independent estimates[197,198]. Z-transformed coherence values were thus calculated for each neuron-LFP pair, across all high recognition trials (novel presentations of the 30 stimuli from each session for which the monkey subsequently showed the best recognition). We considered a pair to have significant spike-field coherence if this Z-transformed gamma-band coherence value was greater than 2 for at least 5 consecutive frequency values (spanning 16.6 Hz).

Spike-spike coherence. Our methods for analyzing the relationship between SSC for visually-responsive neuron pairs and behavior are identical to the analyses applied to SFC data, as described above. Specifically, the Z-transformed coherence values were used to determine neuron-neuron pairs with significant gamma-band coherence, and the nonparametric permutation test described above was used to determine whether spike-spike coherence was significantly correlated with memory performance.

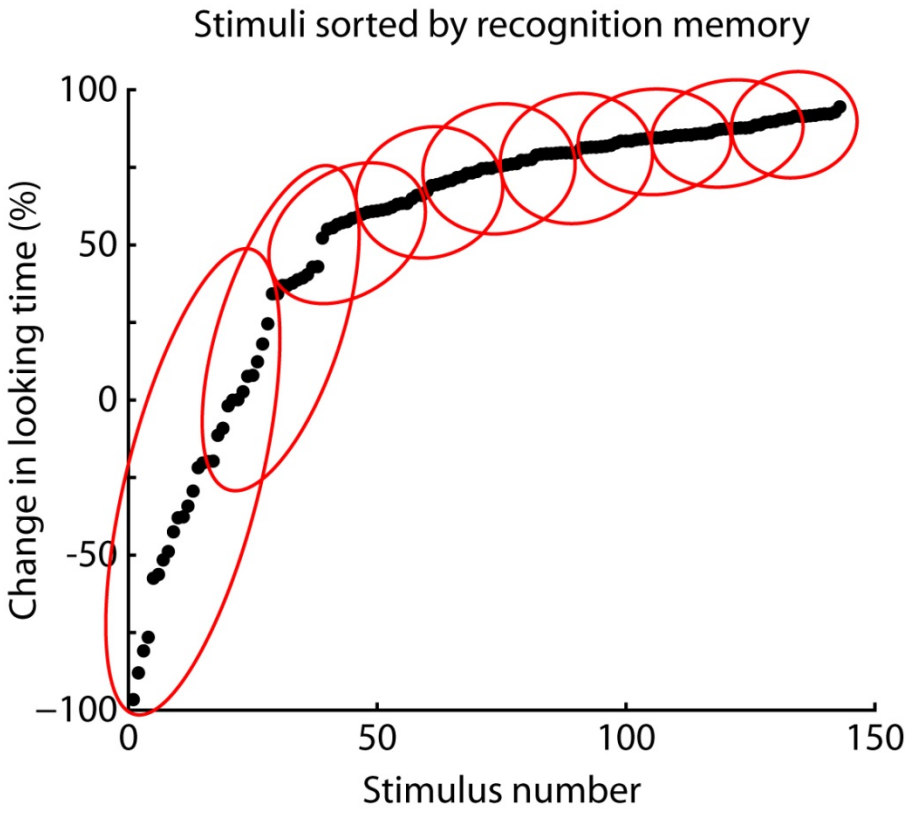

Figure 3.1: Binning analysis of correlation between recognition memory and spike-field coherence. Points represent stimuli from a sample recording session, sorted from lowest to highest recognition memory (i.e., most negative to most positive percent change in looking time). The designation of bins is represented by red circles drawn to encompass 30 stimuli each. Spike-field coherence was calculated for the Novel presentation of all stimuli within each bin and averaged across stimuli to obtain a coherence value for each bin (see Methods).

Correlations with memory and attention: binning analysis

The second analysis we performed to determine the relationship between neuronal activity and performance considered correlations on a trial-by-trial basis. For each recording session, encoding trials were sorted in two ways: in terms of increasing percent change in looking time between the encoding trial and the subsequent repetition of the stimulus (recognition memory performance), and in terms of total looking time for the encoding trial (attention). For each measure, 10 bins of 30 trials each were defined, with

bin centers spaced at equivalent intervals. An equal number of trials per bin was used to avoid sample size biases. As a consequence, in some cases, this resulted in slightly overlapping bins and a few trials that were not included in any bin (Figure 3.1). For each neuron-LFP pair, the frequency range for which the pair showed the highest SFC at 100-400 ms after stimulus onset across all encoding trials was identified, and then the SFC in that frequency range at 100-400 ms was calculated, separately for each bin, across the 30 trials in each bin. Finally, the correlation between the 10 bins of each task parameter value (either recognition memory performance or attention) and coherence during encoding was calculated. Across pairs of recording sites, this resulted in a population of correlation coefficients and slopes for each measure. A sign test was performed on each distribution to determine statistical significance.

For the stimulus-evoked LFP, this analysis was performed in the way described above with one difference: for each bin of trials, we averaged the LFP amplitude from 270-570 ms after stimulus onset for novel trials (the time during which there was a significant difference in the LFP amplitude between High Recognition and Low Recognition trials across all recorded LFPs). The slope and the correlation coefficient were calculated for this trial-averaged LFP amplitude across all bins, separately for each LFP. A sign test was then performed on each distribution of slopes and correlation coefficients.

Correlations with time within session: binning analysis

In order to determine possible changes in behavior or neuronal activity that may have occurred within the session, for each recording session, all 200 stimuli were

organized into the order in which they were presented within each session. Ten bins of 20 stimuli each were then defined, and five measures were calculated for each bin: the mean percent change in looking time from the first to the second presentation (recognition memory performance); the absolute looking time during novel stimulus presentation; the firing rate modulation, defined as the absolute value of the change in firing rate from the 300 ms preceding stimulus onset to the time period 100-500 ms after stimulus onset; gamma-band SFC from 100-400 ms after stimulus onset, using the same frequency window as that used in the binning analysis described above; and LFP amplitude averaged over the time period of 270-570 ms after stimulus onset for each novel stimulus presentation.

Results

Behavioral results

Figure 2.2B depicts an example of the monkey's eye movements during the first (yellow trace) and second (red trace) presentations of a stimulus in the VPLT. In this example, and across the majority of trials, the monkey spent more time looking at a stimulus when it was novel compared to when it was repeated. Across 45 sessions, the monkeys demonstrated robust recognition memory performance. There was a significant ($p < 0.001$) decrease in looking time for the repeated presentation (average looking times for Novel and Repeat trials were 2.7 s and 0.8 s, respectively). The median reduction in looking time was 70.7% (67.3% in Monkey A and 72.8% in Monkey B) (Figure 2.3C).

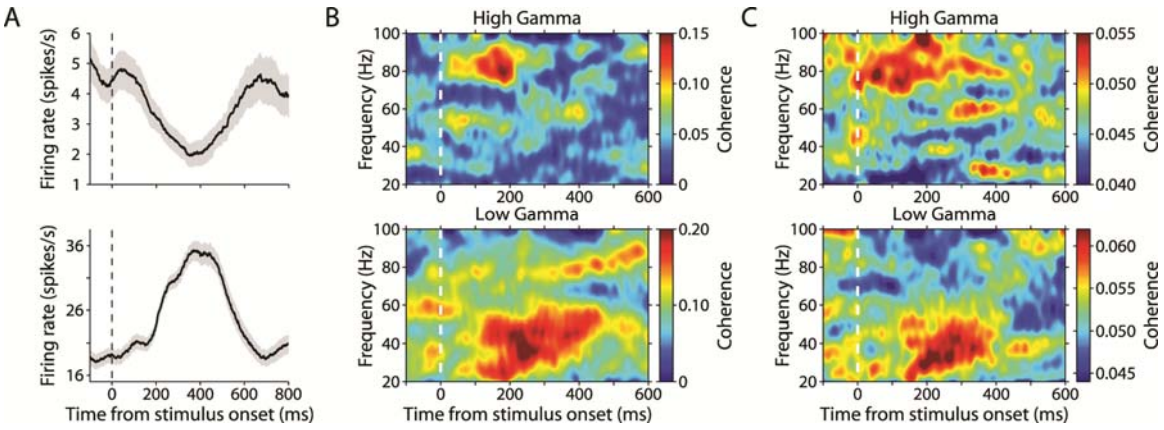

Figure 3.2: Firing Rate and Spike-Field Coherence During Stimulus Encoding. (A) Average firing rates for two example hippocampal neurons during encoding. Shaded areas represent SEM. (B) Spike-field coherence as a function of time (X-Axis) and frequency (Y-Axis) during all encoding trials for the two example neurons shown in (A); coherence was calculated between the neuron on one electrode and the LFP recorded on a separate electrode. (C) Coherence as a function of time and frequency averaged across all encoding trials for high gamma (top) and low gamma (bottom) neurons.

Neuronal activity in the hippocampus

We recorded spikes from 131 isolated single neurons (67 in Monkey A and 64 in Monkey B, respectively) as well as local field potentials (LFPs) in the hippocampal formation in two rhesus monkeys performing the VPLT. Eighty-six neurons (66%) gave a significant response to the first (encoding) presentation of stimuli, with either enhanced (34 neurons) or depressed (52 neurons) responses as compared to baseline (Figure 3.2A; Table 3.1). Consistent with recent findings from human epilepsy patients[100], a substantial proportion of these visually-responsive units (36%) showed a modulation in firing rate based on stimulus novelty.

Neuronal synchronization during the encoding phase of the task was assessed by calculating SFC between each visually-responsive neuron and the LFP recorded simultaneously on a separate electrode (n = 175 neuron-LFP pairs). The LFP results from the extracellular current flow that corresponds primarily to the summed postsynaptic potentials from the dendritic fields of local cell groups[199]. Thus, SFC is a measure of linear predictability that captures phase and amplitude correlations between neuronal input (LFP) and output (spiking activity). SFC typically increased upon visual stimulation, and these increases were most prominent in the 1-8 Hz range (delta/theta-band), and the 30-100 Hz range (gamma-band). Coherence below 20 Hz was not significantly modulated by recognition memory performance on the VPLT. Accordingly, we have confined our analysis and discussion to neuronal synchronization in the gamma band.

Across the population gamma-band SFC tended to cluster in one of two frequency

	Low gamma SFC (30-60 Hz)	High gamma SFC (60-100 Hz)	Total
Firing enhanced by stimuli	20 (58.8%)	14 (41.2%)	34 (**39.5%**)
Firing depressed by stimuli	23 (44.2 %)	29 (55.8%)	52 (**60.5%**)
Total	43 (**50.0%**)	43 (**50.0%**)	**86**

Table 3.1: Neuronal firing and SFC properties. Visually responsive neurons categorized by response properties (enhanced/depressed by stimuli) and frequency of peak gamma-band SFC (high/low). Percentages in bold indicate percentage of total number of cells (n = 86). Other percentages indicate percentage of total cells in corresponding column.

bands: low gamma (30-60 Hz, Figures 3.2B and 3.2C, bottom) and high gamma (60-100 Hz, Figures 3.2B and 3.2C, top). Out of 86 neurons, 42 displayed a range of coherence which included coherence in the 60 Hz band. However, not all those neurons necessarily showed coherence centered around 60 Hz: 20 neurons displayed a band of increased coherence with 60 Hz as either the upper or lower limit, and thus had a substantial portion of increased coherence either above or below 60 Hz. Of the remaining 22 neurons, only 4 showed peak coherence at 60 Hz. For these neurons, we designated each as high or low gamma based on the entire frequency band in which the neuron showed coherence during encoding trials, and whether the bulk of this frequency band lay above or below 60 Hz. Using this method, 3 neurons were designated as high gamma and 1 was designated as low gamma. There was no significant relationship between the peak frequency of gamma-band coherence and the response properties of neurons: 59% of neurons with enhanced firing responses to stimuli exhibited coherence in the low gamma range, while 56% of neurons with depressed firing responses to stimuli exhibited coherence in high gamma ($p > 0.10$). Table 3.1 shows the percentages of enhanced and depressed visually responsive units that displayed SFC in the high gamma and the low gamma frequency bands.

We additionally analyzed all neuron-LFP pairs with visually responsive single units to determine how many pairs exhibited significant SFC during the initial presentation of subsequently well-recognized stimuli. Out of these neuron-LFP pairs, 151 (86%) met the criterion we set for significant gamma-band SFC. Additionally, out of 83 pairs of simultaneously recorded visually-responsive neurons, 54 pairs (65%) showed significant gamma-band SSC during high recognition trials.

Hippocampal gamma-band synchronization reflects recognition memory performance

Figures 3.3A and 3.3B depict the firing rate and SFC for High Recognition and Low Recognition trials for an example recording pair. For this example neuron, and across the population, firing rates during encoding were not significantly modulated by subsequent recognition memory performance ($p > 0.05$; Figure 3.3A). By contrast, for this example (Figure 3.3B) and across the population (Figure 3.3, C-F), gamma-band

Figure 3.3: Gamma-band Spike-field Coherence During Stimulus Encoding Predicts Subsequent Recognition. (A) Average firing rate of an example hippocampal neuron for high recognition (red) and low recognition (blue) trials. There was no difference in firing rate across conditions. Red and blue shaded areas represent SEM. (B) Coherence as a function of time and frequency between the example neuron in (A) and the LFP recorded on a separate electrode, for high recognition (top) and low recognition (bottom) trials. Coherence (52-68 Hz) was significantly enhanced during the encoding of subsequently well-recognized stimuli. (C) Gamma-band coherence expressed as percentage of baseline averaged over 175 hippocampal recording pairs, during high recognition (red) and low recognition (blue) trials, as a function of time from stimulus onset. Red and blue shaded areas represent SEM. Gray shaded area represents time points at which gamma-band coherence was significantly different for the two conditions ($p < 0.01$). (D) Coherence averaged across all high gamma neurons, for high recognition (top) and low recognition (bottom) trials. (E) Same as (D), but for low gamma neurons. (F) Modulation of coherence between high recognition and low recognition trials, for high gamma (top) and low gamma (bottom). Areas of significant coherence modulation are outlined in black (non-parametric randomization test, corrected for multiple comparisons across time and frequency).

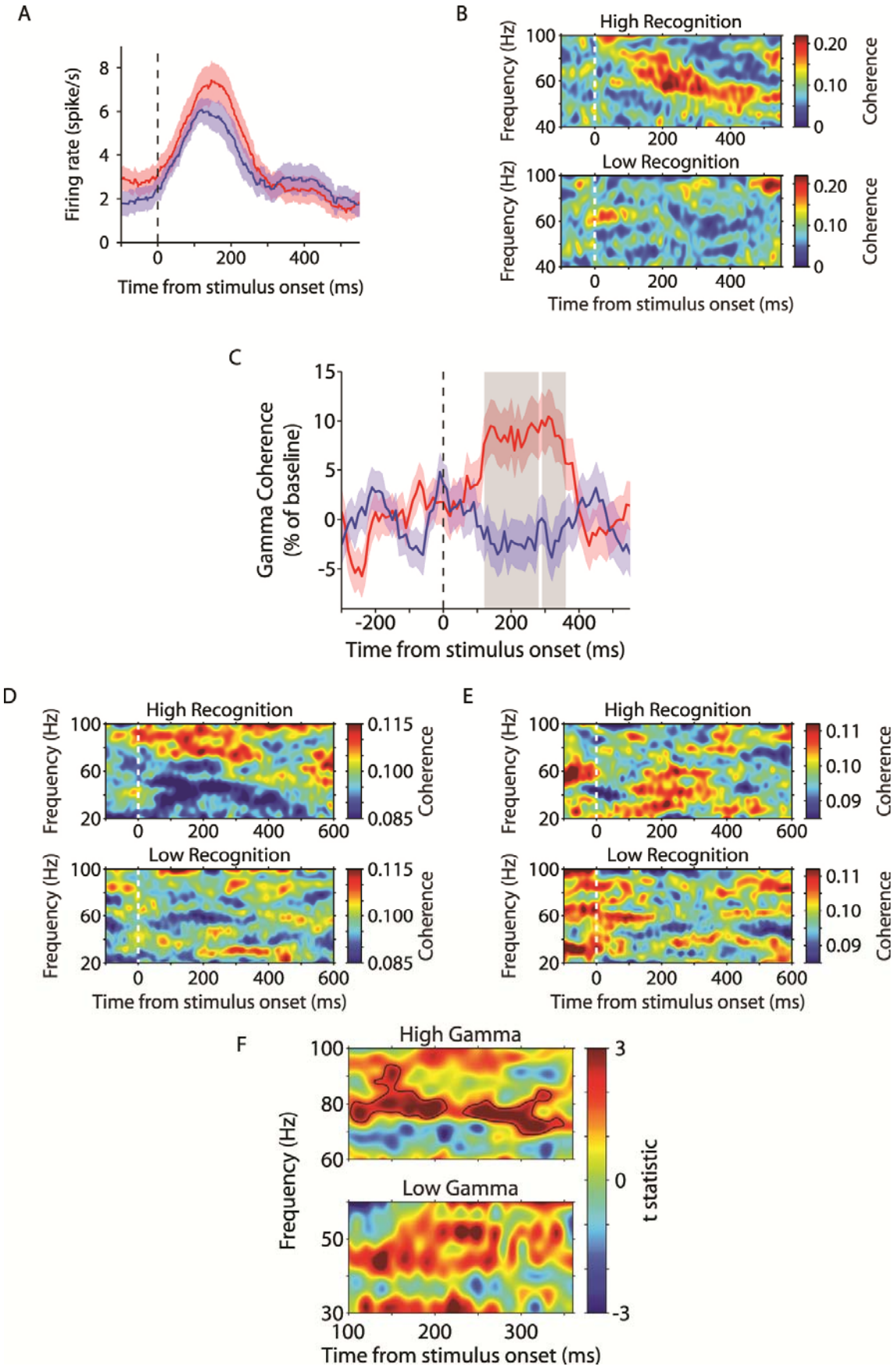
A
Firing rate (spike/s)
Time from stimulus onset (ms)
B
High Recognition
Low Recognition
Frequency (Hz)
Coherence
Time from stimulus onset (ms)
C
Gamma Coherence (% of baseline)
Time from stimulus onset (ms)
D
High Recognition
Low Recognition
Frequency (Hz)
Coherence
Time from stimulus onset (ms)
E
High Recognition
Low Recognition
Frequency (Hz)
Coherence
Time from stimulus onset (ms)
F
High Gamma
Low Gamma
Frequency (Hz)
t statistic
Time from stimulus onset (ms)

coherence was enhanced during the encoding of stimuli that were subsequently well recognized relative to those stimuli that were poorly recognized.

Increases in SFC during the presentation of novel stimuli usually covered limited frequency bands within the broader gamma-band range. This tendency of spikes to lock coherently with LFPs in a narrow band of a particular gamma frequency has also been reported in the rodent neocortex[149]. For this reason, we identified a separate frequency range for each neuron in order to analyze changes in SFC with respect to memory (see Methods). Figure 3.3C shows the average recognition-related modulations in coherence across the population of recording sites. "High Recognition" represents the gamma-band SFC during the encoding of the 30 stimuli in each session with the best subsequent recognition, and "Low Recognition" corresponds to the 30 stimuli with the worst recognition. Across the population, there was an approximately 10% increase in gamma-band synchronization during encoding of stimuli that were subsequently well recognized relative to those stimuli that were poorly recognized. This enhancement reached significance beginning 120 ms after stimulus onset.

Average SFC for the two memory conditions are displayed separately for spike-field pairs displaying high- (above 60 Hz peak frequency, Figure 3.3D) and low-gamma synchronization (below 60 Hz, Figure 3.3E; see Methods for details). The results of the non-parametric permutation analysis revealed that gamma-band coherence was significantly enhanced during high recognition trials as early as 100 ms after stimulus onset for high-gamma spike-field pairs ($p < 0.05$, corrected for multiple comparisons; Figure 3.3F, top panel). Although there was a strong trend for enhanced gamma-band coherence across the low gamma spike-field pairs, this did not reach statistical

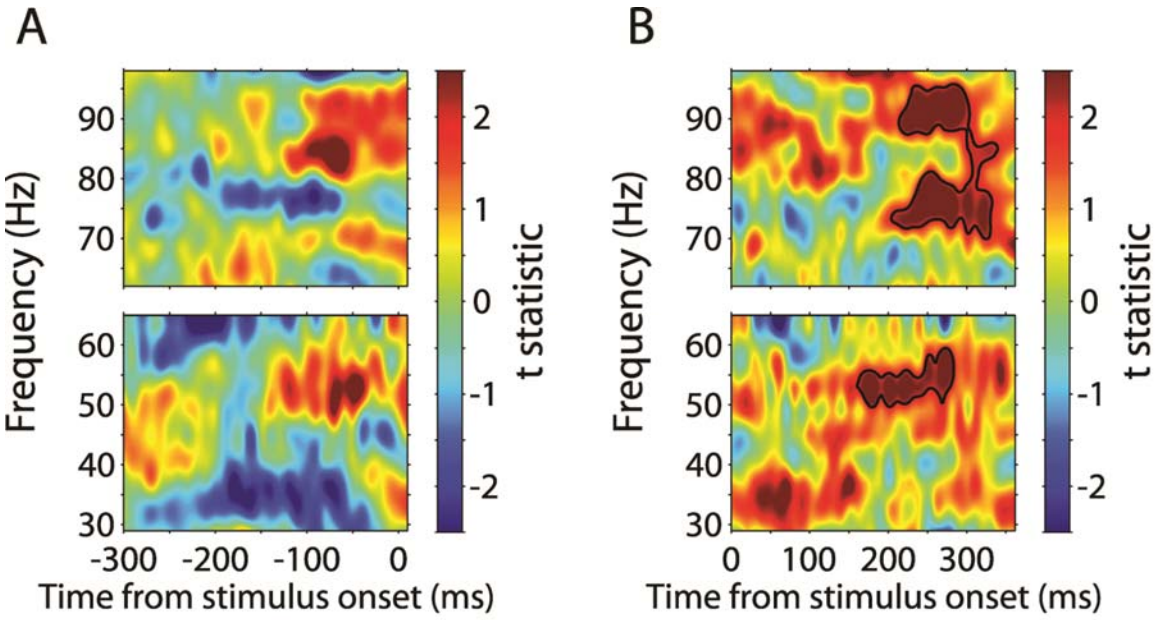

Figure 3.4: Multi-unit Gamma-band Spike-field Coherence. (A) Modulation of multi-unit spike-field coherence between well recognized and poorly recognized stimuli, for high gamma (top) and low gamma (bottom), during pre-stimulus period. There were no areas of significant coherence modulation. (B) Same as (A), but for post-stimulus onset period. Areas of significant coherence modulation are outlined in black (non-parametric randomization test, corrected for multiple comparisons across time and frequency).

significance (Figure 3.3F, bottom panel). This may have been due to a lack of sensitivity because the same analysis using multi-unit activity revealed significant memory-related modulations in gamma-band coherence for both high-gamma and low-gamma pairs (Figure 3.4). Because the sensitivity of coherence measures are proportional to the number of neurons contributing to the analysis, coherence analyses of single unit activity are less sensitive than analyses of multi-unit activity[200]. Therefore, it is possible that single unit spike-field coherence did not reach significance for the Low Gamma group because of a loss in sensitivity compared to the multi-unit analysis.

We also tested whether spike-spike coherence (SSC) was significantly correlated with memory performance using the non-parametric permutation test. Each neuron-

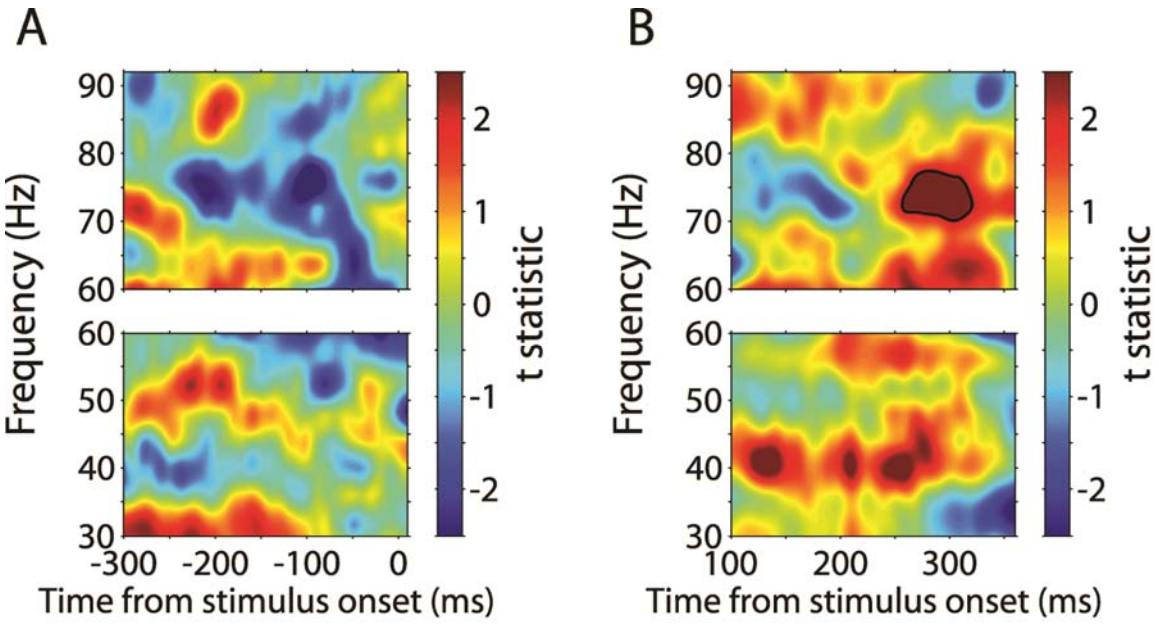

Figure 3.5: Single-unit Gamma-band Spike-spike Coherence. (A) Modulation of single-unit spike-spike coherence between well recognized and poorly recognized stimuli, for high gamma (top) and low gamma (bottom) neuron pairs, during pre-stimulus period. There were no areas of significant coherence modulation. (B) Same as (A), but for post- stimulus onset period. The area of significant coherence modulation is outlined in black (non-parametric randomization test, corrected for multiple comparisons across time and frequency).

neuron pair showing significant coherence was designated as "high gamma" or "low gamma" based on the frequency band in which coherence across all novel stimulus presentations increased in the time period of 100-400 ms after stimulus onset. We applied the permutation test to each group of pairs separately: a small, but significant, cluster of spike-spike coherence (SSC) was seen for the high gamma pairs (n = 32) but not for the low gamma pairs (n = 22; Figure 3.5).

Relationship between Gamma-band Synchronization and Behavior: Memory vs. Attention

It is important to consider whether the observed synchronization among hippocampal neurons primarily reflects successful memory encoding or the attentive state

of the animal. Increased attention to a stimulus likely leads to more successful memory encoding and may cause enhanced neuronal synchronization among hippocampal neurons. With 200 novel stimuli in each recording session, we have to assume that some stimuli are more interesting to the monkey and attract the monkey's attention more than other stimuli. Because the task design allows the monkey to determine the length of stimulus presentation by continuing to look at or looking away from each stimulus, we take as an assumption that the length of looking time for the initial presentation of a stimulus (encoding) reflects the animal's interest in, and attention to, the stimulus. Although other factors may influence looking time in isolated instances, e.g. the monkey's distractibility, over many trials, the monkey's interest in and attention to the stimulus is most likely the overriding factor in determining looking time during novel presentation. If hippocampal synchronization reflects primarily attentive mechanisms, increasing gamma-band coherence in the hippocampus would correlate with increasing length of time spent looking at novel stimuli. To quantify the extent to which neuronal synchronization among hippocampal neurons correlated with recognition memory and attention, for each recording session, we organized all encoding trials into bins, either by increasing recognition memory performance (expressed as the percent change in looking time) or increased attention (expressed as the duration of looking time during the encoding phase). We then correlated the magnitude of spike-field coherence and the behavioral measures of recognition memory performance and attention, as described in Methods. For the example neuron-LFP pair depicted in Figure 3.6A, gamma-band spike-field coherence was significantly correlated with recognition memory performance ($p < 0.005$; Figure 3.6A, left) but not with attention ($p > 0.10$; Figure 3.6A, right). Across the

population, the correlation coefficients and the slopes for all neuron-LFP pairs displayed a significant positive distribution ($p < 0.001$; Figures 3.6B and 3.6C, left) for recognition memory performance, but not for attention ($p > 0.10$; Figures 3.6B and 3.6C, right). A consistent result was obtained when the multiple spike-field coherence results for each single unit were averaged (data not shown). These data suggest that the attentive state of the animal during encoding, as indexed by duration of looking, does not explain the effects of hippocampal gamma-band synchronization on recognition memory

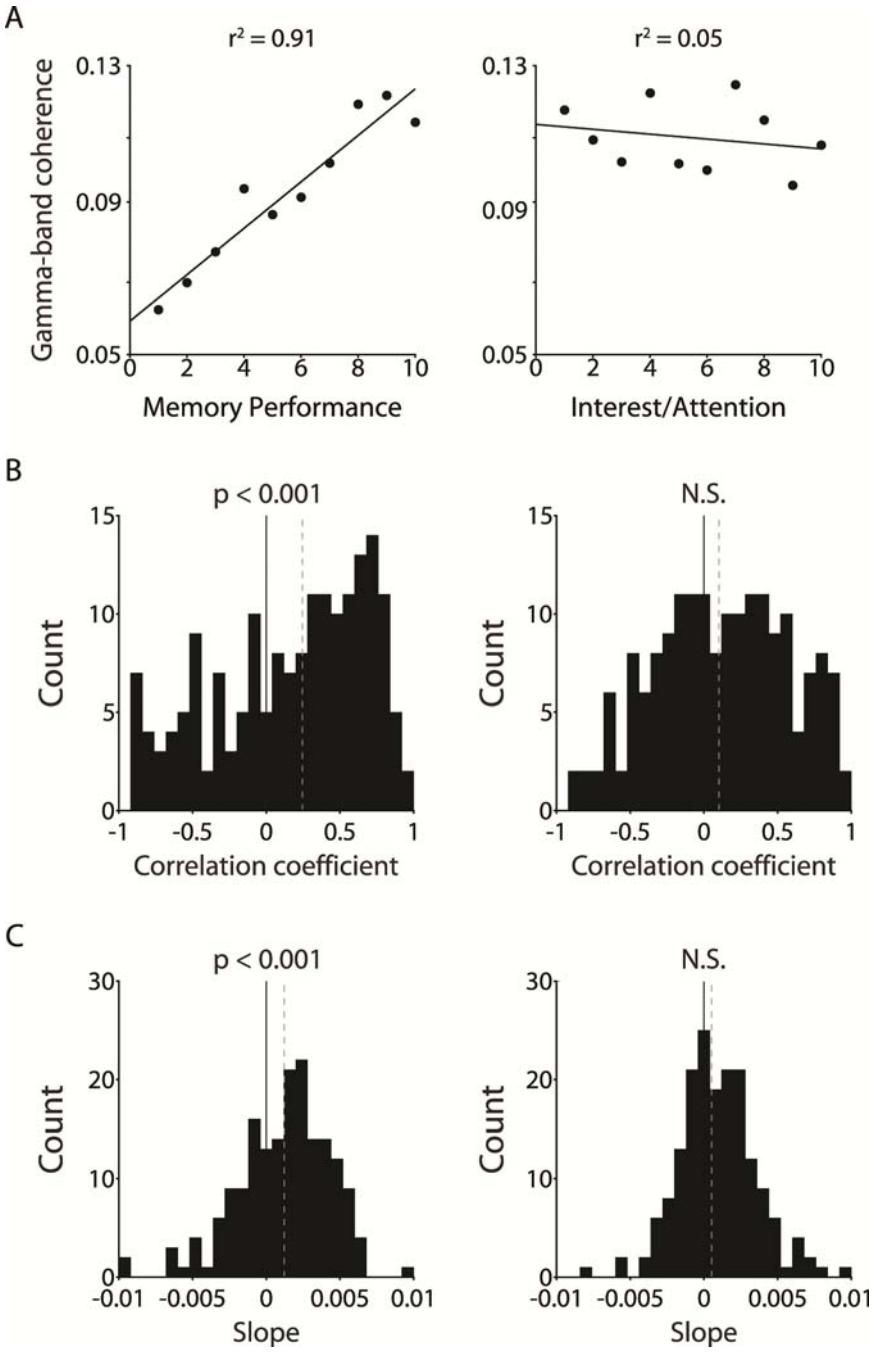

Figure 3.6: Coherence is Correlated with Recognition Memory, but not with Attention. (A) Gamma-band spike-field coherence for one example neuron-LFP pair, binned according to percent change in looking time (left) or looking time during encoding (right). Line indicates linear fit to data. (B) Histograms depicting correlation coefficients between gamma-band spike-field coherence and behavior across all neuron-LFP pairs when binned according to percent change in looking time (left) or looking time during encoding (right). Black line indicates zero; dashed gray line indicates median. (C) Same as (B), but for slopes. Dashed gray line indicates median.

performance.

Previous studies have found that principal cells and interneurons play different roles in the generation of gamma-band oscillations in the hippocampus [119,201,202]. We categorized neurons as putative principal cells or putative interneurons, taking into consideration both the average firing rate during the fixation period preceding stimulus onset and the width of spike waveforms. Both populations of neurons displayed significant gamma-band spike-field coherence modulations during stimulus encoding that predicted subsequent recognition memory (data not shown). Of the 76 visually-responsive putative pyramidal cells, 39 were classified as "high gamma" and 37 as "low gamma". Ten neurons were classified as putative interneurons, 4 of which were designated "high gamma". Accordingly, the data do not suggest that the high vs. low gamma classification was correlated with cell type.

Along with coherence, we also derived power spectra for all LFPs and spike trains. There was no significant effect of memory performance on power in the spike spectra across the population (data not shown). However, LFP power from 40-65 Hz was significantly enhanced during the encoding of well-remembered stimuli compared with the encoding of poorly remembered stimuli approximately 80-300 ms after stimulus onset (Figure 3.7). Although the gamma-band power effects occurred at the same time as the effects in gamma-band coherence, it is important to note that spike-field coherence is normalized by power in both the spike spectrum and the LFP spectrum (see Methods). In other words, coherence represents the consistency of the phase relation between the single unit rhythm and the LFP rhythm, irrespective of the power in either rhythm. Thus, although both signals are correlated with the strength of memory encoding, each

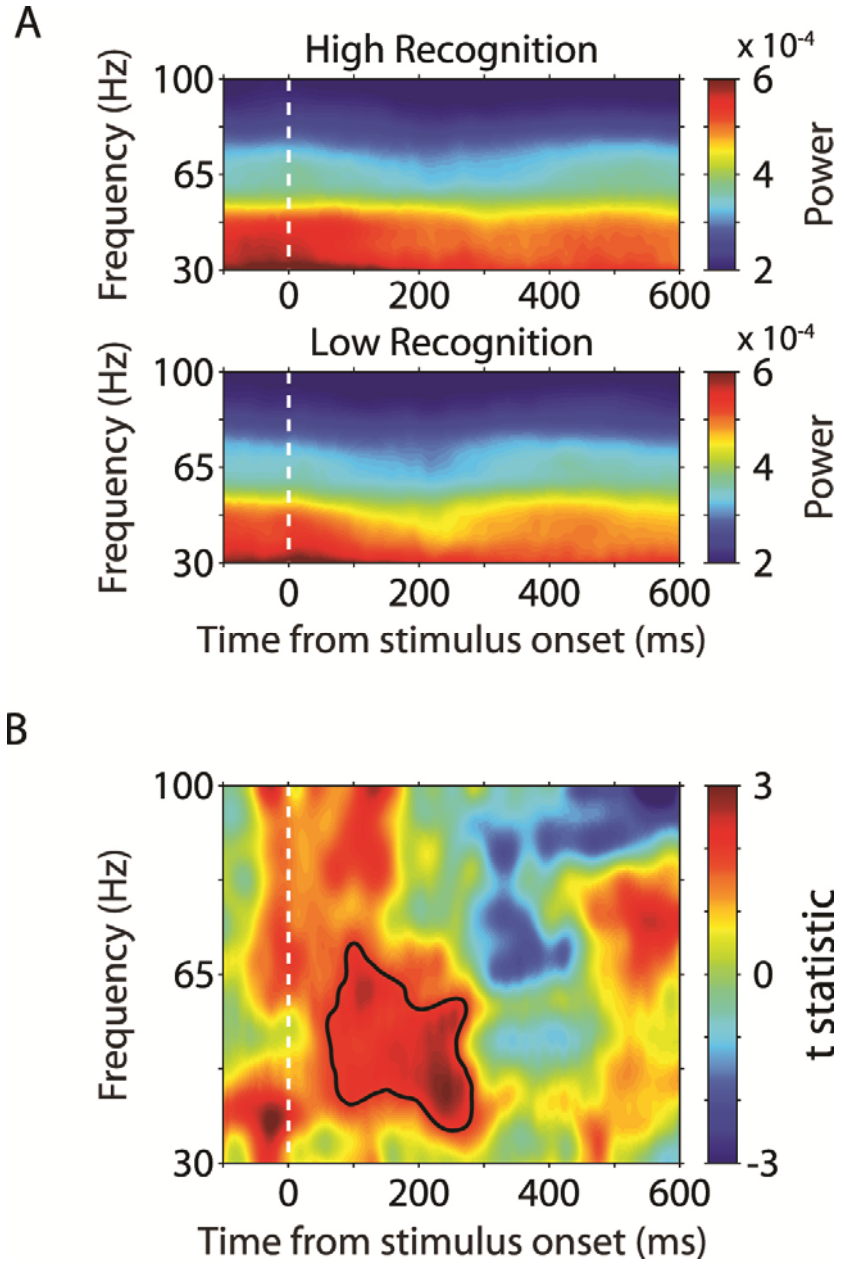

Figure 3.7: Gamma-band LFP Power During Stimulus Encoding Predicts Subsequent Recognition. (A) Gamma-band power averaged across all LFPs during the encoding of high recognition (top) and low recognition (bottom) stimuli. LFP spectra have been normalized by $1/f$ for visualization. (B) Modulation of gamma-band power between high recognition and low recognition stimuli. The area of significant power modulation is outlined in black (non-parametric randomization test, corrected for multiple comparisons across time and frequency).

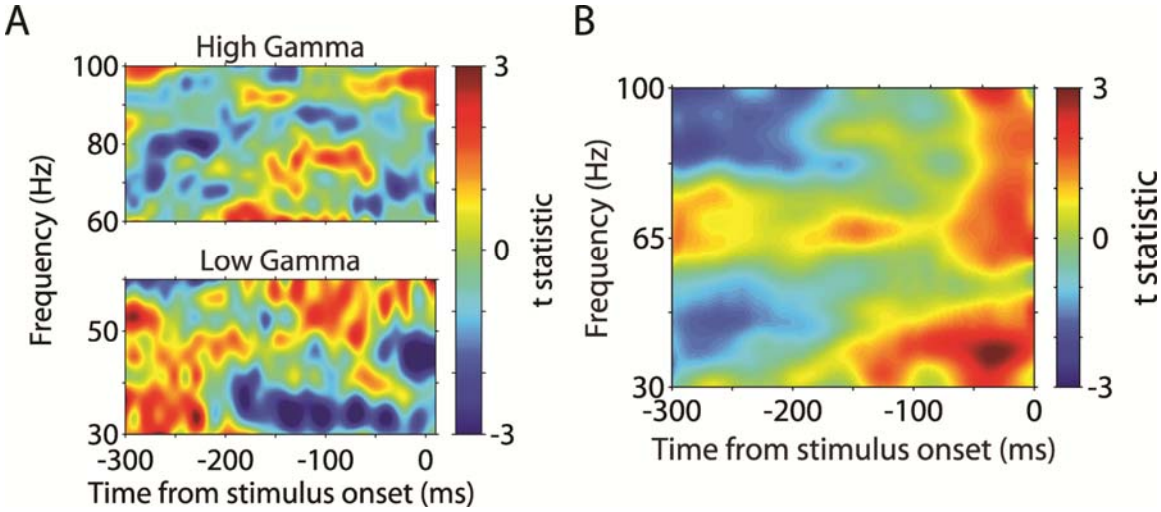

Figure 3.8: Pre-stimulus Gamma-band Spike-field Coherence and Power. (A) Modulation of single-unit spike-field coherence between well recognized and poorly recognized stimuli, for high gamma (top) and low gamma (bottom) neuron pairs, during pre- stimulus period. There were no areas of significant coherence modulation. (B) Modulation of gamma-band power between high recognition and low recognition stimuli during pre- stimulus period. There were no areas of significant coherence modulation.

represents a distinct neural mechanism.

The results from the non-parametric permutation test revealed significant differences between memory conditions for spike-field coherence, spike-spike coherence, and gamma-band power after stimulus onset. However, there were also small clusters of increased gamma-band coherence against background activity prior to stimulus onset (Figures 3.3D and 3.3E). An additional permutation test applied to the baseline period prior to stimulus onset revealed no clusters of significant pre-stimulus modulations for either single-unit SFC (Figure 3.8A), multi-unit SFC (Figure 3.4A), single-unit SSC (Figure 3.5A), or gamma-band power (Figure 3.8B). Therefore, unlike the stimulus-related activity, none of the pre-stimulus activity we recorded was modulated by recognition memory performance.

Relationship between Local Field Potential and Behavior

There have been a number of studies investigating neural activity during presentation of novel or rare stimuli in humans and monkeys. One of the most well-characterized components of this neural response, the P300 component of the event-related potential (ERP), is thought to represent the conscious processing, or encoding, of such stimuli[203,204]. The MTL-P300, recorded via depth electrodes in humans, is a locally generated version of the P300 associated with the hippocampal contribution[205,206]. Figure 3.9A depicts the average stimulus-evoked LFP aligned to stimulus onset for High Recognition and Low Recognition trials, averaged across all 114 LFPs. There was a significant divergence in the signal as early as 270 ms after stimulus onset that predicted subsequent recognition memory performance. We analyzed the magnitude of the stimulus-evoked LFP with respect to memory performance and attention throughout the session using a binning analysis, similar to our previous analysis for spike-field coherence. There was a significant positive relationship between LFP amplitude during stimulus encoding and subsequent recognition memory performance, as well as between LFP amplitude and looking time during encoding (Figure 3.9B-C). These data suggest that unlike gamma-band coherence, changes in the LFP amplitude reflect both attention and memory on a trial-by-trial basis, which is consistent with previous studies associating the P300 with attentional processing[207] and hippocampal-dependent processing of novel stimuli[208]. Interestingly, this P300-like effect did not begin until nearly 170 ms after the earliest effects seen in gamma-band spike-field coherence.

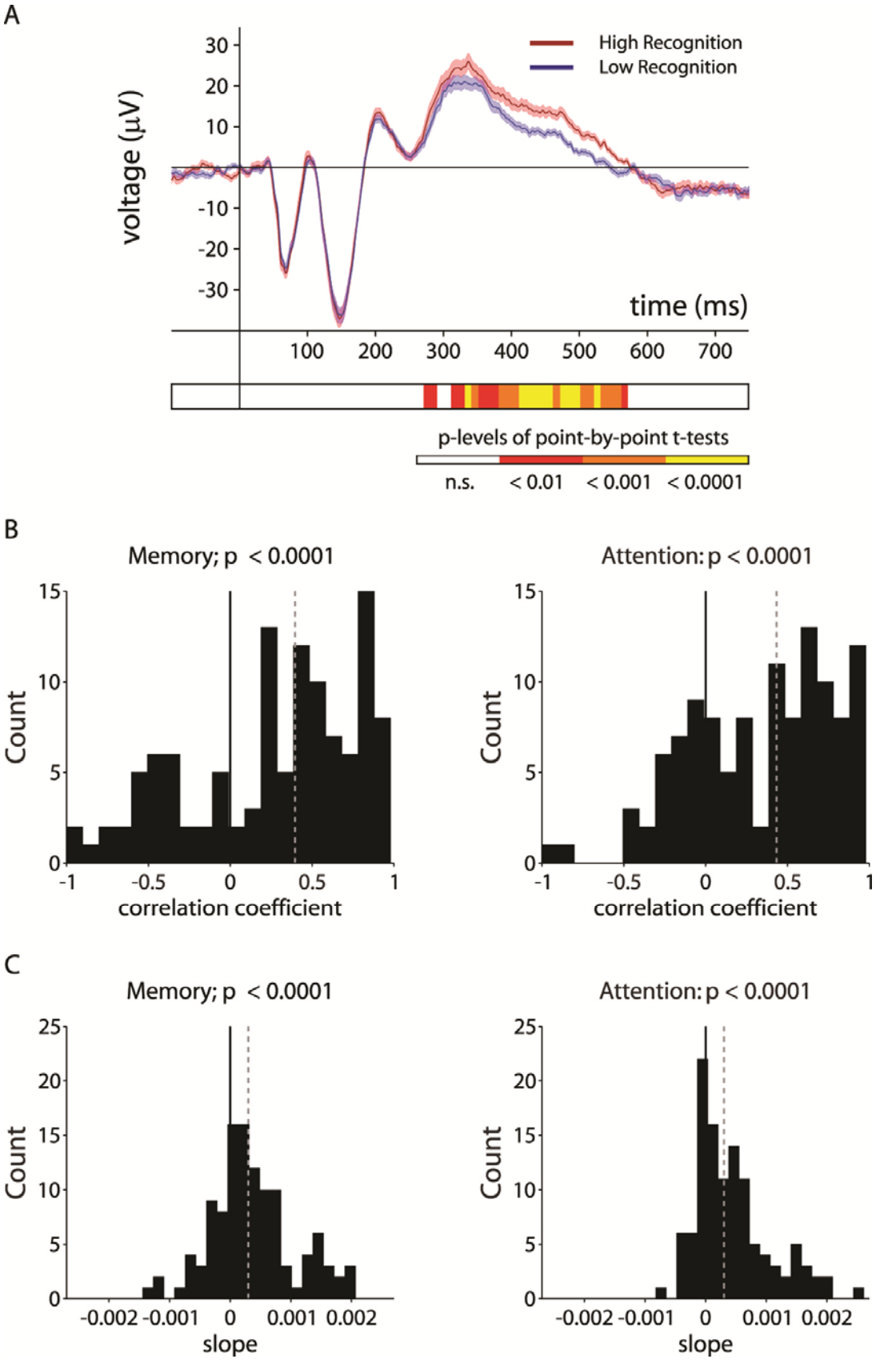
A
High Recognition
Low Recognition
voltage (μV)
30
20
10
-10
-20
-30
time (ms)
100
200
300
400
500
600
700
p-levels of point-by-point t-tests
n.s.
< 0.01
< 0.001
< 0.0001
B
Memory; p < 0.0001
Attention: p < 0.0001
Count
correlation coefficient
C
Memory; p < 0.0001
Attention: p < 0.0001
Count
slope

Figure 3.9: Stimulus-evoked LFP is Modulated by both Attention and Recognition Memory. (A) Stimulus-evoked modulations in LFP amplitude averaged across 114 LFPs during encoding of High Recognition (red) and Low Recognition (blue) stimuli. Shaded areas represent standard error of the mean. *P*-values for significance tests at each consecutive 10 ms time-bin are shown in the color plot below the graph. Time bins shown in yellow represent *p*-values less than 0.0001. (B) Histograms depicting correlation coefficients of the linear functions fit to LFP data across all LFPs when binned according to percent change in looking time (left) or looking time during encoding (right). Black line indicates zero; dashed gray line indicates median. (C) Same as (B), but for slopes. Dashed gray line indicates median.

Additional Behavioral Controls

We also considered the possibility that changes in behavior or neuronal activity through the recording session may affect the interpretation of these results. On average, the monkeys required 58 minutes to complete the session, viewing two presentations of each of 200 stimuli. It is possible that the stimuli presented at the beginning and end of the session evoked different neuronal responses. It is also possible that the monkey experienced fatigue through the session that influenced his performance. To address this issue, we analyzed memory performance, stimulus-evoked firing rates, and the magnitude of SFC with respect to time within the recording session. One-way ANOVAs revealed that there was no significant relationship between time within the session and recognition memory ($F_{(9,439)}$=0.57, p>0.1; Figure 3.10), absolute looking time during novel stimulus presentation ($F_{(9,437)}$=0.39, p>0.1; Figure 3.10A), firing rate modulation ($F_{(9,850)}$=0.28, p>0.1; Figure 3.10B), or gamma-band SFC ($F_{(9,1740)}$=0.96, p>0.1; Figure 3.10C). However, there was a significant negative correlation between LFP amplitude and the time course of the recording session ($F_{(9,1120)}$=2.22, p<0.05; Figure 3.10D). Because this was the only measure which showed any significant correlation with time within the session, it is unclear whether this decline in LFP amplitude is related to fatigue, or some other mechanism.

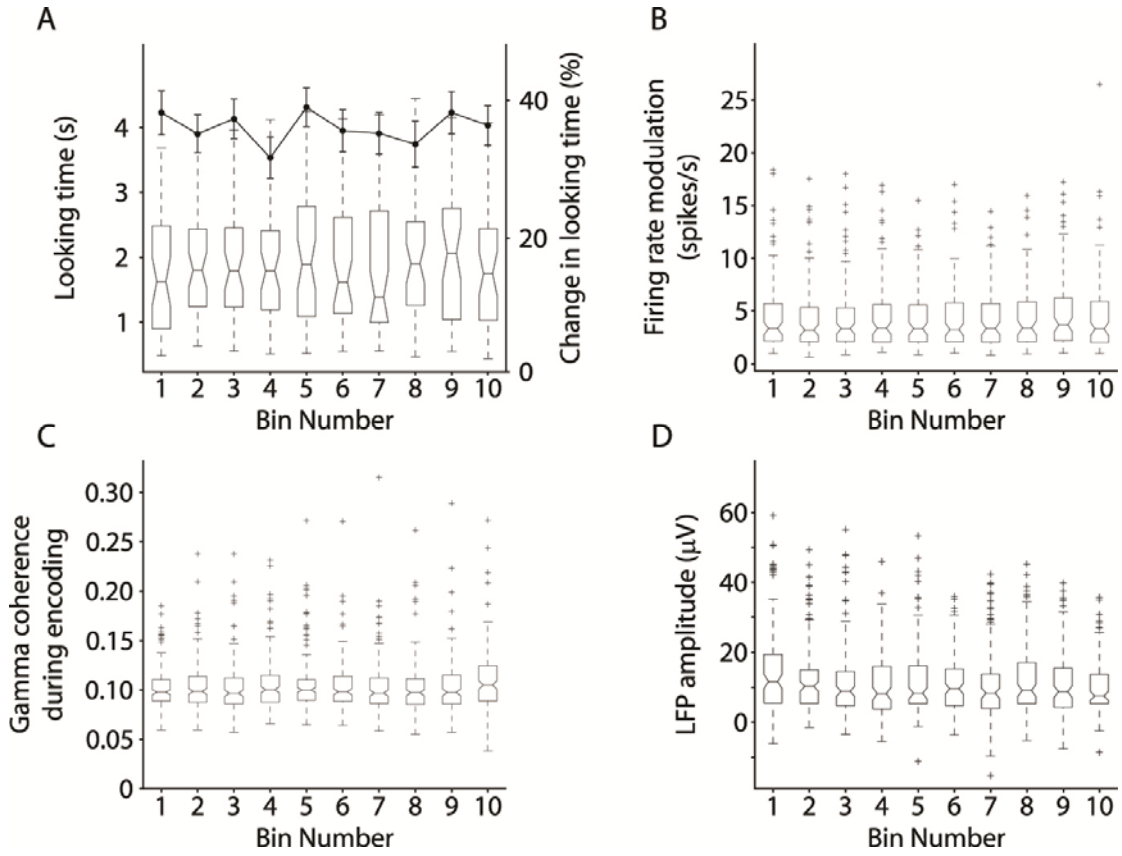

Figure 3.10: Behavioral and Neural Measures as a Function of Time within Session. (A) Box plot: Absolute looking time during novel stimulus presentation, averaged within bins of 20 trials each, across recording sessions. There was no significant effect of bin number on looking time. Line plot: percent change in looking time averaged within bins of 20 trials each, across all recording sessions. There was no significant effect of bin number on behavior across sessions. (B) Magnitude of the response for all visually responsive neurons, averaged within bins of 20 trials each, across recording sessions. There was no significant effect of bin number on firing rate across neurons. (C) Gamma-band spike-field coherence for all visually responsive neurons, averaged within each bin, across recording sessions. There was no significant effect of bin number on coherence across neuron-LFP pairs. (D) LFP amplitude across the 270-570 ms period after novel stimulus onset for all LFPs, averaged within each bin, across recording sessions. There was a significant negative correlation between LFP amplitude and the time course of the recording session (One-way ANOVA, $F_{(9,1120)}=2.22$, $p<0.05$).

Additionally, we determined the amount of time required to achieve fixation before each stimulus presentation. An increased time to achieve fixation would indicate that the monkey's attention or arousal level had declined. Over all 45 recording sessions, we found that that there was no significant difference in this measure between High Recognition and Low Recognition trials ($p > 0.10$). These data suggest that fluctuations in general alertness or arousal levels are not correlated with modulations in gamma-band synchronization in the hippocampus.

Discussion

Our findings show that spikes from isolated single units in the hippocampus are phase locked to each other and to gamma-band oscillations in simultaneously recorded hippocampal LFPs during memory encoding. Further, the magnitude of this phase locking is correlated with subsequent recognition memory performance. These results suggest that memory encoding is accompanied by enhanced coordination between hippocampal neurons.

Fell and colleagues previously showed that successful recognition memory encoding is correlated with increased gamma-band synchronization between local EEG oscillations in the hippocampus and rhinal cortex of human epilepsy patients[117]. The current findings extend these observations to hippocampal neurons, indicating that single units within the hippocampus synchronize the timing of their spikes to the local network oscillations during memory formation, perhaps as a mechanism by which neurons sharing similar response properties might undergo functional coupling. We also found that gamma-band power in hippocampal LFPs during encoding is significantly correlated with

subsequent recognition memory performance. These results are consistent with studies in human epileptic patients that have associated changes in hippocampal gamma-band oscillations with memory[142,209]. Similar observations have been made in monkey parietal cortex in relation to working memory[191]. In that study, both power and coherence in the gamma band were elevated during the delay period of a working memory task. Taken together, these findings suggest that synchronization between spiking activity and oscillatory field activity may be an important mechanism for holding a representation of behaviorally relevant stimuli "on-line".

Previous studies in rodents have linked hippocampal gamma-band synchronization to memory processes[132,210]. In these studies, both the power and the coherence of gamma-band oscillations in hippocampal LFPs were enhanced in relation to the cognitive demands of a hippocampal-dependent task. Consistent with the current study, it was shown that modulations in neuronal synchronization can be dissociated from modulations in firing rate[210], further supporting the notion that changes in the temporal structure of neuronal activity may affect computational outcomes. The current study extends these findings by showing a direct relationship between hippocampal gamma-band coherence and recognition memory performance.

How might gamma-band synchronization in the hippocampus improve encoding? By ensuring that the activity of multiple neurons is correlated within short (i.e., 10 ms) temporal windows, gamma-band synchronization could underlie the transient formation of functional neuronal ensembles[122,211]. For example, a population of neurons may respond to a particular stimulus by synchronizing its firing in the gamma range, and this may contribute spike timing-dependent long-term potentiation[109], thereby strengthening

the connections between these neurons. Gamma-band synchronization among hippocampal neurons may also serve to enhance the impact of hippocampal neurons on output targets in the entorhinal cortex. For example, gamma-band synchronization may result in increased temporal summation of synaptic input on neurons downstream of hippocampal ensembles, thereby increasing the likelihood that these neurons will fire. Such a mechanism would in turn enhance the relay of memory signals to higher-order sensory areas and other areas important for memory storage. Although the difference in average coherence measures between recognition memory conditions is small, evidence from computational studies suggests that small increases in even weakly correlated inputs to neurons can cause substantial increases in the probability of firing of downstream neurons[124].

One caveat is that spike-field coherence does not directly reflect synchronization in the signals being projected to downstream areas, but only implies such an interaction, assuming that some component of the output is reflected in the LFP. Although the results of our analysis of spike-spike coherence provide evidence for synchrony among hippocampal units, future studies are needed to provide a more direct measurement of the degree to which synchronization within the hippocampus affects changes in the activity of downstream targets, e.g. with simultaneous recordings in the hippocampus and the entorhinal cortex.

It is important to consider the extent to which memory effects can be dissociated from attentional effects in assessing performance on the VPLT. Although these processes cannot be completely dissociated with this behavioral task, there is evidence from previous studies that memory and attention depend on different brain regions. In

particular, the finding that monkeys with hippocampal lesions[33] and amnesic patients[30] display intact novelty preference as long as the delay between first and second stimulus presentation is short (1 second, and 0.5 seconds, respectively) but are impaired with increasing delays (10 seconds and longer) supports this idea. At the same time, increased attention during stimulus presentation may lead to better subsequent memory. This could result in neural signals that underlie both processes co-varying with behavioral performance. Our data suggest that gamma-band coherence in the hippocampus more reliably predicts successful recognition memory performance than increased attention to stimuli. In contrast, the stimulus-evoked LFP in the hippocampus appears to reflect both memory encoding and attentional processes.

To our knowledge, this study is unique in its separation of gamma-band oscillations recorded in the primate hippocampus into high and low gamma. A number of recent studies have observed oscillatory synchrony in either high or low gamma in other brain regions, and in many cases these frequency bands have been associated with distinct aspects of cognition [212-215]. Cortical oscillations in the high gamma band tend to exhibit higher phase-locking with theta oscillations in humans[144] and rodents[149]. Additionally, oscillations in the high gamma-band range have been associated with the hemodynamic response measured using BOLD fMRI[216].

In the current study, the results of the non-parametric test for single units revealed a significant difference across memory conditions only for the high gamma neurons. However, analyses including both high and low gamma neurons revealed significant differences between successful (high recognition) and less successful (low recognition) encoding (Figure 3.3C), as well as a significant positive correlation between trial-by-trial

modulations in coherence and recognition memory (Figure 3.6). Nevertheless, these different populations of neurons may make distinct contributions to behavior through their participation in different modes of network activity.

Visual stimuli induced a clear increase in gamma-band synchronization that was associated with recognition memory performance. However, we also observed some gamma-band synchronization prior to stimulus onset. Non-parametric randomization tests applied to the pre-stimulus period revealed that neither gamma-band coherence nor power was correlated with subsequent recognition memory performance during this period (Figures 3.4A, 3.5A, and 3.8), suggesting that the observed level of pre-stimulus synchronization reflects hippocampal processing unrelated to the behavioral task. One possibility is that this pre-stimulus synchronization reflects arousal mechanisms. Timing was held constant throughout the experiment (1 second fixation period), so it would be possible for the monkeys to anticipate the onset of the stimulus. Alternatively, between the end of the previous stimulus presentation and the beginning of the next the monkey may be engaged in retrieving previous stimuli, encoding new information, or some other uncontrolled process. Because some hippocampal function is likely during such processes, the presence of spike-field coherence during this interval is not wholly surprising. Functional imaging studies often employ a separate task during baseline periods because the use of a simple "rest" period can potentially lead to high levels of hippocampal activation[217].

While several studies have identified activity at the cellular level related to recognition memory in the cortex surrounding the hippocampus[85-88,94], there is a notable lack of evidence for recognition memory signals in the hippocampus proper. One

important difference between our task and those used in previous neurophysiological studies is the degree of training involved. The VPLT requires only simple fixation training. In contrast, the tasks used in previous neurophysiology studies require a long period of training (up to 7-10 months), during which monkeys gradually learn a match-to-sample rule. It is conceivable that during this training period, monkeys acquire strategies for performing the task that do not rely on the hippocampus. Similarly, while the VPLT examines the monkey's innate preference for novelty, tasks in previous studies examined the monkey's ability to respond correctly in order to receive a food or juice reward. The reward component of these tasks may encourage the acquisition of strategies that recruit extra-hippocampal structures. Consistent with this idea, the VPLT has been shown to be more sensitive than the delayed non-matching to sample task to restricted lesions of the hippocampus[31,33,42].

In summary, we have utilized spectral analysis to examine the role of precise spike timing in the hippocampus in memory formation. Our results are consistent with the idea that memory encoding in the medial temporal lobe relies on a combination of firing rate changes at the single-cell level, and altered patterns of synchronization at the population level.

Chapter 4

Memory formation is predicted by theta-band phase-locking in the monkey hippocampus[4]

Introduction

Studies in humans and animals suggest that the hippocampus is critical for the successful formation of declarative memories[33,46,159], and memory formation has been associated with a network oscillation in the theta band[150,218,219]. Theta-band oscillations have been studied most extensively in the rodent hippocampus[220], but have also been described in bats[221], cats[222], and, more recently, humans[148,223]. However, there have been no reports of hippocampal theta-band activity in the awake monkey. In rodents, hippocampal theta-band oscillations are modulated by running speed[224], possibly reflecting the rate of sensory input. Primates obtain significant information about their surroundings through visual exploration, and normal exploration of a stationary visual scene through saccadic eye-movements effectively breaks the viewing episode into multiple epochs, each providing a period of incoming sensory information to the brain.

[4] Reproduced with minor edits from manuscript: Jutras, M. J., Killian, N. J., Fries, P. & Buffalo, E. A. Memory formation is predicted by theta-band phase-locking in the monkey hippocampus. In review.

This parsing of visual information into multiple fixation periods may be analogous to information gathering in other species, e.g., sniffing or whisking in rodents, which may be linked to hippocampal theta-band oscillations[225]. Accordingly, we examined primate hippocampal activity related to visual exploration, saccadic eye-movements, and memory formation in monkeys performing a visual recognition memory task.

Methods

Procedures were carried out in accordance with NIH guidelines and were approved by the Emory University Institutional Animal Care and Use Committee. Neuronal recordings were carried out in two adult male rhesus monkeys (Macaca mulatta), which were obtained from the breeding colony at the Yerkes National Primate Research Center. Their mean weight at the start of the experiment was 6.8 ± 1.1 kg, and their mean age was 4 years and 5 months. Prior to implantation of recording hardware, monkeys were scanned with magnetic resonance imaging (MRI) to localize the hippocampus and to guide placement of the recording chamber. Using this information, a cilux plastic chamber (Crist Instrument Co., Hagerstown, MD) for recording neural activity, and a titanium post for holding the head were surgically implanted. We performed post-surgical MRI to fine-tune electrode placement and to determine recording locations.

Behavioral testing procedures

During testing, each monkey sat in a dimly illuminated room, 60 cm from a 19" CRT monitor, running at 120 Hz, non-interlaced refresh rate. Eye movements were

recorded using a non-invasive infrared eye-tracking system (ISCAN, Burlington, Massachusetts). Stimuli were presented using experimental control software (CORTEX, www.cortex.salk.edu). At the beginning of each recording session, the monkey performed a calibration task, which involved holding a touch-sensitive bar while fixating a small (0.3°) gray square, presented on a dark background at various locations on the monitor. The monkey had to maintain fixation within a 3° window until the fixation point changed to an equiluminant yellow at a randomly chosen time between 500 ms and 1100 ms after fixation onset. The monkey was required to release the touch-sensitive bar within 500 ms of the color change for delivery of a drop of applesauce. During this task, the gain and offset of the oculomotor signals were adjusted so that the computed eye position matched targets that were a known distance from the central fixation point.

Visual preferential looking task

Following the calibration task, the monkey was tested on the Visual Preferential Looking Task (VPLT). The monkey initiated each trial by fixating a white cross (1°) at the center of the computer screen. After maintaining fixation on this target for 1 s, the target disappeared and a picture stimulus was presented (11°). The stimulus disappeared when the monkey's direction of gaze moved off the stimulus, or after a maximum looking time of 5 seconds. The VPLT was given in 51 daily blocks of 6, 8, or 10 trials each, chosen pseudorandomly, for a total of 400 trials each day. The median delay between successive presentations was 8.1 seconds. Stimuli were obtained from Flickr (http://www.flickr.com/). A total of 9000 stimuli were used in this study.

Because the monkey controlled the duration of stimulus presentation, the duration of gaze on each stimulus provides a measure of the monkey's preference for the stimulus. We compared the amount of time the monkey spent looking at each stimulus during its first ("Novel") and second ("Repeat") presentation. Adult monkeys show a strong preference for novelty; therefore, a significant reduction in looking time between the two presentations of a stimulus indicated that the monkey had formed a memory of the stimulus and spent less time looking at the now familiar stimulus during its second presentation. To control for varying interest in individual stimuli, recognition memory performance was calculated as the difference in looking time between presentations as a percentage of the amount of time the monkey spent looking at the first presentation of each stimulus: (novel – repeat) ÷ novel.

Reward was not delivered during blocks of the VPLT; however, 5 trials of the calibration task were presented between each block to give the monkey a chance to earn some reward and to verify calibration. The number of trials in each VPLT block was varied to prevent the monkey from knowing when to expect the rewarded calibration trials.

Electrophysiological recording methods

The recording apparatus consisted of a multi-channel microdrive (FHC Inc., Bowdoinham, Maine) holding a manifold consisting of a 23-gauge guide tube containing 4 independently moveable tungsten microelectrodes (FHC Inc., Bowdoin, Maine), with each electrode inside an individual polyamide tube. Electrode impedance was in the range of 1-2 MΩ, and electrode tips were separated horizontally by 190 μm. For each

recording, the guide tube was slowly lowered through the intact dura mater and advanced to ~3.5 mm dorsal to the hippocampus with the use of coordinates derived from the MRI scans. The electrodes were then slowly advanced out of the guide tube to the hippocampus. No attempt was made to select neurons based on firing pattern. Instead, we collected data from the first neurons we encountered in the hippocampus. At the end of each recording session, the microelectrodes and guide tube were retracted. All recordings took place in the anterior part of the left hippocampus. Recording sites were located in the CA3 field, dentate gyrus, and subiculum. For the example recording shown in Figure 4.3, an axial array electrode was used, consisting of a laminar electrode array mounted on a tungsten microelectrode (12-site, 150 μm spacing, 0.5 mm from the tip; FHC Inc., Bowdoin, Maine).

Data amplification, filtering, and acquisition were performed with a Multichannel Acquisition Processor (MAP) system from Plexon Inc. (Dallas, TX). The neural signal was split to separately extract the spike and the LFP components. For spike recordings, the signals were filtered from 250 Hz – 8 kHz, further amplified and digitized at 40 kHz. A threshold was set interactively, in order to separate spikes from noise, and spike waveforms were stored in a time window from 150 μs before to 650 μs after threshold crossing. Each recording typically yielded 2 to 6 units; single units were sorted offline using Offline Sorter (Plexon, Inc.). For LFP recordings, the signals were filtered with a passband of 0.7-170 Hz, further amplified and digitized at 1 kHz; any additional filtering was performed in Matlab (see Data Analysis for details). Eye movement data were digitized and stored with a 240 Hz resolution.

Data analysis

All analyses were performed using custom programming in Matlab (The Mathworks, Inc., Natick, MA) and using FieldTrip (http://www.ru.nl/fcdonders/fieldtrip/), an open source toolbox for the analysis of neurophysiological data, and CircStat (www.kyb.mpg.de/~berens/circStat.html) an open source toolbox for the calculation of circular statistics.

Eye movement data were analyzed in order to isolate fixation periods occurring between saccades. Saccades were detected by first applying a low-pass filter with a high-cut frequency limit of 40 Hz to the horizontal and vertical eye position data to remove high-frequency noise, differentiating and combining these signals to obtain the eye velocity, and setting a threshold of 25 degrees/second in order to define saccades. The start and end of each saccade was considered to occur when the first order derivative of the eye velocity reached zero before the upward crossing and after the downward crossing of this threshold, respectively. For the analysis of neural data, only fixation periods with durations of at least 100 ms (excluding the fixation period immediately following stimulus onset) were considered in order to focus analysis on eye movements that were more likely to reflect a shift in attention to a new target rather than readjustments in gaze on a current target.

We recorded from 131 hippocampal units in two monkeys (67 in Monkey A and 64 in Monkey B, respectively). For each neuron, the average firing rate was calculated for the period including pre-stimulus fixation as well as stimulus presentation, for each trial. A baseline period of 800 ms preceding stimulus onset was used to calculate the average background firing rate for each neuron. We categorized neurons as putative

principal cells or putative interneurons, taking into consideration both the average firing rate during the fixation period preceding stimulus onset and the width of spike waveforms. Spike waveforms were examined to determine the duration, defined as the time, in μs, from waveform trough to peak. All neurons with baseline firing rates above 15 spikes/second were classified as putative interneurons, and all other neurons were classified as putative principal neurons. With this classification, the average waveform duration for putative interneurons was significantly shorter than that for putative principal cells (independent t-test, $p < 0.05$). Based on this analysis, 12 recorded neurons were classified as putative interneurons.

The powerline artifacts were removed from the LFP in the following way: We estimated the amplitude of the powerline fluctuations with a Discrete Fourier Transformation (DFT) of long data segments which contained the data epochs of interest. We then computed the DFT at 60 and 120 Hz. Because the powerline artifact is of a perfectly constant frequency and amplitude, and because the long data segments contained integer cycles of the artifact frequencies, essentially all the artifact energy is contained in those DFTs. We constructed sine waves with the amplitudes and phases as estimated by the respective DFTs, and subtracted those sine waves from the original long data segments. The epoch of interest was then cut out of the cleaned epoch. Power spectra of the cleaned epochs demonstrated that all artifact energy was eliminated, leaving a notch of a bin width of 0.1 Hz in the monkey recordings.

For the calculation of inter-saccade coherence and power spectra, we used a single Hanning taper and applied fast Fourier transforms to overlapping 500 ms segments of Hanning-tapered data in 10 ms steps. The 500 ms segment length allowed a frequency

resolution of 2 Hz. Coherence spectra were calculated between the LFP signal and the start of each fixation period to produce the inter-saccade coherence. Like normal coherence, inter-saccade coherence assumes a value of 1 for perfect phase-locking and a value of 0 for fully random phase relations. Both inter-saccade coherence and power analyses were limited to LFPs derived from electrodes that also had isolated single units in order to ensure that LFPs were obtained from cell layers.

We investigated the degree of coupling between gamma-band power and theta-band oscillations by first taking the inverse Fourier transform of overlapping 50 ms segments of each Hanning-tapered LFP signal in 1 ms steps, centred at 60 Hz, after windowing in the frequency domain. This method produced a measure of the power of the LFP signal in the 30-90 Hz range around the onset of each fixation period. Due to the spectral smoothing inherent in this method, the 0.1 Hz notch that resulted from powerline artifact removal became invisible. We then calculated the coherence between this signal and the LFP on the same channel using the multi-taper method of spectral estimation[193]. Overlapping 500 ms segments of data (in 10 ms steps) were each multiplied by a data taper, followed by Fourier transformation. A variety of tapers can be used, but an optimal family of orthogonal tapers is given by the prolate spheroidal functions or Slepian functions. For time length T and bandwidth frequency W, up to K=2TW-1 tapers are concentrated in frequency and suitable for use in spectral estimation. We used three Slepian tapers, providing an effective taper smoothing of ±4 Hz. For each taper, the data segment was multiplied with that taper and Fourier transformed, giving the windowed Fourier transform, $\tilde{x}_k(f)$:

$$\tilde{x}_k(f) = \sum_{1}^{N} w_k(t) x_t e^{-2\pi i f t}$$

where x_t, (t = 1,2,..., N) is the time series of the signal under consideration and $w_k(t)$, (k = 1,2,..., K) are K orthogonal taper functions. The multitaper estimates for the spectrum $S_x(f)$ and the cross-spectrum $S_{yx}(f)$ are given by the following:

$$S_x(f) = \frac{1}{K}\sum_{1}^{K}\left|\widetilde{x}_k(f)\right|^2$$

$$S_{yx}(f) = \frac{1}{K}\sum_{1}^{K}\widetilde{y}_k(f)\widetilde{x}_k^*(f)$$

Spectra and cross-spectra are averaged over trials before calculating the coherency $C_{yx}(f)$ as follows:

$$C_{yx}(f) = \frac{S_{yx}(f)}{\sqrt{S_x(f)S_y(f)}}$$

Coherency is a complex quantity. Its absolute value is termed coherence and ranges from 0 to 1. A coherence value of 1 indicates that the two signals have a constant phase relationship (and amplitude covariation), and a value of 0 indicates the absence of any phase relationship. Thus, coherence is a measure of linear predictability that captures phase and amplitude correlations.

To relate the phase at fixation onset to recognition memory, the stimuli from each session were ranked in order of increasing recognition performance, quantified as the percent change in looking time between Novel and Repeat presentations for each stimulus. The 30 encoding trials with the lowest percent change were designated “Low Recognition” and the 30 trials with the highest percent change were designated “High Recognition”. Only those trials in which the monkey made at least three saccades during Novel stimulus presentation without looking away from the image were used. LFPs recorded during Novel trials were then filtered with a band-pass filter of 3-8 Hz, using a

zero-phase-shift fourth-order Butterworth filter. The phase at fixation onset was calculated by using the Hilbert transform to extract the phase of the LFP at each time point, and determining the phase at the onset of each fixation period, i.e. the end of each saccade. The collection of phases was then averaged for each of the 30 trials in each condition, for each LFP, in order to obtain 30 phases for High Recognition trials and 30 phases for Low Recognition trials for each LFP. This was done for each of 110 LFPs obtained from electrodes on which single unit activity was also recorded; thus, the final distributions used for the statistical analysis contained an equal number of phase angle measurements (n = 3300). Finally, a non-parametric multi-sample test for equal medians was used to determine whether the distributions were significantly different.

The relationship between single unit spiking activity and LFP phase was examined by first calculating the spike-triggered average of the LFP in a 500 ms window around each spike. Because filtering to separate spike waveforms from lower-frequency components of the LFP took place at data acquisition, the raw LFP was assumed to be clean of artifacts from spiking activity recorded on the same electrode. Regardless, we used a cubic spline interpolation method in a window of 5 ms before to 15 ms after each spike timestamp on each LFP obtained from the same electrode in order to rule out the influence of spike artifacts on the analysis. We next designated a 500 ms segment of LFP data around each spike and multiplied each segment by a Hanning window before Fourier transforming it, giving the spike-triggered LFP spectrum. This allowed us to calculate the phase angle of each spike at each frequency (with a resolution of 2 Hz) in the range of 0-20 Hz. To test whether a neuron was significantly phase-locked to the theta-band oscillation, the collection of all phase angles at each frequency was compared to a

random (uniform) distribution using the Rayleigh test. A threshold of 0.05, Bonferroni-corrected for multiple comparisons, was set for each frequency (4-14 Hz in 2 Hz steps; thus, the threshold was set to 0.005). A neuron was designated as theta phase-locked if the *p* value of the Rayleigh statistic fell below this threshold for at least one of the frequencies in the theta range (4, 6, or 8 Hz).

To determine the degree of phase synchronization between spikes and LFP oscillations, and the degree to which phase synchronization varied with memory, we calculated the pairwise phase consistency (PPC). This measure of synchronization is completely bias-free, even for small sample sizes (in our case, the number of spikes and the length of trials, which varied according to recognition memory performance), is linearly related to existing phase-locking statistics, and has been extensively validated on simulated and real data[226]. We used the Fourier transform of the Hanning-tapered 500 ms data segment around each spike to obtain a single LFP phase value per trial. The sample estimate of the PPC is defined as:

$$\hat{D} \equiv \frac{2}{N(N-1)} \sum_{j=1}^{N-1} \sum_{k=(j+1)}^{N} d(\theta_j, \theta_k)$$

where $d(\varphi,\omega)$ is the absolute angular distance defined as:

$$d(\varphi, \omega) \equiv |\varphi - \omega| \bmod \pi$$

and θ_j and θ_k are the relative phases from two observations. Thus, $\hat{D}$ calculates the average absolute angular distance between all observed spike phases (with a total of $N^2 - N$) pairs). The population pairwise phase consistency is then defined by the Riemannn Stieltjes integral as follows:

$$D \equiv \int_{-\pi}^{\pi} \int_{-\pi}^{\pi} d(\varphi, \omega) dP_{\varphi}(\varphi) dP_{\omega}(\omega)$$

with $P_{\varphi}(\varphi) = P_{\omega}(\omega)$ defined as the cumulative probability distribution of the relative phase θ_j. Note that the expected value of the PPC $E\{\hat{D}\}$ does not depend on the number of pairs in the sample. To obtain the same dynamic range as the phase-locking value, we normalize the PPC by $\hat{D}^* = \frac{\pi - 2\hat{D}}{\pi}$, which results in $\hat{D}^*$ ranging from −1 to 1, and in expected values ranging from 0 to 1, with 1 indicating complete phase consistency and 0 indicating the absence of phase consistency (e.g., as for a uniform circular distribution or a mixture of two von Mises distributions with an orthogonal mean phase and equal dispersion). Note that values below 0 are possible. However, the expected value is always greater than or equal to zero, with values smaller than zero indicative of a complete absence of phase consistency.

Results

We recorded single unit activity and local field potentials (LFPs) simultaneously from four to twelve electrodes in two rhesus monkeys performing the Visual Preferential Looking Task[227,228] (see Figure 2.3). Each recording session, monkeys were presented with two-hundred novel complex stimuli (11° x 11° in size) on a computer screen. Each stimulus was presented twice during a given session, with up to 8 intervening stimuli between successive presentations. The monkeys' eye movements were measured with a non-invasive infrared eye-tracking system. Each stimulus remained on the screen until the monkey's gaze moved off the stimulus or for a maximum of 5 seconds. Figure 4.1 depicts an example of a monkey's eye movements during the first ("Novel", yellow trace) and second ("Repeat", blue trace) presentations of a stimulus. Monkeys demonstrated

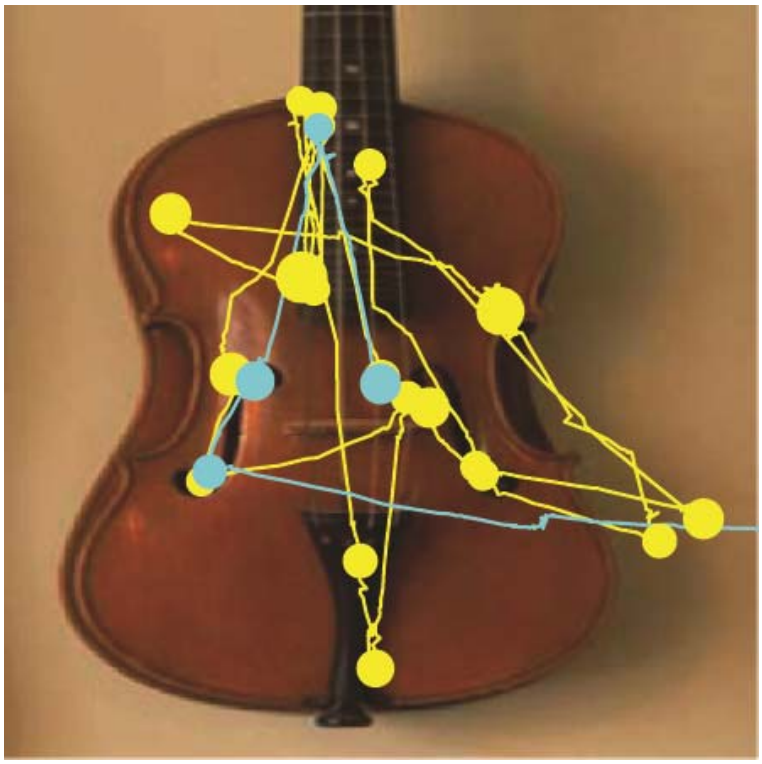

Figure 4.1: Example of saccadic eye movements during VPLT. This figure shows a representative example of one monkey's scan path, showing that the monkey spent more time looking at the image when it was novel (yellow) compared to when it was repeated (blue). Circles represent points of fixation between saccades, with the size of each circle proportional to the duration of the fixation period.

recognition memory by spending less time exploring the stimulus when it was repeated compared to when it was novel. Across 45 sessions, the monkeys demonstrated robust recognition memory performance. There was a significant decrease in looking time for the repeated presentation (average looking times for Novel and Repeat trials were 2.3 s and 0.8 s, respectively; paired t-test, $p < 0.001$). To control for varying interest in individual stimuli, recognition memory performance was calculated as the difference in looking time between presentations as a percentage of the amount of time the monkey spent looking at the first presentation of each stimulus. The median reduction in looking time was 70.7% (67.3% in Monkey A and 72.8% in Monkey B; Figure 2.3C). Similar

	Putative principal cells	Putative interneurons
n	119	12
Baseline firing rate (spk/s)	4.9 ± 0.3	23.2 ± 1.3
Mean waveform duration (μs)	278.4 ± 4.8	241.2 ± 10.2
Theta phase-locked (n)	42 (35.3%)	10 (83.3%)

Table 4.1: Properties of putative principal cells and interneurons. Values represent mean ± SEM.

tasks which examine recognition memory through preference for novelty have been shown to depend on the integrity of the hippocampus in rodents, monkeys, and humans[30,33,34,42]. Because the task involves minimal training, the behavior thus measured may more closely approximate the activity that animals exhibit naturally.

Across 45 recording sessions, we isolated 131 single units (67 from Monkey A and 64 from Monkey B, primarily from CA3; see Figure 2.1) and we recorded a total of 110 LFPs. Putative pyramidal cells fired, on average, 4.9 ± 0.3 spikes per second, and putative interneurons fired 23.2 ± 1.3 spikes per second (Table 4.1). In the LFP, we observed a prominent theta-band oscillation while monkeys actively explored novel images (Figure 4.2). Some of our recordings were performed using an axial array electrode which permitted simultaneous recordings across 12 contacts, spaced at 150 microns (Methods; Figure 4.3). With these recordings, we observed a gradual phase shift in the theta-band oscillation across cell layers, consistent with findings from the rodent hippocampus[201].

We next considered whether there was any relationship between theta oscillations and saccadic eye-movements. Saccades were defined as eye movements that surpassed a velocity of 25 degrees/second (Figure 4.4A). Monkeys typically explored each picture

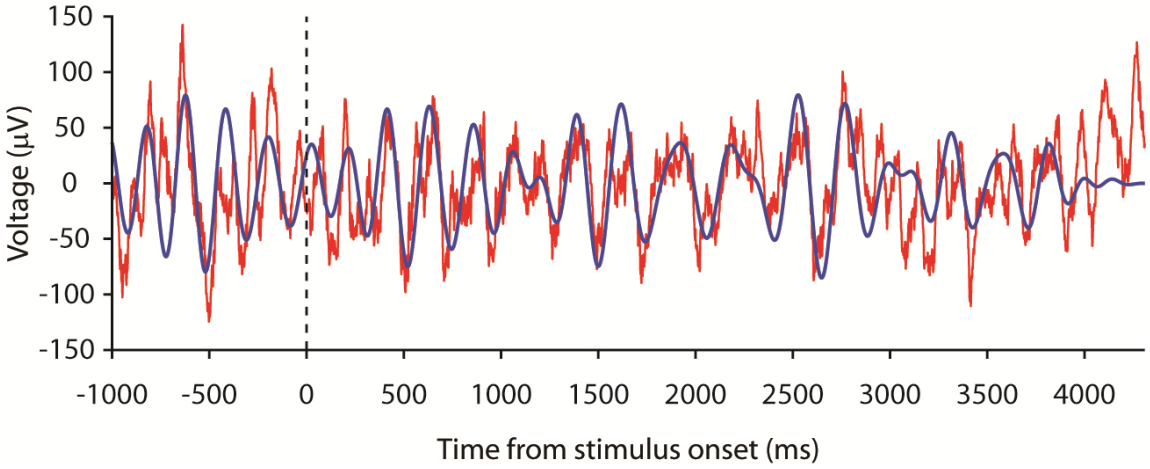

Figure 4.2: Example LFP trace showing theta activity. Unfiltered (red) and 3-6 Hz filtered (blue) LFP from a representative Novel trial, showing prominent theta-band oscillatory activity during stimulus exploration. The trial lasted approximately 4.3 seconds, until the monkey made a saccade outside the boundaries of the image.

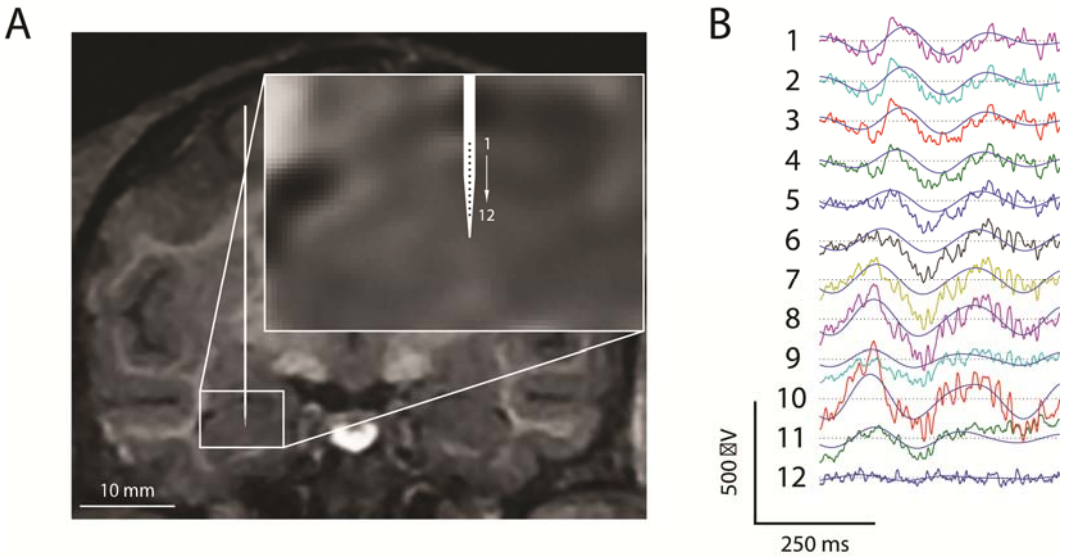

Figure 4.3: Axial array recording of theta-band oscillations across cell layers in the hippocampus. (A) Coronal MRI image of Monkey A showing the hippocampal formation with schematic of axial array electrode superimposed, showing the approximate location of each contact during a representative recording (location of array estimated using post-operative MRI scan in combination with coordinates obtained during recording). (B) Data obtained from hippocampal recording in the same monkey with axial array electrode located as shown in (A) during the exploration period of the VPLT. Unfiltered LFP traces obtained at each contact are shown along with the 3-8 Hz filtered LFPs in blue. A clear phase shift across contacts can be seen in the theta oscillation.

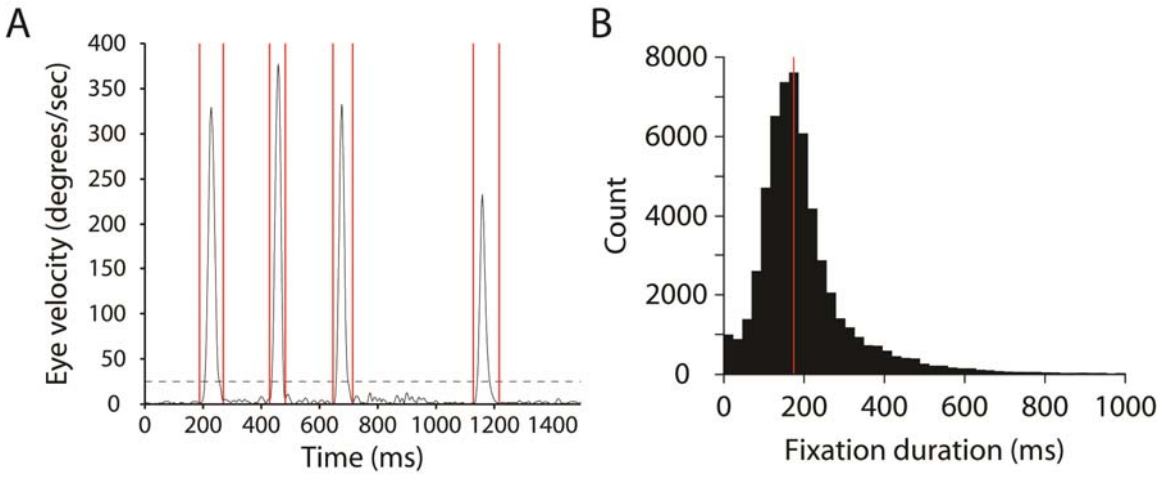

Figure 4.4: Saccade detection and inter-saccade intervals. (A) Representative eye velocity trace after low-pass filtering (40 Hz high-cut) showing four peaks in velocity, indicating the occurrence of saccades. Vertical red lines indicate the start and end of each saccade based on the algorithm used to define saccades. Dashed line: velocity threshold for defining saccades (25 degrees/sec). (B) Distribution of inter-saccade intervals for all Novel trials across 45 test sessions of the VPLT. Red line: median (177 ms).

during its first presentation with 2-20 fixations. These occurred with a median inter-saccade interval (i.e. fixation duration) of 177 ms (corresponding to a saccade frequency of 5.6 Hz; Figure 4.4B).

Interestingly, this exploratory saccade rate falls within the theta-frequency band, consistent with human behavior during scene perception tasks[229]. In order to identify whether saccades were related to rhythmic hippocampal activity, we transformed the LFP signal into a time-frequency representation by calculating the inter-saccade coherence on each channel, which represented the phase-locking of the LFP aligned to the end of each saccade (i.e. the beginning of each fixation period; Methods). Around the end of each saccade and initiation of the fixation period, there was a marked increase in inter-saccade coherence in the theta band (Figure 4.5A). These data suggest that upon each new fixation onset, the hippocampal LFP exhibited a change in oscillatory phase. This change

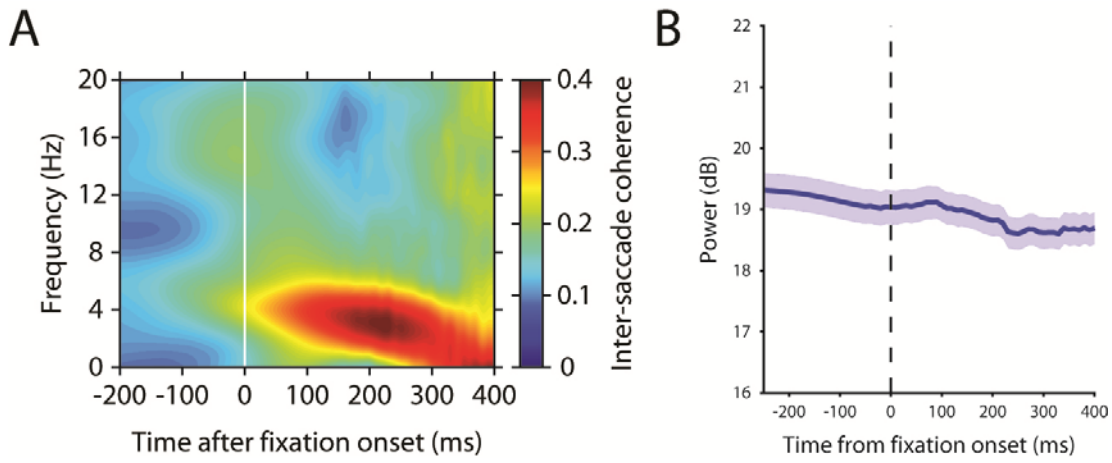

Figure 4.5: Theta-band phase resetting at fixation onset. (A) Inter-saccade coherence aligned to fixation onset, averaged across all hippocampal LFPs. (B) LFP theta-band power aligned to fixation onset. Average power in the theta-band (4-8 Hz) frequency range across 110 LFPs, aligned to fixation onset. Shaded area: SEM across LFPs. Power after fixation onset was not significantly higher than power before fixation onset ($p > 0.05$).

in theta-frequency oscillatory phase constituted a phase resetting in the LFP oscillation because each saccade occurred while an oscillation induced by a previously-occurring event was already underway and because there was no concomitant increase in power (Figure 4.5B)[230].

Neuronal ensembles generally oscillate at multiple frequencies simultaneously, and oscillations across frequencies are often correlated. For example, coupling between theta-band phase and gamma-band power is thought to coordinate processing across neuronal ensembles in multiple brain regions[143,144,231]. We tested for the presence of fixation-locked cross-frequency coupling in the monkey hippocampus by calculating, for each LFP, the coherence between gamma-band (30-90 Hz) power and LFP phase. Figure 4.6 depicts the average cross-frequency coherence across 110 LFPs, aligned to fixation onset. Cross-frequency coherence increased slightly before fixation onset and continued

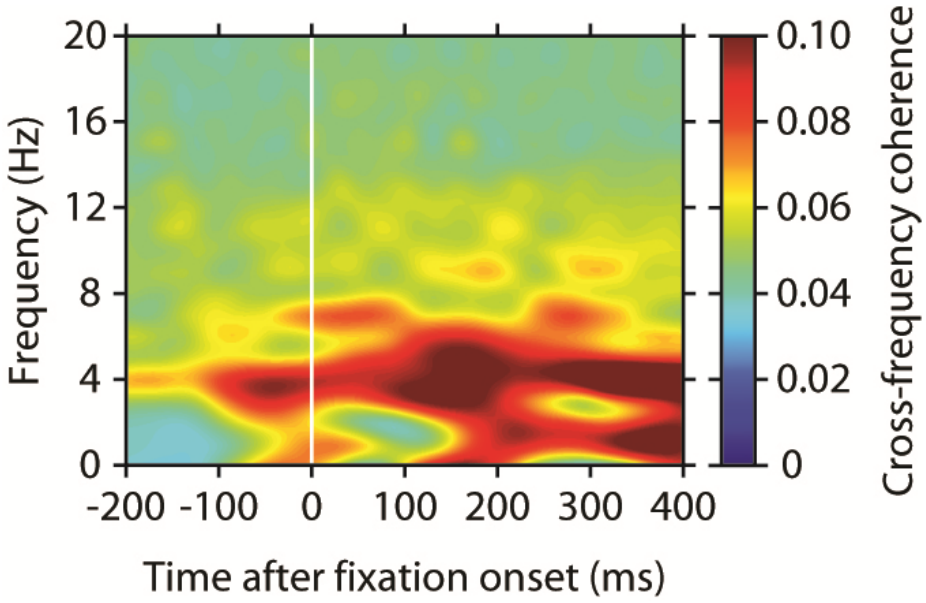

Figure 4.6: Gamma-band power is coherent with theta-band activity. Cross-frequency coupling between gamma-band (30-90 Hz) power and LFP phase, aligned to fixation onset, averaged across all hippocampal LFPs.

throughout the course of the fixation period, following a similar time-course as the increase in inter-saccade coherence. Because gamma-band power[228] and coherence[117,228] in the primate medial temporal lobe increases during successful memory formation, this increase in coupling between theta phase and gamma power could be a mechanism by which memory-related processes in the hippocampus are modulated by eye movements.

We next considered whether there was any relationship between these fixation-related modulations in neural activity and memory formation in terms of performance on the VPLT. Many factors affect the success of memory formation, including attention, arousal, and novelty, and the brain can become entrained to predictable stimulus presentation in a way that optimizes information processing[143]. Accordingly, we first examined the possibility that the absolute phase to which the LFP was reset upon fixation onset predicted encoding strength. We defined recognition memory strength as the

difference in looking times for the Novel and Repeat presentations, normalized to the looking time during the Novel presentation. We calculated the phase at fixation onset in the 3-8 Hz filtered LFP, during the Novel presentations of the 30 stimuli for which the monkey showed the best subsequent recognition memory (High Recognition) and the 30 stimuli for which the monkey showed the worst subsequent recognition memory (Low Recognition). Across the population, there was a significant difference in phase at fixation onset between trials with the best and worst subsequent memory performance. Trials with the best subsequent memory performance were associated with a phase of 326.4° +/- 36.5°, while trials with the worst subsequent memory performance were associated with a phase of 47.5° +/- 23.9°; these distributions were significantly different (non-parametric multi-sample test for equal medians, $p < 0.01$; Figure 4.7).

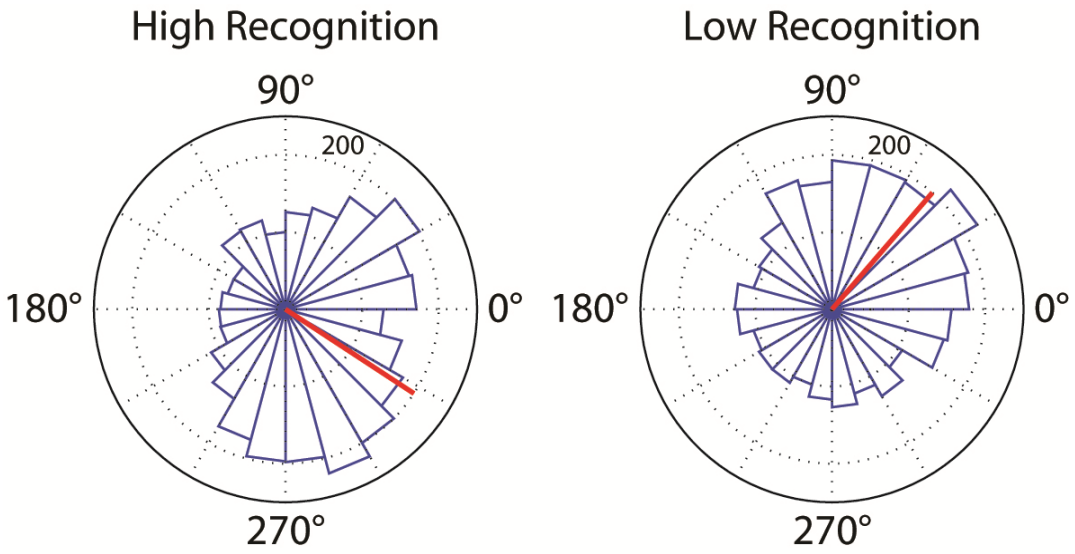

Figure 4.7: Theta-band phase-resetting at fixation onset is correlated with memory encoding. Distribution of instantaneous phases at fixation onset in theta-filtered (3-8 Hz) LFPs for High Recognition (left) and Low Recognition (right) trials, across all hippocampal LFPs. Red lines: mean phase for each distribution (High Recognition: 326.4°; Low Recognition: 47.5°). The peak of the theta-band oscillation occurs at 0°.

Second, we examined the relationship between single unit activity and theta-band oscillations in the LFP. It has been recently reported that neurons in the human hippocampus are phase-locked to the LFP in the theta band, and this phase-locking is predictive of memory performance[148]. We tested for theta-band phase-locking among neurons in the monkey hippocampus by calculating the spike-triggered spectrum for each single unit with the LFP recorded on the same electrode during stimulus presentation, and using a Rayleigh test[232] for significant spike-field phase-locking within the frequency range of interest. Any neuron with a *p* value less than 0.01 at any frequency range within the theta band (3-8 Hz) was considered significantly phase-locked. A substantial proportion of neurons (52, or 39.7% of total neurons) met this criterion (an example neuron is shown in Figure 4.8). Neurons had a range of phase preferences, with the

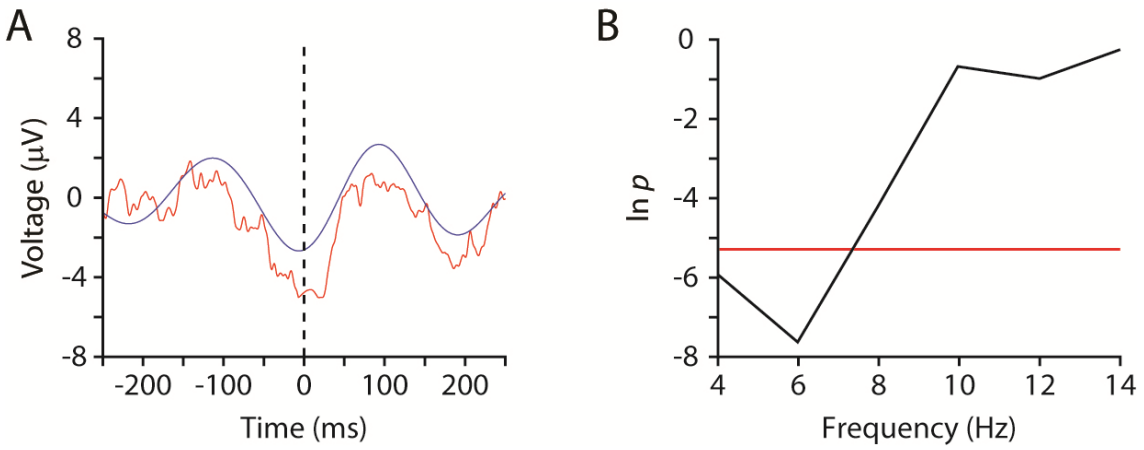

Figure 4.8: Hippocampal neurons are phase-locked to LFP theta. (A) Spike-triggered average LFP for a representative hippocampal neuron, showing prominent theta-band oscillatory activity surrounding each spike. Red: raw LFP; blue: 3-8 Hz filtered LFP. (B) Significance of phase-locking for the representative neuron shown in (A) as a function of frequency (natural logarithm plotted for visualization). Red line: Bonferroni-corrected threshold for significance of Rayleigh statistic ($p = 0.005$; 0.05/10).

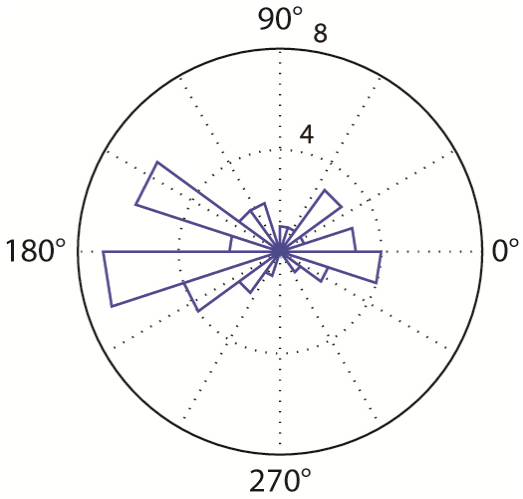

Figure 4.9: Theta-band phase preference of putative principal neurons. Distribution of preferred phases of all theta-locked putative principal neurons ($n = 42$), at the frequency for which each neuron showed the most phase-locking (highest significance from Rayleigh test).

majority of putative principal neurons firing close to the trough of the theta-frequency oscillation (Figure 4.9).

To determine whether theta-band phase-locking of hippocampal neurons during novel stimulus presentation was predictive of subsequent memory, we calculated the pairwise phase consistency (PPC) of each theta phase-locked neuron with its respective LFP, for High Recognition and Low Recognition stimuli. Pairwise phase consistency measures the phase synchronization between two signals. The expected PPC value is identical to the expected squared phase-locking value, while avoiding biases introduced into the latter by variable spike counts and trial lengths[226]. The PPC measures for the example neuron in Figure 4.8, calculated separately for High and Low Recognition trials, are shown in Figure 4.10A. In this example, and across all theta phase-locked neurons

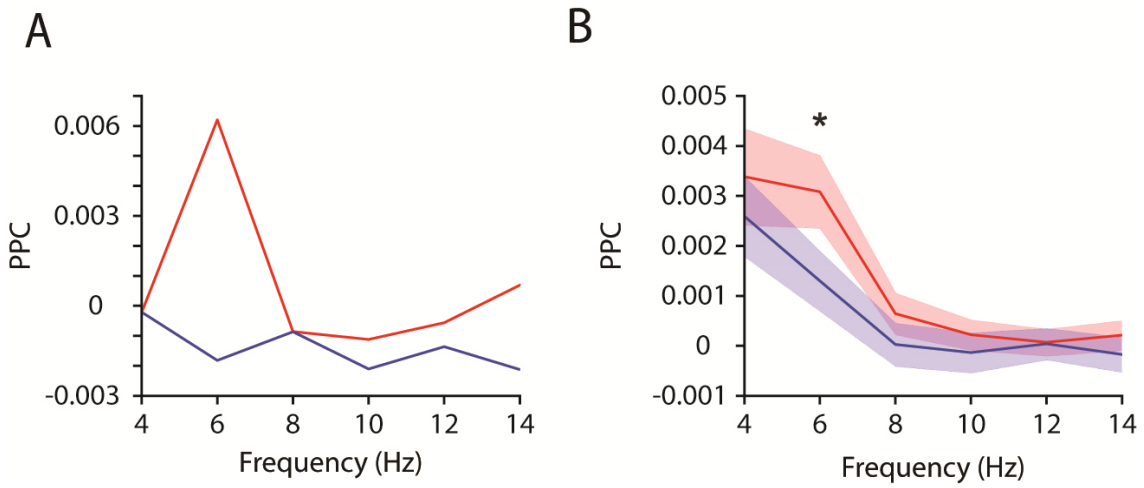

Figure 4.10: Theta-band phase synchronization between neurons and LFPs is correlated with recognition memory. (A) Pairwise phase consistency (PPC) as a function of frequency for the representative neuron shown in Figure 4.8 for the High Recognition (red) and Low Recognition (blue) conditions. (B) PPC as a function of frequency for the High Recognition (red) and Low Recognition (blue) condition averaged across all theta-locked putative principal neurons ($n = 42$). Shading represents SEM.

(Figure 4.10B), there was a significant increase in PPC for High Recognition trials compared with Low Recognition trials, indicating a significantly higher degree of phase-locking with the theta oscillation during successful memory formation (paired t-test, $p < 0.05$ at 6 Hz).

Discussion

What, then, is the functional significance of the theta rhythm in monkey hippocampus? The correlation with visual exploration suggests that this rhythm may play a role in "active sensing"[233], providing a mechanism for synchronizing ongoing hippocampal activity with incoming visual information. In particular, the phase resetting observed upon fixation onset may ensure that sensory input occurs at an "ideal" phase of the LFP theta-band oscillation, as suggested by the correlation between theta-band phase at fixation onset and performance on the memory task. Theta-band phase is thought to contain information related to memory encoding and retrieval[150], and neural stimulation in rat hippocampus can induce either LTP or LTD depending on the phase of the theta oscillation during stimulation[157,234], suggesting that the timing of spiking activity relative to the ongoing theta oscillation may play an important role in memory formation. In addition, studies in rats[147] and humans[144] have provided evidence that theta-band oscillations modulate gamma-band oscillations. We have previously shown that gamma-band phase synchronization between single unit activity and local field activity in the macaque hippocampus during encoding is predictive of subsequent recognition[228]. The current study provides evidence that these hippocampal processes are under the control of theta-rhythmic eye movements. Taken together, these data suggest that rhythmic activity

in the hippocampus is organized at multiple levels, is related to the strength of memory formation, and is intimately connected to the active exploration behavior of the animal.

Chapter 5

Discussion

In this dissertation, I present findings supporting involvement of the monkey hippocampus in recognition memory. I also provide data indicating potential mechanisms whereby hippocampal neurons, at the level of single cells and at the network level, may support the encoding of representations of visual information into memory. This chapter will provide an overview of the current findings and a general discussion of how these data relate to what is currently known concerning memory and its underlying physiological mechanisms.

Summary

The primary goals of this research project were twofold. The first goal was to investigate potential neural substrates for recognition memory in primate hippocampus as a way of characterizing the involvement of the hippocampus in this cognitive process. This goal was motivated by previous findings in humans and nonhuman primates which strongly supported a critical role for cortical areas of the MTL in memory but were more

ambiguous regarding the contribution of the hippocampus. Because these previous findings have often been highly dependent on the particular task used to assess recognition memory, there was a strong incentive to develop a specific task that is both sensitive to hippocampal damage and amenable to use in neurophysiological studies. The use of the VPLT was therefore chosen for all three experiments in this project, as it provided a way of comparing multiple measures of neural activity on a task paradigm that is known to involve the hippocampus.

The second goal of this project was to learn about the processes underlying memory encoding by investigating multiple, simultaneously-occurring neuronal mechanisms of information processing, some of which have only been fully appreciated in recent years. For instance, while it was certainly informative to analyze the firing rates of individual neurons and multi-unit activity as well as field oscillations recorded from microelectrodes, the technological and analytical tools we used to measure the intricate dynamics of local network processing are relatively recent developments, especially in primates. Investigations of neuronal synchronization have been ongoing for a number of years in the context of perception and attentional mechanisms in the brain[235-237], yet until recently, few studies had applied these methods to investigating the mechanisms underlying learning and memory[191,238]. This study provided a unique opportunity to not only analyze brain activity using classic methods of spike rate analysis and analysis of oscillatory power in field potentials, but also to rigorously investigate the precise timing of coordinated neuronal activity and its role in cognition. In order to accomplish these two goals, the experiments incorporating each of the three aims of this project were developed.

Encoding is modulated through neuronal spiking and network synchrony

For the first aim, we recorded spiking activity of neurons in the hippocampus as monkeys performed the VPLT and correlated rates of firing during stimulus presentation with behavioral measures. Unlike many previous studies, the VPLT uses stimuli which are completely novel to the monkey. We found that a substantial proportion of visually responsive neurons showed modulations in firing activity depending on whether the visual stimuli inducing this activity were novel or had been previously seen by the monkey. Most interestingly, the amplitude of this modulation was correlated with the degree of memory shown, such that greater evidence of recognition by the monkey was associated with a greater change in firing rate from the novel to the repeat presentation.

Chapter 3 of the current thesis addressed the third aim, in which we investigated gamma-band neuronal synchronization in the hippocampus during performance of the VPLT. Here, we found that spike-field coherence, both for single units and multi-unit activity, increased after the onset of novel stimuli in a manner that predicted how well these stimuli were subsequently remembered during the second presentation. Similar relationships were seen for spike-spike coherence and gamma-band LFP power, suggesting that different aspects of this neural network could synchronize in a manner that would facilitate memory formation. While there were indications of a linear correlation between gamma-band coherence during encoding and subsequent recognition, this correlation did not hold up when coherence was related to looking time during the presentation of novel stimuli, suggesting that this mechanism is related to encoding rather than interest in, or attention to, the stimuli.

Taken together with the first aim, these two main results provide a glimpse into possible mechanisms for memory storage in the brain. During the presentation of novel stimuli in the VPLT, visually responsive neurons exhibit changes in firing rates, while also modulating the timing of their spikes to increase phase synchronization with the underlying gamma oscillation in the LFP. This process could contribute to spike timing-dependent long-term potentiation[109], thereby strengthening associations among neurons encoding a representation of the stimulus into memory. This in turn would result in modulation of neuronal firing rates when the stimulus is presented a second time and the memory is accessed. Alternatively, gamma-band synchronization among multiple neurons (as measured, for example, through spike-spike coherence) may serve to enhance the impact of hippocampal neurons on downstream targets in the entorhinal cortex or other output regions through increased temporal summation of synaptic input, thus strengthening pathways important for information storage in other parts of the brain. Interestingly, the time-course of this enhancement was extremely similar to gamma-band synchronization seen in between the hippocampus and rhinal cortex in humans, using a similar behavioral paradigm[117] (Figure 5.1). This suggests that gamma-band synchronization may reflect a basic mechanism for the neuronal interactions that are critical for successful memory encoding.

Active sensing and the role of hippocampal theta in memory

The second aim, addressed in the fourth chapter of this thesis, dealt with mechanisms related to oscillatory LFP activity. The theta-band activity we observed during visual exploration of images in the VPLT underwent a phase reset with the onset

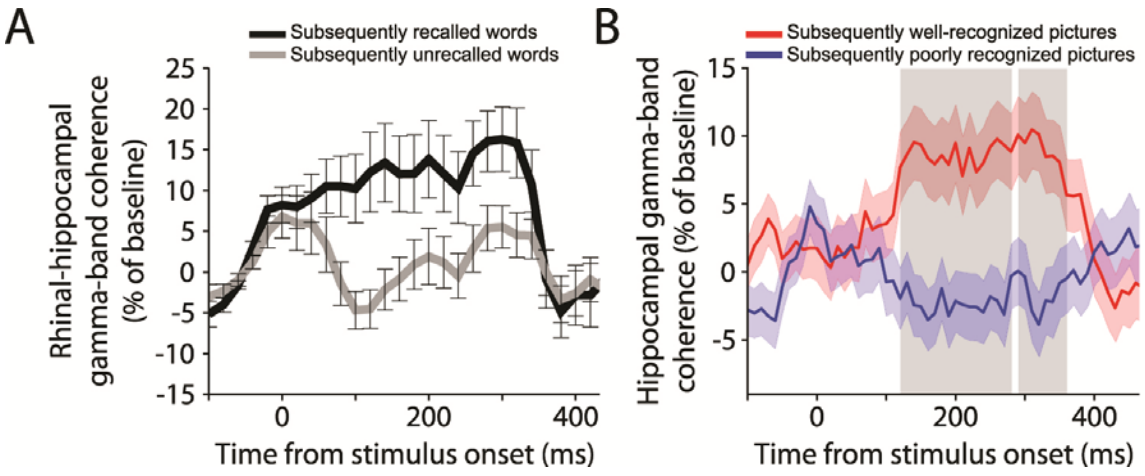

Figure 5.1: Gamma-band synchronization in the medial temporal lobe during memory encoding is associated with the degree of subsequent recognition. (A) Gamma-band phase synchronization (coherence) between the human hippocampus and the rhinal cortex during word study, as a function of time from stimulus onset. Coherence was significantly higher during the encoding of words that are subsequently recalled (black) than for words that were not later recalled (gray). Error bars indicate SEM. Modified from Fell et al., 2001. (B) Gamma-band spike-field coherence in the monkey hippocampus during the encoding of pictures, as a function of time from stimulus onset. Coherence was significantly higher for stimuli which monkeys subsequently showed a high degree of recognition (red) than for stimuli which were not well recognized (blue). Red and blue shaded areas represent SEM. Gray shaded area represents time points at which gamma-band coherence was significantly different for the two conditions ($p < 0.01$). Modified from Jutras et al., 2009.

of each fixation period after the monkey made a saccade. Interestingly, the phase of the theta oscillation at fixation onset was correlated with memory performance, with certain phases being more conducive to subsequent recognition than others. While similar effects have been seen in other areas of the brain, such as visual cortex[153], where an "ideal" phase was predictive of subsequently higher firing activity, in this case we observed correlations between theta phase and both gamma band power and single unit firing activity in the hippocampus. These, in turn, were tied to behavior through the relationship between theta-band oscillations and eye movements.

These data may give some clue as to the effectiveness of the VPLT in evoking hippocampal activity, since unlike tasks which have typically been used in neurophysiology experiments to record memory signals, the VPLT allows for free exploration of images. The case has been made that exploration of the environment, whether through visual or somatosensory methods, occurs through "active sensing" which is largely determined through motor or attentional sampling routines, and is rhythmic in nature[233]. It is possible that in this respect, the theta rhythm which we observed to modulate other modes of neuronal activity actually provides a mechanism for synchronizing ongoing hippocampal activity with incoming visual information, which is obtained in a rhythmic nature during VPLT performance through saccadic eye movements. In particular, the theta-band phase resetting observed upon fixation onset may ensure that sensory input occurs at an "ideal" phase of the LFP theta-band oscillation, as suggested by the correlation between theta-band phase at fixation onset and performance on the memory task. Recent studies have shown multiple processes in the brain that are modulated by the hippocampal theta rhythm[147,149,239], as well as links between hippocampal theta and behavior in the human[148,223]. Our findings suggest that in the primate, hippocampal theta-band oscillations and the processes they regulate are under the control of theta-rhythmic eye movements.

While these findings pertain to the relationship between hippocampal theta-band oscillations, saccadic eye movements in the primate, and recognition memory, they also hint at the possibility of such a relationship in other mammalian species in which hippocampal theta-band oscillations have been studied. For example, previous studies of hippocampal theta in the rodent, incorporating modeling with electrophysiological

methods, have suggested that this oscillation actually consists of distinct functional phases, allowing for the temporal segregation of neural processes related to memory encoding and retrieval[147,150]. Thus, encoding of new memories optimally occurs when synaptic input from the entorhinal cortex to the hippocampus is in phase with the oscillatory changes that induce long-term potentiation of synaptic inputs from CA3 to CA1, while activity related to memory retrieval, i.e. synaptic current from CA3, occurs out of phase with encoding-related processes in order to reduce interference from previously-encoded information[150]. This proposed relationship between theta-band phase and memory encoding/retrieval is consistent with several phenomena that have been observed in the rodent. For example, theta phase precession, in which the firing of a hippocampal place cell systematically advances to earlier phases of the ongoing theta oscillation as the animal moves through the cell's place field[240,241], may be interpreted as the shift from retrieval-related processing (as the animal approaches the place field) to encoding-related processing driven by sensory information when the animal is within the place field[150]. Other examples of coordination between behavioral events and specific phases of hippocampal theta include the phase-resetting of theta-band oscillations with the onset of visual or auditory stimuli in a working memory task[151] and the locking of sniff cycles to particular phases of hippocampal theta in rodents[225]. If optimal encoding is associated with a specific phase of the hippocampal theta-band oscillation, then these instances of phase-locking between hippocampal theta and behavioral processes or events relevant to memory encoding may serve to time the arrival of sensory information into the hippocampus precisely at this ideal phase of the theta oscillation. Furthermore, rhythmic exploratory behaviors occurring in the theta frequency range in the rodent, such

as sniffing[225] and whisking[242], may occur synchronously with the hippocampal theta-band oscillation, and thus may be analogous to the active sensing mechanisms utilized by the visual system in primates. Taken together with previous findings, the results from this aim suggest that the hippocampal theta oscillation serves the common purpose of providing a temporal background to organize sensory information during exploration in a way that ensures the optimal encoding, and later retrieval, of this information.

Future directions

In this thesis, I have described a series of experiments in which certain modes of neuronal activity in the hippocampus are correlated with performance on a recognition memory task. While the implication of these results is fairly broad in terms of what they may tell us about the network activity underlying memory storage in the brain, there are still a number of questions that arise. While the activity I have described here is associated entirely with hippocampal circuitry, it is important to bear in mind that the hippocampus does not function in isolation, but is in fact part of a system which mediates the continuous transfer of information to and from the hippocampus, for instance through the entorhinal cortex, as memories are stored and accessed. A greater understanding of the role of coherent network activity would thus be informed by paired recordings in the hippocampus and the entorhinal cortex, in order to ascertain whether increasing synchrony in the hippocampus has any downstream effect via feedforward pathways from the hippocampus back to the deep layers of the entorhinal cortex.

While the current findings regarding the functional implications of enhanced hippocampal synchronization for learning and memory are correlational in nature, they

do provide insight as to the specific mechanisms that may underlie normal memory function, thus offering a potential target for detection of cognitive impairment as well as for therapeutic intervention in future translational and clinical studies. Future studies in this realm may involve experimentally enhancing or reducing synchronization, perhaps by taking advantage of modulations in phase resetting. Alternatively, there are a number of already existing models of memory loss where insights gathered from the study of synchronous activity during active sensing may inform our understanding of what is happening in the brain when memory becomes deficient. Studies such as these may offer great promise for predicting the onset of memory loss and developing therapies for treating patients suffering from these deficits.

References

1 Hebb, D. O. *The organization of behavior; a neuropsychological theory*. (Wiley, 1949).

2 Bliss, T. V. & Lomo, T. Long-lasting potentiation of synaptic transmission in the dentate area of the anaesthetized rabbit following stimulation of the perforant path. *J Physiol* **232**, 331-356, (1973).

3 von Bechterew, W. Demonstration eines gehirns mit zerstörung der vorderen und inneren theile der hirnrinde beider schläfenlappen. *Neurologische Zeitenblatte* **19**, 990-991, (1900).

4 Glees, P. & Griffith, H. B. Bilateral destruction of the hippocampus (cornu ammonis) in a case of dementia. *Monatsschr Psychiatr Neurol* **123**, 193-204, (1952).

5 Grünthal, E. Über das klinische Bild nach umschriebenem beiderseitigem Ausfall der Ammonshornrinde. *Monatsschr Psychiatr Neurol* **113**, 1-16, (1947).

6 Hegglin, K. Über einen Fall von isolierter linkseitiger Ammonshornerweichung bei präseniler Dementz. *Monatsschr Psychiatr Neurol* **125**, 170-186, (1953).

7 Scoville, W. B. The Limbic Lobe in Man. *J Neurosurg* **11**, 64-66, (1954).

8 Scoville, W. B. & Milner, B. Loss of recent memory after bilateral hippocampal lesions. *J Neurochem* **20**, 11-21, (1957).

9 Knowlton, B. J., Mangels, J. A. & Squire, L. R. A Neostriatal Habit Learning System in Humans. *Science* **273**, 1399-1402, (1996).

10 Orbach, J., Milner, B. & Rasmussen, T. Learning and Retention in Monkeys After Amygdala-Hippocampus Resection. *Arch Neurol* **3**, 230-251, (1960).

11 Kimble, D. P. The effects of bilateral hippocampal lesions in rats. *J Comp Physiol Psychol* **56**, 273-283, (1963).

12 Milner, B. Disorders of learning and memory after temporal lobe lesions in man. *Clinical neurosurgery* **19**, 421-446, (1972).

13 Bayley, P. J., Frascino, J. C. & Squire, L. R. Robust habit learning in the absence of awareness and independent of the medial temporal lobe. *Nature* **436**, 550-553, (2005).

14 Mishkin, M., Malamut, B. & Bachevalier, J. in *Neurobiology of human learning and memory* (eds G. Lynch, J. L. McGaugh, & N. M. Weinberger) 65-77 (Guilford, 1984).

15 Teng, E., Stefanacci, L., Squire, L. R. & Zola, S. M. Contrasting Effects on Discrimination Learning after Hippocampal Lesions and Conjoint Hippocampal-Caudate Lesions in Monkeys. *J Neurosci* **20**, 3853-3863, (2000).

16 Gaffan, D. Recognition impaired and association intact in the memory of monkeys after transection of the fornix. *J Comp Physiol Psychol* **86**, 1100-1109, (1974).

17 Mishkin, M. & Delacour, J. An analysis of short-term visual memory in the monkey. *J Exp Psychol Anim Behav Process* **1**, 326-334, (1975).

18 Meunier, M., Hadfield, W., Bachevalier, J. & Murray, E. A. Effects of rhinal cortex lesions combined with hippocampectomy on visual recognition memory in rhesus monkeys. *J Neurophysiol* **75**, 1190-1205, (1996).

19 Zola-Morgan, S., Squire, L., Clower, R. & Rempel, N. Damage to the perirhinal cortex exacerbates memory impairment following lesions to the hippocampal formation. *J Neurosci* **13**, 251-265, (1993).

20 Mishkin, M. Memory in monkeys severely impaired by combined but not by separate removal of amygdala and hippocampus. *Nature* **273**, 297-298, (1978).

21 Murray, E. & Mishkin, M. Severe tactual as well as visual memory deficits follow combined removal of the amygdala and hippocampus in monkeys. *J Neurosci* **4**, 2565-2580, (1984).

22 Murray, E. & Mishkin, M. Visual recognition in monkeys following rhinal cortical ablations combined with either amygdalectomy or hippocampectomy. *J Neurosci* **6**, 1991-2003, (1986).

23 Mahut, H., Zola-Morgan, S. & Moss, M. Hippocampal resections impair associative learning and recognition memory in the monkey. *J Neurosci* **2**, 1214-1220, (1982).

24 Zola-Morgan, S. & Squire, L. R. Medial temporal lesions in monkeys impair memory on a variety of tasks sensitive to human amnesia. *Behav Neurosci* **99**, 22-34, (1985).

25 Zola-Morgan, S. & Squire, L. R. Memory impairment in monkeys following lesions limited to the hippocampus. *Behav Neurosci* **100**, 155-160, (1986).

26 Fantz, R. A method for studying early visual development. *Perceptual and Motor Skills* **6**, 13-16, (1956).

27 Fagan, J. F. Memory in the infant. *J Exp Child Psychol* **9**, 217-226, (1970).

28 Gunderson, V. M. & Sackett, G. P. Development of pattern recognition in infant pigtailed macaques (Macaca nemestrina). *Developmental Psychology* **20**, 418-426, (1984).

29 Ennaceur, A. & Delacour, J. A new one-trial test for neurobiological studies of memory in rats. 1: Behavioral data. *Behav Brain Res* **31**, 47-59, (1988).

30 McKee, R. D. & Squire, L. R. On the development of declarative memory. *J Exp Psychol Learn Mem Cogn* **19**, 397-404, (1993).

31 Pascalis, O. & Bachevalier, J. Neonatal aspiration lesions of the hippocampal formation impair visual recognition memory when assessed by paired-comparison task but not by delayed nonmatching-to-sample task. *Hippocampus* **9**, 609-616, (1999).

32 Bachevalier, J., Brickson, M. & Hagger, C. Limbic-dependent recognition memory in monkeys develops early in infancy. *NeuroReport* **4**, 77-80, (1993).

33 Zola, S. M. *et al.* Impaired recognition memory in monkeys after damage limited to the hippocampal region. *J Neurosci* **20**, 451-463, (2000).

34 Clark, R. E., Zola, S. M. & Squire, L. R. Impaired recognition memory in rats after damage to the hippocampus. *J Neurosci* **20**, 8853-8860, (2000).

35 Suzuki, W. A. & Amaral, D. G. Topographic organization of the reciprocal connections between the monkey entorhinal cortex and the perirhinal and parahippocampal cortices. *J Neurosci* **14**, 1856, (1994).

36 Suzuki, W. A. & Amaral, D. G. Perirhinal and parahippocampal cortices of the macaque monkey: cortical afferents. *J Comp Neurol* **350**, 497, (1994).

37 Witter, M. P. & Amaral, D. G. Entorhinal cortex of the monkey: V. Projections to the dentate gyrus, hippocampus, and subicular complex. *J Comp Neurol* **307**, 437-459, (1991).

38 Witter, M. P., Van Hoesen, G. W. & Amaral, D. G. Topographical organization of the entorhinal projection to the dentate gyrus of the monkey. *J Neurosci* **9**, 216-228, (1989).

39 Zola-Morgan, S., Squire, L., Amaral, D. & Suzuki, W. Lesions of perirhinal and parahippocampal cortex that spare the amygdala and hippocampal formation produce severe memory impairment. *J. Neurosci.* **9**, 4355-4370, (1989).

40 Meunier, M., Bachevalier, J., Mishkin, M. & Murray, E. A. Effects on visual recognition of combined and separate ablations of the entorhinal and perirhinal cortex in rhesus monkeys. *J Neurosci* **13**, 5418-5432, (1993).

41 Suzuki, W., Zola-Morgan, S., Squire, L. & Amaral, D. Lesions of the perirhinal and parahippocampal cortices in the monkey produce long-lasting memory impairment in the visual and tactual modalities. *J. Neurosci.* **13**, 2430-2451, (1993).

42 Nemanic, S., Alvarado, M. C. & Bachevalier, J. The hippocampal/parahippocampal regions and recognition memory: insights from visual paired comparison versus object-delayed nonmatching in monkeys. *J Neurosci* **24**, 2013-2026, (2004).

43 Buffalo, E. A. *et al.* Dissociation between the effects of damage to perirhinal cortex and area TE. *Learning & Memory* **6**, 572, (1999).

44 Murray, E. A. & Mishkin, M. Object Recognition and Location Memory in Monkeys with Excitotoxic Lesions of the Amygdala and Hippocampus. *J Neurosci* **18**, 6568-6582, (1998).

45 Baxter, M. G. & Murray, E. A. Opposite relationship of hippocampal and rhinal cortex damage to delayed nonmatching-to-sample deficits in monkeys. *Hippocampus* **11**, 61-71, (2001).

46 Beason-Held, L. L., Rosene, D. L., Killiany, R. J. & Moss, M. B. Hippocampal formation lesions produce memory impairment in the rhesus monkey. *Hippocampus* **9**, 562-574, (1999).

47 Zola, S. M. & Squire, L. R. Relationship between magnitude of damage to the hippocampus and impaired recognition memory in monkeys. *Hippocampus* **11**, 92-98, (2001).

48 Baxter, M. G. & Murray, E. A. Effects of hippocampal lesions on delayed nonmatching-to-sample in monkeys: A reply to Zola and Squire (2001). *Hippocampus* **11**, 201-203, (2001).

49 Pascalis, O., Hunkin, N. M., Holdstock, J. S., Isaac, C. L. & Mayes, A. R. Visual paired comparison performance is impaired in a patient with selective hippocampal lesions and relatively intact item recognition. *Neuropsychologia* **42**, 1293-1300, (2004).

50 Manns, J. R., Stark, C. E. L. & Squire, L. R. The visual paired-comparison task as a measure of declarative memory. *Proc Natl Acad Sci U S A* **97**, 12375-12379, (2000).

51 Brown, M. W. & Aggleton, J. P. Recognition memory: What are the roles of the perirhinal cortex and hippocampus? *Nat Rev Neurosci* **2**, 51-61, (2001).

52 Eichenbaum, H., Otto, T. & Cohen, N. J. Two functional components of the hippocampal memory system. *Behav Brain Sci* **17**, 449-472, (1994).

53 O'Keefe, J. & Nadel, L. *The Hippocampus as a Cognitive Map*. (Oxford University Press, 1978).

54 Stark, C. E. L., Bayley, P. J. & Squire, L. R. Recognition Memory for Single Items and for Associations Is Similarly Impaired Following Damage to the Hippocampal Region. *Learning & Memory* **9**, 238-242, (2002).

55 Wirth, S. *et al.* Single Neurons in the Monkey Hippocampus and Learning of New Associations. *Science* **300**, 1578-1581, (2003).

56 Wilson, F. A. W. & Goldman-Rakic, P. S. Viewing preferences of rhesus monkeys related to memory for complex pictures, colours and faces. *Behav Brain Res* **60**, 79-89, (1994).

57 Gross, C. G. in *Handbook of Sensory Physiology* Vol. 7, Part 3B (ed R. Jung) 451-482 (Springer-Verlag, 1973).

58 Saul, L. J. & Davis, H. Action currents in the central nervous system. *Arch Neurol Psychiatry* **29**, 255-259, (1933).

59 Jung, R. & Kornmüller, A. Eine methodik der ableitung lokalisierter potential schwankingen aus subcorticalen hirnyebieten. *Arch Psychiat Neruenkr* **109**, 1-30, (1938).

60 Renshaw, B., Forbes, A. & Morison, B. R. Activity of isocortex and hippocampus: electrical studies with micro-electrodes. *J Neurophysiol* **3**, 74-105, (1940).

61 Cragg, B. G. & Hamlyn, L. H. Action potentials of the pyramidal neurones in the hippocampus of the rabbit. *J Physiol* **129**, 608-627, (1955).

62 Cragg, B. G. & Hamlyn, L. H. Some commissural and septal connexions of the hippocampus in the rabbit. A combined histological and electrical study. *J Physiol* **135**, 460-485, (1957).

63 Rolls, E. T. A theory of hippocampal function in memory. *Hippocampus* **6**, 601-620, (1996).

64 Bennett, M. R., Gibson, W. G. & Robinson, J. Dynamics of the CA3 Pyramidal Neuron Autoassociative Memory Network in the Hippocampus. *Philosophical Transactions of the Royal Society of London. Series B: Biological Sciences* **343**, 167-187, (1994).

65 Buckmaster, P. S. & Soltesz, I. Neurobiology of hippocampal interneurons: A workshop review. *Hippocampus* **6**, 330-339, (1996).

66 Cobb, S. R., Buhl, E. H., Halasy, K., Paulsen, O. & Somogyi, P. Synchronization of neuronal activity in hippocampus by individual GABAergic interneurons. *Nature* **378**, 75-78, (1995).

67 Aika, Y., Ren, J. Q., Kosaka, K. & Kosaka, T. Quantitative analysis of GABA-like-immunoreactive and parvalbumin-containing neurons in the CA1 region of the rat hippocampus using a stereological method, the disector. *Exp Brain Res* **99**, 267-276, (1994).

68 Woodson, W., Nitecka, L. & Ben-Ari, Y. Organization of the GABAergic system in the rat hippocampal formation: A quantitative immunocytochemical study. *J Comp Neurol* **280**, 254-271, (1989).

69 Halasy, K., Buhl, E. H., Lörinczi, Z., Tamás, G. & Somogyi, P. Synaptic target selectivity and input of GABAergic basket and bistratified interneurons in the CA1 area of the rat hippocampus. *Hippocampus* **6**, 306-329, (1996).

70 Li, X. G., Somogyi, P., Tepper, J. M. & Buzsáki, G. Axonal and dendritic arborization of an intracellularly labeled chandelier cell in the CA1 region of rat hippocampus. *Exp Brain Res* **90**, 519-525, (1992).

71 Sik, A., Penttonen, M., Ylinen, A. & Buzsaki, G. Hippocampal CA1 interneurons: an in vivo intracellular labeling study. *J Neurosci* **15**, 6651-6665, (1995).

72 Whittington, M. A., Traub, R. D. & Jefferys, J. G. R. Synchronized oscillations in interneuron networks driven by metabotropic glutamate receptor activation. *Nature* **373**, 612-615, (1995).

73 Traub, R. D. *et al.* Gap Junctions between Interneuron Dendrites Can Enhance Synchrony of Gamma Oscillations in Distributed Networks. *J Neurosci* **21**, 9478-9486, (2001).

74 Traub, R. D., Schmitz, D., Jefferys, J. G. R. & Draguhn, A. High-frequency population oscillations are predicted to occur in hippocampal pyramidal neuronal networks interconnected by axoaxonal gap junctions. *Neuroscience* **92**, 407-426, (1999).

75 Buzsaki, G. & Chrobak, J. J. Temporal structure in spatially organized neuronal ensembles: a role for interneuronal networks. *Curr Opin Neurobiol* **5**, 504-510, (1995).

76 Ranck, J. B., Jr. Studies on single neurons in dorsal hippocampal formation and septum in unrestrained rats. I. Behavioral correlates and firing repertoires. *Exp Neurol* **41**, 461-531, (1973).

77 O'Keefe, J. & Dostrovsky, J. The hippocampus as a spatial map. Preliminary evidence from unit activity in the freely-moving rat. *Brain Research* **34**, 171-175, (1971).

78 Fox, S. E. & Ranck Jr, J. B. Localization and anatomical identification of theta and complex spike cells in dorsal hippocampal formation of rats. *Exp Neurol* **49**, 299-313, (1975).

79 Skaggs, W. E. *et al.* EEG Sharp Waves and Sparse Ensemble Unit Activity in the Macaque Hippocampus. *J Neurophysiol* **98**, 898-910, (2007).

80 Viskontas, I. V., Ekstrom, A. D., Wilson, C. L. & Fried, I. Characterizing interneuron and pyramidal cells in the human medial temporal lobe in vivo using extracellular recordings. *Hippocampus* **17**, 49-57, (2007).

81 Horel, J. A. The neuroanatomy of amnesia. *Brain* **101**, 403-445, (1978).

82 Gaffan, D. Hippocampus: Memory, Habit and Voluntary Movement. *Philosophical Transactions of the Royal Society of London. B, Biological Sciences* **308**, 87-99, (1985).

83 Squire, L. R. Mechanisms of memory. *Science* **232**, 1612-1619, (1986).

84 Weiskrantz, L. Comparative Aspects of Studies of Amnesia. *Philosophical Transactions of the Royal Society of London. B, Biological Sciences* **298**, 97-109, (1982).

85 Miller, E. K., Li, L. & Desimone, R. A neural mechanism for working and recognition memory in inferior temporal cortex. *Science* **254**, 1377-1379, (1991).

86 Miller, E. K., Li, L. & Desimone, R. Activity of neurons in anterior inferior temporal cortex during a short-term memory task. *J Neurosci* **13**, 1460, (1993).

87 Suzuki, W. A., Miller, E. K. & Desimone, R. Object and place memory in the macaque entorhinal cortex. *J Neurophysiol* **78**, 1062-1081, (1997).

88 Riches, I. P., Wilson, F. A. W. & Brown, M. W. The effects of visual stimulation and memory on neurons of the hippocampal formation and the neighboring parahippocampal gyrus and inferior temporal cortex of the primate. *J Neurosci* **11**, 1763-1779, (1991).

89 Brown, M. W., Wilson, F. A. W. & Riches, I. P. Neuronal evidence that inferomedial temporal cortex is more important than hippocampus in certain processes underlying recognition memory. *Brain Research* **409**, 158-162, (1987).

90 Wilson, F. A. W., Brown, M. W. & Riches, I. P. in *Cellular Mechanisms of Conditioning and Behavioral Plasticity* (eds C. D. Woody, D. L. Alkon, & J. L. McGaugh) 313-328 (Plenum, 1988).

91 Wilson, F. A., Riches, I. P. & Brown, M. W. Hippocampus and medial temporal cortex: neuronal activity related to behavioural responses during the performance of memory tasks by primates. *Behav Brain Res* **40**, 7-28, (1990).

92 Xiang, J. Z. & Brown, M. W. Differential neuronal encoding of novelty, familiarity and recency in regions of the anterior temporal lobe. *Neuropharmacology* **37**, 657-676, (1998).

93 Rolls, E. T., Cahusac, P. M. B., Feigenbaum, J. D. & Miyashita, Y. Responses of single neurons in the hippocampus of the macaque related to recognition memory. *Exp Brain Res* **93**, 299-306, (1993).

94 Sobotka, S. & Ringo, J. L. Investigation of long-term recognition and association memory in unit responses from inferotemporal cortex. *Exp Brain Res* **96**, 28-38, (1993).

95 Miller, E. K. & Desimone, R. Parallel neuronal mechanisms for short-term memory. *Science* **263**, 520, (1994).

96 Colombo, M. & Gross, C. G. Responses of Inferior Temporal Cortex and Hippocampal Neurons During Delayed Matching to Sample in Monkeys (Macaca fascicularis). *Behav Neurosci* **108**, 443-455, (1994).

97 Rolls, E. T. *et al.* Hippocampal neurons in the monkey with activity related to the place in which a stimulus is shown. *J Neurosci* **9**, 1835-1845, (1989).

98 Hampson, R. E., Pons, T. P., Stanford, T. R. & Deadwyler, S. A. Categorization in the monkey hippocampus: A possible mechanism for encoding information into memory. *Proc Natl Acad Sci U S A* **101**, 3184-3189, (2004).

99 Porrino, L. J., Daunais, J. B., Rogers, G. A., Hampson, R. E. & Deadwyler, S. A. Facilitation of task performance and removal of the effects of sleep deprivation by an ampakine (CX717) in nonhuman primates. *PLoS Biology* **3**, e299, (2005).

100 Rutishauser, U., Mamelak, A. N. & Schuman, E. M. Single-trial learning of novel stimuli by individual neurons of the human hippocampus-amygdala complex. *Neuron* **49**, 805-813, (2006).

101 Mitzdorf, U. Current source-density method and application in cat cerebral cortex: investigation of evoked potentials and EEG phenomena. *Physiol Rev* **65**, 37-100, (1985).

102 Mitzdorf, U. Properties of the evoked potential generators: current source-density analysis of visually evoked potentials in the cat cortex. *Int J Neurosci* **33**, 33-59, (1987).

103 Kamondi, A., Acsady, L., Wang, X. J. & Buzsaki, G. Theta oscillations in somata and dendrites of hippocampal pyramidal cells in vivo: activity-dependent phase-precession of action potentials. *Hippocampus* **8**, 244-261, (1998).

104 Buzsaki, G. & Kandel, A. Somadendritic backpropagation of action potentials in cortical pyramidal cells of the awake rat. *J Neurophysiol* **79**, 1587-1591, (1998).

105 Gustafsson, B. Afterpotentials and transduction properties in different types of central neurones. *Arch Ital Biol* **122**, 17-30, (1984).

106 Caporale, N. & Dan, Y. Spike timing-dependent plasticity: a Hebbian learning rule. *Annu Rev Neurosci* **31**, 25-46, (2008).

107 Zhang, L. I., Tao, H. W., Holt, C. E., Harris, W. A. & Poo, M. A critical window for cooperation and competition among developing retinotectal synapses. *Nature* **395**, 37-44, (1998).

108 Levy, W. B. & Steward, O. Temporal contiguity requirements for long-term associative potentiation/depression in the hippocampus. *Neuroscience* **8**, 791-797, (1983).

109 Bi, G. Q. & Poo, M. M. Synaptic modifications in cultured hippocampal neurons: dependence on spike timing, synaptic strength, and postsynaptic cell type. *J Neurosci* **18**, 10464-10472, (1998).

110 Debanne, D., Gahwiler, B. H. & Thompson, S. M. Long-term synaptic plasticity between pairs of individual CA3 pyramidal cells in rat hippocampal slice cultures. *J Physiol* **507 (Pt 1)**, 237-247, (1998).

111 Markram, H., Lubke, J., Frotscher, M. & Sakmann, B. Regulation of synaptic efficacy by coincidence of postsynaptic APs and EPSPs. *Science* **275**, 213-215, (1997).

112 Rao, R. P. & Sejnowski, T. J. Spike-timing-dependent Hebbian plasticity as temporal difference learning. *Neural Computation* **13**, 2221-2237, (2001).

113 Froemke, R. C., Poo, M. M. & Dan, Y. Spike-timing-dependent synaptic plasticity depends on dendritic location. *Nature* **434**, 221-225, (2005).

114 Sjostrom, P. J. & Hausser, M. A cooperative switch determines the sign of synaptic plasticity in distal dendrites of neocortical pyramidal neurons. *Neuron* **51**, 227-238, (2006).

115 Letzkus, J. J., Kampa, B. M. & Stuart, G. J. Learning rules for spike timing-dependent plasticity depend on dendritic synapse location. *J Neurosci* **26**, 10420-10429, (2006).

116 Gruber, T., Tsivilis, D., Montaldi, D. & Muller, M. M. Induced gamma band responses: an early marker of memory encoding and retrieval. *Neuroreport* **15**, 1837-1841, (2004).

117 Fell, J. *et al.* Human memory formation is accompanied by rhinal-hippocampal coupling and decoupling. *Nat Neurosci* **4**, 1259-1264, (2001).

118 Sederberg, P. B., Kahana, M. J., Howard, M. W., Donner, E. J. & Madsen, J. R. Theta and gamma oscillations during encoding predict subsequent recall. *J Neurosci* **23**, 10809-10814, (2003).

119 Csicsvari, J., Jamieson, B., Wise, K. D. & Buzsaki, G. Mechanisms of gamma oscillations in the hippocampus of the behaving rat. *Neuron* **37**, 311-322, (2003).

120 Hajos, N. & Paulsen, O. Network mechanisms of gamma oscillations in the CA3 region of the hippocampus. *Neural Netw* **22**, 1113-1119, (2009).

121 Papp, E., Leinekugel, X., Henze, D. A., Lee, J. & Buzsaki, G. The apical shaft of CA1 pyramidal cells is under GABAergic interneuronal control. *Neuroscience* **102**, 715-721, (2001).

122 Womelsdorf, T. ***et al.*** Modulation of neuronal interactions through neuronal synchronization. *Science* **316**, 1609-1612, (2007).

123 Konig, P., Engel, A. K. & Singer, W. Integrator or coincidence detector? The role of the cortical neuron revisited. *Trends in Neurosciences* **19**, 130-137, (1996).

124 Salinas, E. & Sejnowski, T. J. Impact of correlated synaptic input on output firing rate and variability in simple neuronal models. *J Neurosci* **20**, 6193-6209, (2000).

125 Salinas, E. & Sejnowski, T. J. Correlated neuronal activity and the flow of neural information. *Nat Rev Neurosci* **2**, 539-550, (2001).

126 Fries, P., Reynolds, J. H., Rorie, A. E. & Desimone, R. Modulation of oscillatory neuronal synchronization by selective visual attention. *Science* **291**, 1560-1563, (2001).

127 Fries, P., Womelsdorf, T., Oostenveld, R. & Desimone, R. The effects of visual stimulation and selective visual attention on rhythmic neuronal synchronization in macaque area V4. *J Neurosci* **28**, 4823-4835, (2008).

128 Womelsdorf, T., Fries, P., Mitra, P. P. & Desimone, R. Gamma-band synchronization in visual cortex predicts speed of change detection. *Nature* **439**, 733-736, (2006).

129 Taylor, K., Mandon, S., Freiwald, W. A. & Kreiter, A. K. Coherent oscillatory activity in monkey area V4 predicts successful allocation of attention. *Cereb Cortex* **15**, 1424-1437, (2005).

130 Muzzio, I. A. ***et al.*** Attention Enhances the Retrieval and Stability of Visuospatial and Olfactory Representations in the Dorsal Hippocampus. *PLoS Biology* **7**, e1000140, (2009).

131 Jeewajee, A., Lever, C., Burton, S., O'Keefe, J. & Burgess, N. Environmental novelty is signaled by reduction of the hippocampal theta frequency. *Hippocampus* **18**, 340-348, (2008).

132 Montgomery, S. M. & Buzsaki, G. Gamma oscillations dynamically couple hippocampal CA3 and CA1 regions during memory task performance. *Proc Natl Acad Sci U S A* **104**, 14495-14500, (2007).

133 Jacobs, J., Kahana, M. J., Ekstrom, A. D. & Fried, I. Brain oscillations control timing of single-neuron activity in humans. *J Neurosci* **27**, 3839-3844, (2007).

134 Jensen, O., Kaiser, J. & Lachaux, J. P. Human gamma-frequency oscillations associated with attention and memory. *Trends in Neurosciences* **30**, 317-324, (2007).

135 Fell, J. *et al.* Rhinal-hippocampal theta coherence during declarative memory formation: interaction with gamma synchronization? *European Journal of Neuroscience* **17**, 1082-1088, (2003).

136 Fell, J., Ludowig, E., Rosburg, T., Axmacher, N. & Elger, C. E. Phase-locking within human mediotemporal lobe predicts memory formation. *Neuroimage* **43**, 410-419, (2008).

137 Fell, J. *et al.* Rhinal-hippocampal coupling during declarative memory formation: dependence on item characteristics. *Neuroscience Letters* **407**, 37-41, (2006).

138 Fell, J., Klaver, P., Elger, C. E. & Fernandez, G. The interaction of rhinal cortex and hippocampus in human declarative memory formation. *Reviews in the Neurosciences* **13**, 299-312, (2002).

139 Mormann, F. *et al.* Independent delta/theta rhythms in the human hippocampus and entorhinal cortex. *Frontiers in Human Neuroscience* **2**, 3, (2008).

140 Mormann, F. *et al.* Phase/amplitude reset and theta-gamma interaction in the human medial temporal lobe during a continuous word recognition memory task. *Hippocampus* **15**, 890-900, (2005).

141 Guderian, S., Schott, B. H., Richardson-Klavehn, A. & Duzel, E. Medial temporal theta state before an event predicts episodic encoding success in humans. *Proc Natl Acad Sci U S A* **106**, 5365-5370, (2009).

142 Sederberg, P. B. *et al.* Hippocampal and neocortical gamma oscillations predict memory formation in humans. *Cereb Cortex* **17**, 1190-1196, (2007).

143 Lakatos, P. *et al.* An Oscillatory Hierarchy Controlling Neuronal Excitability and Stimulus Processing in the Auditory Cortex. *J Neurophysiol* **94**, 1904-1911, (2005).

144 Canolty, R. T. *et al.* High gamma power is phase-locked to theta oscillations in human neocortex. *Science* **313**, 1626-1628, (2006).

145 Jensen, O. & Colgin, L. L. Cross-frequency coupling between neuronal oscillations. *Trends in Cognitive Sciences* **11**, 267-269, (2007).

146 Osipova, D., Hermes, D. & Jensen, O. Gamma power is phase-locked to posterior alpha activity. *PLoS One* **3**, e3990, (2008).

147 Colgin, L. L. *et al.* Frequency of gamma oscillations routes flow of information in the hippocampus. *Nature* **462**, 353-357, (2009).

148 Rutishauser, U., Ross, I. B., Mamelak, A. N. & Schuman, E. M. Human memory strength is predicted by theta-frequency phase-locking of single neurons. *Nature* **464**, 903-907, (2010).

149 Sirota, A. *et al.* Entrainment of neocortical neurons and gamma oscillations by the hippocampal theta rhythm. *Neuron* **60**, 683-697, (2008).

150 Hasselmo, M. E., Bodelon, C. & Wyble, B. P. A proposed function for hippocampal theta rhythm: separate phases of encoding and retrieval enhance reversal of prior learning. *Neural Computation* **14**, 793-817, (2002).

151 Givens, B. Stimulus-evoked resetting of the dentate theta rhythm: relation to working memory. *Neuroreport* **8**, 159-163, (1996).

152 Tesche, C. D. & Karhu, J. Theta oscillations index human hippocampal activation during a working memory task. *Proc Natl Acad Sci U S A* **97**, 919-924, (2000).

153 Rajkai, C. *et al.* Transient Cortical Excitation at the Onset of Visual Fixation. *Cereb Cortex* **18**, 200-209, (2008).

154 Lakatos, P., Chen, C.-M., O'Connell, M. N., Mills, A. & Schroeder, C. E. Neuronal Oscillations and Multisensory Interaction in Primary Auditory Cortex. *Neuron* **53**, 279-292, (2007).

155 Huerta, P. T. & Lisman, J. E. Bidirectional synaptic plasticity induced by a single burst during cholinergic theta oscillation in CA1 in vitro. *Neuron* **15**, 1053-1063, (1995).

156 Hyman, J. M., Wyble, B. P., Goyal, V., Rossi, C. A. & Hasselmo, M. E. Stimulation in hippocampal region CA1 in behaving rats yields long-term potentiation when delivered to the peak of theta and long-term depression when delivered to the trough. *J Neurosci* **23**, 11725-11731, (2003).

157 McCartney, H., Johnson, A. D., Weil, Z. M. & Givens, B. Theta reset produces optimal conditions for long-term potentiation. *Hippocampus* **14**, 684-687, (2004).

158 Melloni, L., Schwiedrzik, C. M., Rodriguez, E. & Singer, W. (Micro)Saccades, corollary activity and cortical oscillations. *Trends in Cognitive Sciences* **13**, 239-245, (2009).

159 Zola-Morgan, S., Squire, L. R. & Amaral, D. G. Human amnesia and the medial temporal region: enduring memory impairment following a bilateral lesion limited to field CA1 of the hippocampus. *J Neurosci* **6**, 2950-2967, (1986).

160 Rempel-Clower, N. L., Zola, S. M., Squire, L. R. & Amaral, D. G. Three Cases of Enduring Memory Impairment after Bilateral Damage Limited to the Hippocampal Formation. *J Neurosci* **16**, 5233-5255, (1996).

161 Manns, J. R., Hopkins, R. O., Reed, J. M., Kitchener, E. G. & Squire, L. R. Recognition memory and the human hippocampus. *Neuron* **37**, 171-180, (2003).

162 Reed, J. M. & Squire, L. R. Impaired recognition memory in patients with lesions limited to the hippocampal formation. *Behav Neurosci* **111**, 667-675, (1997).

163 Alvarez, P., Zola-Morgan, S. & Squire, L. R. Damage limited to the hippocampal region produces long-lasting memory impairment in monkeys. *J Neurosci* **15**, 3796-3807, (1995).

164 Vargha-Khadem, F. *et al.* Differential effects of early hippocampal pathology on episodic and semantic memory. *Science* **277**, 376-380, (1997).

165 Mayes, A. R., Holdstock, J. S., Isaac, C. L., Hunkin, N. M. & Roberts, N. Relative sparing of item recognition memory in a patient with adult-onset damage limited to the hippocampus. *Hippocampus* **12**, 325-340, (2002).

166 Baddeley, A., Vargha-Khadem, F. & Mishkin, M. Preserved recognition in a case of developmental amnesia: implications for the acquisition of semantic memory? *J Cogn Neurosci* **13**, 357-369, (2001).

167 Brown, E. N., Nguyen, D. P., Frank, L. M., Wilson, M. A. & Solo, V. An analysis of neural receptive field plasticity by point process adaptive filtering. *Proc Natl Acad Sci U S A* **98**, 12261-12266, (2001).

168 Adlam, A. L., Malloy, M., Mishkin, M. & Vargha-Khadem, F. Dissociation between recognition and recall in developmental amnesia. *Neuropsychologia* **47**, 2207-2210, (2009).

169 Bastin, C. *et al.* Dissociation between recall and recognition memory performance in an amnesic patient with hippocampal damage following carbon monoxide poisoning. *Neurocase* **10**, 330-344, (2004).

170 Holdstock, J. S., Mayes, A. R., Gong, Q. Y., Roberts, N. & Kapur, N. Item recognition is less impaired than recall and associative recognition in a patient with selective hippocampal damage. *Hippocampus* **15**, 203-215, (2005).

171 Yonelinas, A. P. *et al.* Effects of extensive temporal lobe damage or mild hypoxia on recollection and familiarity. *Nat Neurosci* **5**, 1236-1241, (2002).

172 Squire, L. R., Wixted, J. T. & Clark, R. E. Recognition memory and the medial temporal lobe: a new perspective. *Nat Rev Neurosci* **8**, 872-883, (2007).

173 Dunn, J. C. Remember-know: a matter of confidence. *Psychol Rev* **111**, 524-542, (2004).

174 Kirwan, C. B., Wixted, J. T. & Squire, L. R. Activity in the Medial Temporal Lobe Predicts Memory Strength, Whereas Activity in the Prefrontal Cortex Predicts Recollection. *J Neurosci* **28**, 10541-10548, (2008).

175 Donaldson, W. The role of decision processes in remembering and knowing. *Memory & Cognition* **24**, 523-533, (1996).

176 Wixted, J. T. & Stretch, V. In defense of the signal detection interpretation of remember/know judgments. *Psychon Bull Rev* **11**, 616-641, (2004).

177 Wais, P. E., Mickes, L. & Wixted, J. T. Remember/know judgments probe degrees of recollection. *J Cogn Neurosci* **20**, 400-405, (2008).

178 Fried, I., MacDonald, K. A. & Wilson, C. L. Single Neuron Activity in Human Hippocampus and Amygdala during Recognition of Faces and Objects. *Neuron* **18**, 753-765, (1997).

179 Brown, M. W. Hippocampal and perirhinal functions in recognition memory. *Nat Rev Neurosci* **9**, 405; author reply 405, (2008).

180 Squire, L. R., Wixted, J. T. & Clark, R. E. Review authors' response. *Nat Rev Neurosci* **9**, 405-405, (2008).

181 Ranganath, C. Working memory for visual objects: complementary roles of inferior temporal, medial temporal, and prefrontal cortex. *Neuroscience* **139**, 277-289, (2006).

182 Rissman, J., Gazzaley, A. & D'Esposito, M. Dynamic adjustments in prefrontal, hippocampal, and inferior temporal interactions with increasing visual working memory load. *Cereb Cortex* **18**, 1618-1629, (2008).

183 Ranganath, C., Cohen, M. X. & Brozinsky, C. J. Working memory maintenance contributes to long-term memory formation: neural and behavioral evidence. *J Cogn Neurosci* **17**, 994-1010, (2005).

184 Forwood, S. E., Winters, B. D. & Bussey, T. J. Hippocampal lesions that abolish spatial maze performance spare object recognition memory at delays of up to 48 hours. *Hippocampus* **15**, 347-355, (2005).

185 Mumby, D. G. Perspectives on object-recognition memory following hippocampal damage: lessons from studies in rats. *Behav Brain Res* **127**, 159-181, (2001).

186 Viskontas, I. V., Knowlton, B. J., Steinmetz, P. N. & Fried, I. Differences in Mnemonic Processing by Neurons in the Human Hippocampus and Parahippocampal Regions. *J Cogn Neurosci* **18**, 1654-1662, (2006).

187 Cameron, K. A., Yashar, S., Wilson, C. L. & Fried, I. Human Hippocampal Neurons Predict How Well Word Pairs Will Be Remembered. *Neuron* **30**, 289-298, (2001).

188 Suzuki, W. A. & Eichenbaum, H. The neurophysiology of memory. *Annals of the New York Academy of Sciences* **911**, 175-191, (2000).

189 Bichot, N. P., Rossi, A. F. & Desimone, R. Parallel and serial neural mechanisms for visual search in macaque area V4. *Science* **308**, 529-534, (2005).

190 Buschman, T. J. & Miller, E. K. Top-Down Versus Bottom-Up Control of Attention in the Prefrontal and Posterior Parietal Cortices. *Science* **315**, 1860-1862, (2007).

191 Pesaran, B., Pezaris, J. S., Sahani, M., Mitra, P. P. & Andersen, R. A. Temporal structure in neuronal activity during working memory in macaque parietal cortex. *Nat Neurosci* **5**, 805-811, (2002).

192 Mishra, J., Fellous, J. M. & Sejnowski, T. J. Selective attention through phase relationship of excitatory and inhibitory input synchrony in a model cortical neuron. *Neural Netw* **19**, 1329-1346, (2006).

193 Mitra, P. P. & Pesaran, B. Analysis of dynamic brain imaging data. *Biophys J* **76**, 691-708, (1999).

194 Jarvis, M. R. & Mitra, P. P. Sampling properties of the spectrum and coherency of sequences of action potentials. *Neural Computation* **13**, 717-749, (2001).

195 Nichols, T. E. & Holmes, A. P. Nonparametric permutation tests for functional neuroimaging: A primer with examples. *Human Brain Mapping* **15**, 1-25, (2002).

196 Maris, E. & Oostenveld, R. Nonparametric statistical testing of EEG- and MEG-data. *J Neurosci Methods* **164**, 177-190, (2007).

197 Rosenberg, J. R., Amjad, A. M., Breeze, P., Brillinger, D. R. & Halliday, D. M. The Fourier approach to the identification of functional coupling between neuronal spike trains. *Prog Biophys Mol Biol* **53**, 1-31, (1989).

198 Kilner, J. M., Baker, S. N., Salenius, S., Hari, R. & Lemon, R. N. Human cortical muscle coherence is directly related to specific motor parameters. *J Neurosci* **20**, 8838-8845, (2000).

199 Buzsaki, G. Large-scale recording of neuronal ensembles. *Nat Neurosci* **7**, 446-451, (2004).

200 Zeitler, M., Fries, P. & Gielen, S. Assessing Neuronal Coherence with Single-Unit, Multi-Unit, and Local Field Potentials. *Neural Computation* **18**, 2256-2281, (2006).

201 Bragin, A. *et al.* Gamma (40-100 Hz) oscillation in the hippocampus of the behaving rat. *J Neurosci* **15**, 47-60, (1995).

202 Chrobak, J. J. & Buzsaki, G. High-frequency oscillations in the output networks of the hippocampal-entorhinal axis of the freely behaving rat. *J Neurosci* **16**, 3056-3066, (1996).

203 Soltani, M. & Knight, R. T. Neural origins of the P300. *Crit Rev Neurobiol* **14**, 199-224, (2000).

204 Polich, J. Updating P300: an integrative theory of P3a and P3b. *Clin Neurophysiol* **118**, 2128-2148, (2007).

205 Halgren, E., Marinkovic, K. & Chauvel, P. Generators of the late cognitive potentials in auditory and visual oddball tasks. *Electroencephalogr Clin Neurophysiol* **106**, 156-164, (1998).

206 Fell, J. *et al.* Neural bases of cognitive ERPs: more than phase reset. *J Cogn Neurosci* **16**, 1595-1604, (2004).

207 Kok, A. On the utility of P3 amplitude as a measure of processing capacity. *Psychophysiology* **38**, 557-577, (2001).

208 Knight, R. Contribution of human hippocampal region to novelty detection. *Nature* **383**, 256-259, (1996).

209 Sederberg, P. B. *et al.* Gamma oscillations distinguish true from false memories. *Psychological Science* **18**, 927-932, (2007).

210 Robbe, D. *et al.* Cannabinoids reveal importance of spike timing coordination in hippocampal function. *Nat Neurosci* **9**, 1526-1533, (2006).

211 Fries, P. A mechanism for cognitive dynamics: neuronal communication through neuronal coherence. *Trends in Cognitive Sciences* **9**, 474-480, (2005).

212 Edwards, E., Soltani, M., Deouell, L. Y., Berger, M. S. & Knight, R. T. High Gamma Activity in Response to Deviant Auditory Stimuli Recorded Directly From Human Cortex. *J Neurophysiol* **94**, 4269-4280, (2005).

213 Hoogenboom, N., Schoffelen, J.-M., Oostenveld, R., Parkes, L. M. & Fries, P. Localizing human visual gamma-band activity in frequency, time and space. *Neuroimage* **29**, 764-773, (2006).

214 Wyart, V. & Tallon-Baudry, C. Neural dissociation between visual awareness and spatial attention. *J Neurosci* **28**, 2667-2679, (2008).

215 Wyart, V. & Tallon-Baudry, C. How ongoing fluctuations in human visual cortex predict perceptual awareness: baseline shift versus decision bias. *J Neurosci* **29**, 8715-8725, (2009).

216 Niessing, J. *et al.* Hemodynamic Signals Correlate Tightly with Synchronized Gamma Oscillations. *Science* **309**, 948-951, (2005).

217 Stark, C. E. & Squire, L. R. When zero is not zero: the problem of ambiguous baseline conditions in fMRI. *Proc Natl Acad Sci U S A* **98**, 12760-12766, (2001).

218 Winson, J. Loss of hippocampal theta rhythm results in spatial memory deficit in the rat. *Science* **201**, 160-163, (1978).

219 Lisman, J. E. & Idiart, M. A. Storage of 7 +/- 2 short-term memories in oscillatory subcycles. *Science* **267**, 1512-1515, (1995).

220 Buzsaki, G. Theta Oscillations in the Hippocampus. *Neuron* **33**, 325-340, (2002).

221 Ulanovsky, N. & Moss, C. F. Hippocampal cellular and network activity in freely moving echolocating bats. *Nat Neurosci* **10**, 224-233, (2007).

222 Brown, B. B. Frequency and phase of hippocampal theta activity in the spontaneously behaving cat. *Electroencephalogr Clin Neurophysiol* **24**, 53-62, (1968).

223 Ekstrom, A. D. *et al.* Human hippocampal theta activity during virtual navigation. *Hippocampus* **15**, 881-889, (2005).

224 Slawinska, U. & Kasicki, S. The frequency of rat's hippocampal theta rhythm is related to the speed of locomotion. *Brain Res.* **796**, 327-331, (1998).

225 Macrides, F., Eichenbaum, H. B. & Forbes, W. B. Temporal relationship between sniffing and the limbic theta rhythm during odor discrimination reversal learning. *J Neurosci* **2**, 1705-1717, (1982).

226 Vinck, M., van Wingerden, M., Womelsdorf, T., Fries, P. & Pennartz, C. M. A. The pairwise phase consistency: A bias-free measure of rhythmic neuronal synchronization. *Neuroimage* **51**, 112-122, (2010).

227 Jutras, M. J. & Buffalo, E. A. Recognition memory signals in the macaque hippocampus. *Proc. Natl. Acad. Sci. U. S. A.* **107**, 401-406, (2010).

228 Jutras, M. J., Fries, P. & Buffalo, E. A. Gamma-band synchronization in the macaque hippocampus and memory formation. *J Neurosci* **29**, 12521-12531, (2009).

229 Irwin, D. E. & Zelinsky, G. J. Eye movements and scene perception: memory for things observed. *Percept Psychophys* **64**, 882-895, (2002).

230 Shah, A. S. *et al.* Neural Dynamics and the Fundamental Mechanisms of Event-related Brain Potentials. *Cereb. Cortex.* **14**, 476-483, (2004).

231 Jensen, O. & Colgin, L. L. Cross-frequency coupling between neuronal oscillations. *Trends Cogn. Sci.* **11**, 267-269, (2007).

232 Fisher, N. I. *Statistical analysis of circular data*. (Cambridge University Press, 1993).

233 Schroeder, C. E., Wilson, D. A., Radman, T., Scharfman, H. & Lakatos, P. Dynamics of Active Sensing and perceptual selection. *Curr Opin Neurobiol* **20**, 172-176, (2010).

234 Holscher, C., Anwyl, R. & Rowan, M. J. Stimulation on the Positive Phase of Hippocampal Theta Rhythm Induces Long-Term Potentiation That Can Be Depotentiated by Stimulation on the Negative Phase in Area CA1 In Vivo. *J Neurosci* **17**, 6470-6477, (1997).

235 Gray, C. M., Engel, A. K., Konig, P. & Singer, W. Synchronization of oscillatory neuronal responses in cat striate cortex: temporal properties. *Vis Neurosci* **8**, 337-347, (1992).

236 Halgren, E., Babb, T. L. & Crandall, P. H. Human hippocampal formation EEG desynchronizes during attentiveness and movement. *Electroencephalogr Clin Neurophysiol* **44**, 778-781, (1978).

237 Fries, P., Roelfsema, P. R., Engel, A. K., Konig, P. & Singer, W. Synchronization of oscillatory responses in visual cortex correlates with perception in interocular rivalry. *Proc Natl Acad Sci U S A* **94**, 12699-12704, (1997).

238 Lee, H., Simpson, G. V., Logothetis, N. K. & Rainer, G. Phase locking of single neuron activity to theta oscillations during working memory in monkey extrastriate visual cortex. *Neuron* **45**, 147-156, (2005).

239 Siapas, A. G., Lubenov, E. V. & Wilson, M. A. Prefrontal Phase Locking to Hippocampal Theta Oscillations. *Neuron* **46**, 141-151, (2005).

240 O'Keefe, J. & Recce, M. L. Phase relationship between hippocampal place units and the EEG theta rhythm. *Hippocampus* **3**, 317-330, (1993).

241 Skaggs, W. E., McNaughton, B. L., Wilson, M. A. & Barnes, C. A. Theta phase precession in hippocampal neuronal populations and the compression of temporal sequences. *Hippocampus* **6**, 149-172, (1996).

242 Semba, K. & Komisaruk, B. R. Neural substrates of two different rhythmical vibrissal movements in the rat. *Neuroscience* **12**, 761-774, (1984).